Technische Universität München

TUM School of Life Sciences

# Effect of Pathogen Quiescence on Epidemiological Models of Infectious Diseases

Usman Sanusi

Vollständiger Abdruck der von der TUM School of Life Sciences der Technischen Universität München zur Erlangung des akademischen Grades eines

Doktors der Naturwissenschaften (Dr. rer. nat.)

genehmigten Dissertation.

| | |
|---|---|
| Vorsitzende: | Prof. Donna Ankerst, Ph.D. |
| Prüfer der Dissertation: | 1. Prof. Dr. Aurélien Tellier |
| | 2. Prof. Dr. Johannes Müller |

Die Dissertation wurde am 05.12.2022 bei der Technischen Universität München eingereicht und durch die TUM School of Life Sciences am 26.01.2023 angenommen.

# Kurzfassung

Erreger-Ruhephase ist die Fähigkeit eines Parasiten, für eine gewisse Zeit inaktiv zu werden, bezüglich Stoffwechsel und Infektiosität, und anschließend wieder aktiv (infektiös) zu werden. Erreger-Ruhephase ist eine Strategie, die bei vielen Pilzen, Bakterien, wirbellosen Tieren und Pflanzen zu finden ist. Diese Strategie hat sich entwickelt, um die Auswirkungen schwieriger Bedingungen zu überleben und die Fortpflanzung während günstiger Bedingungen zu optimieren. Die Strategie des "bet-hedging" entwickelt sich mit der Zeit, wenn das Individuum (Pilz, Bakterium, wirbelloses Tier) oder die Nachkommenschaft des Individuums (wirbelloses Tier, Pflanze) in eine Ruhephase mit niedrigem Stoffwechselzustand eintritt, was bei vielen menschlichen Parasiten (Tuberkulose, Malaria, ...) der Fall ist. Während dieser Ruhephase finden Evolution und Reproduktion im aktiven Teil der Population statt. Die Ruhephase von Parasiten wird im Allgemeinen unterschätzt und hat Konsequenzen für die Verbesserung der Krankheitsbewältigung und -kontrolle. In dieser Arbeit diskutiere ich die Auswirkungen der Erregerruhe auf die Epidemiologie von Infektionskrankheiten. Dazu entwickle ich ein Susceptible-Infected-Quiescent-Susceptible (SIQS)-Modell, um die Auswirkung der Ruhephase auf die Zeit bis zum Aussterben und die quasistationäre Verteilung des stochastischen SIQS-Modells zu verstehen. Ich stelle fest, dass die Ruhezeit die Zeit bis zum Aussterben verlängert und die quasistationäre Verteilung beeinflusst, indem sie eine der bekannten Formen der Verteilung bricht, nämlich die abnehmende Form. Außerdem entwickle ich ein deterministisches Koevolutionsmodell mit zwei Parasitentypen, die einen Wirtstyp infizieren, und untersuche analytisch die Stabilität des dynamischen Systems. Insbesondere leite ich eine Stabilitätsbedingung für ein fünf-mal-fünf-Gleichungssystem mit Ruhezustand ab. Außerdem entwickle ich eine stochastische Version des Modells, um den Einfluss der Ruhephase auf die Stochastizität der Systemdynamik zu untersuchen. Ich berechne die stationäre Verteilung der Parasitentypen, die einer multivariaten Normalverteilung folgt, und erhalte numerische Lösungen für die Kovarianzmatrix des Systems bei symmetrischen und asymmetrischen Ruhephasenraten zwischen Parasitentypen. Wenn die Parasitenstämme identisch sind, erhöht die Ruhephase die Varianz der Anzahl der infizierten Individuen bei hoher Übertragungsrate und umgekehrt, wenn die Übertragungsrate niedrig ist. Wenn jedoch ein Wettbewerb zwischen Parasitenstämmen mit unterschiedlichen Ruhezeiten besteht, führt die Ruhezeit zu einem gleitenden Mittelwert, der die Stochastizität dämpft und die Varianz der Anzahl der infizierten Wirte verringert. Der Stamm mit der höchsten Rate des Eintritts in die Ruhephase bestimmt die Stärke des gleitenden Durchschnitts und das Ausmaß der Verringerung der Stochastizität. Abschließend entwickle ich ein Koinfektionsmodell, das die Dynamik der Epidemiologie bei Koinfektionen mit zwei Stämmen und einem Wirtstyp erfasst, bei denen einer der Stämme das Ruheverhalten zeigt. Überraschenderweise beobachte ich ein neues Verhalten, nämlich dass die Ruhephase die Korrelation zwischen der Anzahl der von beiden Stämmen Infizierten beeinflusst. Ich schließe die Arbeit mit einer Diskussion über die Relevanz der durchgeführten Forschung und einer kurzen Analyse der epidemiologischen Daten über die Verbreitung von Malariaparasiten in Brasilien.

# Abstract

Quiescence is the ability for a parasite to become inactive, with respect to metabolism and infectiousness, for some amount of time and then active (infectious) again. Quiescence is a bet-hedging strategy that is commonly found in many fungi, bacteria, invertebrates and plants. This strategy developed to survive the effect of harsh conditions and to optimise reproduction during favourable conditions. The strategy of bet-hedging in time evolves when the individuals (fungus, bacteria, invertebrates) or the progeny of the individual (invertebrate, plants) enters quiescence with a low metabolic state and is common in many human parasites (tuberculosis, malaria,...). During this dormancy period, evolution and reproduction take place in the active part of the population. Parasite quiescence is generally under appreciated and has consequences for improving disease management and control. In this Thesis, I discuss the effect of pathogen quiescence on infectious disease epidemiology. Therefore, I build a Susceptible-Infected-Quiescent-Susceptible (SIQS) model to understand the effect of quiescence/dormancy on the time to extinction and the quasi-stationary distribution of the stochastic SIQS model. I find that quiescence increases the time to extinction and affects the quasi-stationary distribution by breaking one of the known shapes of the distribution, namely the decreasing shape. Furthermore, I develop a deterministic coevolutionary model with two parasite types infecting one host type and study analytically the stability of the dynamical system. I specifically derive a stability condition for a five-by-five system of equations with quiescence. I also develop a stochastic version of the model to study the influence of quiescence on stochasticity of the system dynamics. I compute the steady state distribution of the parasite types which follows a multivariate normal distribution, and obtain numerical solutions for the covariance matrix of the system under symmetric and asymmetric quiescence rates between parasite types. When parasite strains are identical, quiescence increases the variance of the number of infected individuals at high transmission rate and vice versa when the transmission rate is low. However, when there is competition between parasite strains with different quiescent rates, quiescence generates a moving average behaviour which dampens off stochasticity and decreases the variance of the number of infected hosts. The strain with the highest rate of entering quiescence determines the strength of the moving average and the magnitude of reduction of stochasticity. Finally, I develop a co-infections model that captures the dynamics of epidemiology with co-infections with two strains, one host type, in which one of the strains exhibits the quiescence behaviour. Surprisingly, I observe a new behaviour, namely quiescence affects the correlation between the number of infected by either strains. I conclude the thesis with a discussion of the relevance of the conducted research and include a short analysis of epidemiological data of malaria parasites disease prevalence in Brazil.

# Acknowledgement

First and foremost, I thank Allah, the Lord of all that exists who gave me knowledge and opportunity to conduct this research. I would like to use this opportunity to express my heartfelt gratitude to my supervisors Aurélien Tellier and Johannes Müller for their constant support, guidance, keeping me going even when things were really arduous and follow-up on my work progress throughout this journey. I really consider myself lucky to have work under these great gentle men. I would also like to acknowledge and thank Donna Ankerst. I also like to thank my advisor Sona John for her support especially during the early time of this work. I would like to express my special appreciation to Silke Bauer (popgen), Daniela Scheikl (Popgen), Anke Friebel (IGSSE) , Katharina Geiselmann (IGSSE), Lydia Weber (Maths), Isabella Wiegand (Maths) for offering me invaluable advices especially on administrative issues. My sincere thanks also go to Eva Stadler, Augustine Okolie, Berly Musundi, Kevin Korfmann, Thibaut Sellinger, Matthias Neumair, Lukas Metzger, Gustabo Adolfo Silva Arias, Heng Liang, Moritz Hackbarth, Annalena Matzner, Sidra Tul Muntaha, Murtala Bindawa and all people whom I work with both at section of Population Genetics and Maths Department for their collaborative research support and advice. I extend my heartfelt gratitude to my sponsors, Petroleum Technology Development Fund (PTDF) of Nigeria for sponsoring the whole PhD programme and International Graduate School of Science and Engineering (IGSSE) for supporting me through Deutsche Forschungsgemeinschaft (DFG) grant. I equally thank Umaru Musa Yar'adua University Katsina (UMYUK), Nigeria for the opportunity to follow the TUM PhD programme.

I would like to acknowledge and express my sincere appreciation to my wife, Aisha Kabir Wurgi, my sons, Abudullahi Usman Sanusi and Sanusi Usman Sanusi for the their support, love, care , concern, understanding, encouragement during this work and for being patient of my long absence, I really appreciate it, I love you all.

A special recognition goes to my parents, family and friends. Words cannot express how grateful I am to my parents, Mr. Sanusi Rabo and Malama Hauwa'u Abdul-aziz for their financial support/ Investing heavenly in my educational pursuit. Your prayers to my humble self are what kept me going thus far. I also thank my mother-in law, father-in-law, Baba Hafizu and all members of my family for the love shown to me during this critical time.

Last but not the least, I would like to thank Maths department, School of Life Sciences, International Graduate of Science and Engineering (IGSSE), German Goverment and Nigerian Government for providing me a world-class learning environment to carry out this novel research.

# Contents

# Chapter 1

# Introduction

Since the seminal early work [18, 65, 12], mathematical models have been refined in their modern version to understand and predict the spread of infectious diseases [8, 78]. The use of such mathematical models contributes immensely to the control of various infectious diseases in human, wild and domesticated animals and plants [9, 43, 32, 56, 55]. Modelling helps us to utilise our limited resources more effectively in case of a pandemic such as managing the occupancy rate of hospitalisations [85], with the ultimate aim for human diseases to decrease the rate of death (as we have recently witnessed during the Covid-19 pandemic). A main first control measure of an infectious disease in humans and animals include vaccination [64, 72, 77, 111] which was first develop by *Edward Jenner* in the year 1796 against smallpox [69, 92, 59]. Later on, the wide use of the vaccine successfully helped to eradicate the said disease. Note that this is the one and only disease that has been completely eradicated globally to date. Vaccination acts by stimulating immune response of susceptible individuals which in turn become immunised against the disease. Secondly, isolation and quarantine are key measures and consist in isolating from the rest of the population an already infected person who has been identified or suspected to have contracted the disease. The result is to reduce the potential transmission rate of the disease. Isolation / quarantine is the oldest disease management method which is known for centuries, and has been successfully applied for example 1) in Italy by implementing a policy that blocked all ships coming from an already plague infected region in the middle-ages, or 2) in the UK in the year 1665 when people in the village of Eyam in Derbyshire isolated themselves in an effort to contain the spread of plague to neighbouring villages [91]. Isolation has been also used recently to curtail the spread of SARS in the year 2003 [63], and in early 2020 to slow down the spread of the Covid-19 epidemics. Isolation of infected individuals and quarantine measures is one of the simplest control measure to be applied. In our modern world, travel restrictions are also one of the methods used to control the spread of infectious diseases [5]. However, these measures carry a social and economic cost because activities are slowed down or even paralysed. We finally need to mention contact tracing, which is in itself not a control measure, but a tool used for

disease management [87]. Contact tracing is a process by which a patient is asked about his behaviour and potential contacts with other individuals. These contacts can then either be isolated, vaccinated or even hospitalised depending on their health conditions. Contact tracing can be done as we witnessed during the Covid-19 epidemics at an early stage of the epidemics when the number of infected cases is not too large. The feasibility of tracing infection patterns becomes cumbersome, if not impossible, when the number of infected individuals is too large.

With these practical tools at hand, the aim of health authorities is to control the spread of or, if possible, to eradicate the infectious disease. As the only infectious disease that has been successfully eradicated to this moment is smallpox, it is obvious that disease eradication is an extremely difficult task. Nevertheless, with the help of mathematicians, there has been a tremendous achievement towards the control of some diseases such as polio, malaria, etc. Recently, mathematical modelling is being used to contain the spread of Corona-virus COVID-19 by applying the above mentioned control measures [23, 74, 35, 36, 97, 47]. Indeed, mathematical modeling is a tool that can be used to predict the efficacy of different measures for controlling the disease spread. No doubt that mathematicians worked tirelessly towards giving insights on how it spreads from one person to other and what need to be done to curtail the spread of the disease. The models uses mathematics as a language to precisely described the real world problem, albeit models remain simplifications of the reality and are based on a certain number of hypotheses. In disease epidemiology, mathematical models allow us to put societal behaviour into an equations, termed differential equations, allowing analyses and simulations to make a predictions on the spread of infectious disease, predict whether a disease can become a pandemic and the long term behaviour of the disease (endemic status).

The transmission of infectious disease is characterised by the level / amount of pathogens present within the host. In other words, the pathogen has to present a certain amount of infectious propagules to enable the disease transmission from one infected person to another. Initially, it is often assumed that all individuals are susceptible to the disease, and that there is no pathogen present in the population. At time $t = 0$, one person becomes infected by the pathogen. The pathogen grows and multiplies in the host individual over time. At the early time after infection, the infected individual may show no symptoms, but the pathogen is growing. Such individual is referred to as being exposed and the disease is said to be at the latent stage. Please note already that this phenomenon is different from the quiescence stage, which I study later on, at which the pathogen stops growing inside the host. In the event that the pathogen in the host reaches a sufficiently high level or population size of infectious propagules, disease transmission can occur and the host is said to be infectious. If the host's immune system is able to clear the pathogen during the latent phase or after an infectious period, the host is so-called recovered. Classically in epidemiological models, we assume that a single individual becomes infectious, and we then follow the fate of infection from that individual to assess if the disease persists or becomes pandemic. The Basic Reproduction Number $R_0$, calculated in many occasion in my thesis such as in equations (1.3.2 and 1.3.4), is the most important epidemic number

which determine at the beginning of the outbreak of the disease if the disease becomes pandemic or not [7]. It is defined as the average number of people an infectious individual does infect during the pandemic in a totally susceptible population.

In the first chapter of this thesis, I present a general introduction to the problem of choice and main topic of my work, namely the role of pathogen quiescence in epidemiology. I will explain why we are interested in studying the influence of quiescence and how we can used mathematics to answer some interesting questions. I will also define the basic reproduction number, the most important quantity in epidemiology, and basic notations of mathematical models of epidemiology used in this thesis. I begin with the standard SIS model which is mathematical model use to understand and predict the spread of infectious diseases without host immunity in a constant population. This model can be applied to study the transmission of malaria disease in Nigeria and the world at large, a topic which is close to my long term interests. We aim to study the long term behaviour of the infectious disease mathematically, taking two approaches: deterministic and stochastic. The deterministic version has a threshold parameter called the basic reproduction number $R_0 = 1$. If $R_0 > 1$, then the infection becomes endemic, while the infection dies out if $R_0 < 1$. This fact does not hold in the stochastic version (with birth and death processes), as the disease dies out regardless of the value of $R_0$ [84] due to the influence of stochasticity.

## 1.1 Motivation

Let me start with a short outline of a concrete issue which motivates my research in this thesis. Malaria is a deadly disease caused by *Plasmodium sp.* parasites and passed to humans by the *Anopheles sp.* mosquito through bite. Once bitten, the parasite propagules (known as sporozoites) multiply in the patient's liver and then infect and destroy the red blood cells. Malaria is recognised as a world health issue since the initial stage of the human historical times [95]. The progression of this disease in human population is estimated to have begun approximately 42,000 years back [79]. The disease can be controlled and treated if diagnosed early. Unfortunately, this is not possible in some areas where medical facilities are lacking and malaria outbreaks frequently occur. Presently, an effective malaria vaccine is yet to be discovered. Today, despite sophisticated prevention measures such a insecticide-treated bed nets and effective antimalarial drugs, malaria infects approximately 227 million people and kills about 409,000 people all over the world in 2019 (WHO World Malaria Report 2020). As a result other forms of preventive measures, chiefly against mosquito populations, have to be taken by various health agencies and governments in a bid to eliminate the disease. This effort succeeded in decreasing drastically the disease epidemics in some regions of the world such as in Southern Europe, the former USSR, and some countries of North Africa and the Middle East [2].

In Nigeria, the government in collaboration with health agencies is working hard to achieve the goal of eradicating malaria. Some of the measures taken to this effect include:

- Prompt diagnosis and treatment with effective medicines.
- Distribution of insecticide-treated nets (ITNs) to achieve coverage of populations at risk especially children under the age of five and pregnant women.
- Indoor residual spraying (IRS) to curtail transmission.
- Prevention of malaria in pregnancy through intermittent preventive treatment.

Notwithstanding, malaria continues to be a menace to the increasing population of Nigeria and in the world at large. As such there is the need to further explore other forms of measures that can produce the required effect of eradicating the parasite or reducing it to a minimum. Malaria is a serious global health issue generating a strong disease burden worldwide [101]. There are five species of malaria known to infect human: *P. falciparum, P. vivax, P. ovale, P. malariae*, and *P. knowlesi*. Out of these five, two, namely *P. falciparum* and *P. vivax* are the main causes of malaria cases globally with P. falciparum the deadliest [58, 75] while *P. vivax* is the most geographically widespread plasmodium species. The latter can cause severe, even fatal infections and results in significant global morbidity and mortality [16, 25, 94, 104] .

**Plasmodium life cycle**

The *Plasmodium* life cycle shown in (Figure 1.1) is similar for the five plasmodium species that caused malaria in the human population [117]. There are three stages:

- Infection of a human with the parasite (sporozoites) by a female mosquito,
- Asexual reproduction inside the human body,
- Sexual reproduction.

Note that the first two stages take place inside the body of an infected individual, while the third stage starts in the human body and ends in the female *Anopheles* mosquito.

Malaria infection starts when an infected female mosquito bites a healthy person (individual), injecting parasites at the sporozoites stage into the blood circulation. That constitutes the first life stage of parasite (infection stage). These sporozoites then migrate to the liver, multiply and mature into *trophozoites* which then spread into red blood cells. This is achieved by asexual reproduction forming many *merozoites* which then move freely and invade red blood cells. Some merozoites also develop into *gametocytes*. At this stage, a female mosquito biting an infected (and thus infectious) person, becomes infected with the parasite (gametocytes) too. At the last (part of third) stage, the gametocytes develop and reproduce sexually, inside the mosquito's stomach, to produce sporozoites which migrates to the salivary glands. Then disease transmisison to another human individual can be achieved via the mosquito bites [110] .

It should be noted that in the cases of *P.vivax* and *P. ovalae*, sporozoites might not follow the reproduction step and rather become dormant (call hypnozoites) in the liver. These hypnozoites may be reactivated after a long period of time leading to relapses, because they

enter the blood stream as merozoites. These hypnozoites can stay dormant (quiescent) for weeks, months or even years before they wake up and are reactivated. When these propagules exit the quiescence phase, they continue the life cycle as described above [24].

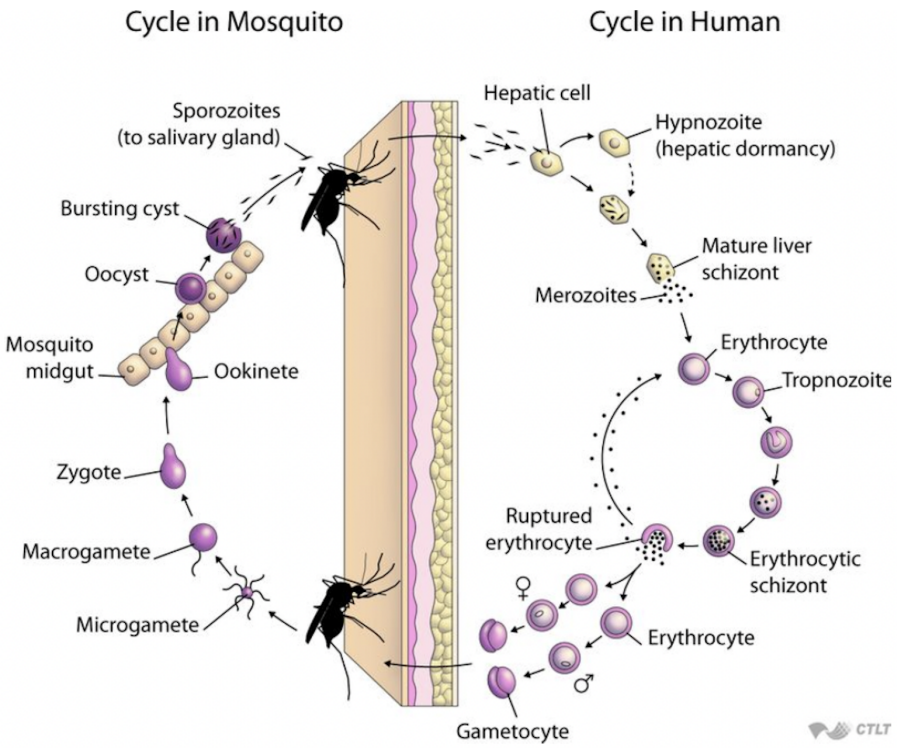


Figure 1.1: Plasmodium life cycle; the image was taken from The Medical Invincible Group (MIG)[45]

## 1.2 Quiescence/dormancy

Quiescence or dormancy is defined, in this thesis, as the ability for a parasite to become inactive for sometime and then wake up again. It is a bet-hedging strategy that is commonly found in many fungi, bacteria [76, 70], invertebrates [81] and plants. This strategy developed to survive the effect of harsh condition and to optimise the reproduction during favorable conditions [98]. The strategy of bet-hedging in time evolves when the individuals (fungus, bacteria, invertebrates) or the progeny of the individual (invertebrate, plants) enters quiescence with a low metabolic state for some time. During this period, evolution and reproduction take place in the active part of the population. Quiescence likely evolves as bet-hedging mechanism for parasites to damp off fluctuating environment such a when it is subjected to antibiotic/drug treatment, competition under density dependent selection or prey-predator competitive interactions. Quiescent individual forms a reservoir which is generally known as the seed bank (in our case quiescent propagule bank) and can be reactivated and enter into the active population later on. Quiescence (dormancy) generates an

overlapping between generations, a storage effect, and a delay in the generation time [99]. At the population level, dormancy is shown to slow down the rate of genetic drift, that is increasing the time to random loss or fixation of neutral alleles. Moreover, seed banks also slow down the action of natural selection by increasing the time to fixation (loss) of the positively (deleterious) selected alleles [51, 68, 108]. We note the use of the term dormancy preferably for plant seeds or crustacean eggs (*e.g. Daphnia sp.*), while quiescence refers to individual bacteria, fungi or malaria propagules switching between "on" and "off" metabolic states. As we focus on microparasites such as malaria in the following, we prefer the term quiescence from now on.

The quiescent strategy makes it hard to get rid of the parasites. We note that parasite dormancy has been a long neglected topic in parasitology research despite its huge impact on management of diseases. Parasite quiescence is a strategy of microparasites (bacteria, fungi) becoming inactive inside an infected host for some period of time. During this period, the disease does not progress in the host and the host can express symptoms or be asymptomatic. Parasite quiescence has well known but yet underappreciated consequences for disease management. During quiescence, the parasite are often resistant to the application of drugs, antibiotics or fungicides [27, 28, 122, 121]. Furthermore, applying antibiotics can trigger the switching of bacteria from active to the inactive (quiescent) state. *Plasmodium falciparum* has the ability to lurk in the hepatocytes of some patients, remaining inactive but being resistance to drug treatments, causing later on disease relapse [29, 46]. *P. vivax*, another malarial agent, exhibits also the ability to become dormant in the liver of a host for some weeks, months and in some cases even a year or more which makes the it difficult to eradicate the disease [118, 105, 26]. Therefore, it is important to determine 1) conditions for the evolution of parasite quiescence, and 2) influence of quiescence on the sustainability of parasite populations.

## 1.3 Review of the Basic Epidemic Models; SIS and SIR

In this section, we review some basic epidemiological models on which the further complicated epidemic models which include quiescence in this thesis are build on. Therefore, it is important to lay down the definitions and understand the dynamics of these basic models. Both $SIS$ and $SIR$ models are call compartmental model because individuals in the population are divided into mutually excluded compartments (classes) based on their disease status. These models are approximately 100-years old and date back to Kermack and Mckendrick 1927 [65], who first studied an SIR model to understand the mechanism behind the exponential growth and decay of the number of cases during an epidemics in London [1]. Since then the models have been applied to numerous infectious diseases such influenza, malaria, common cold, sexually transmitted diseases, the infamous Covid-19 and many bacterial infections [4, 63].

The total population is divided into two mutually exclusive compartments, namely: S -the susceptible sub-population (people who are currently healthy but may get the disease in the future from a successful encounter with an infectious person), and I- the infected sub-population (these are individuals who are currently carrying the disease and are capable of passing it to other people upon contact).

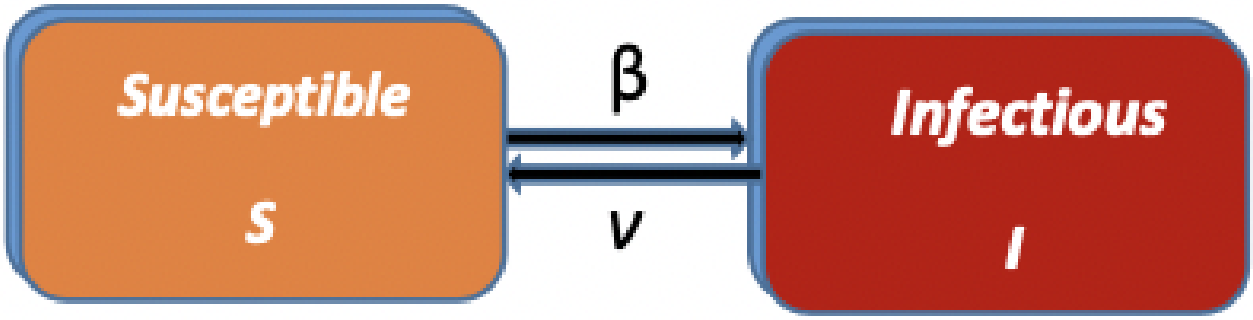


Figure 1.2: Flow diagram of the SIS model described in equation (1.3.1).

The two couple differential equations describe the flux (rate of change) of the individual in each compartment, the compartments are susceptible and infected class. $N$ is the total population size, $\beta$ is the infection rate and $\nu$ is the recovery rate.

$$\begin{aligned} \frac{dS}{dt} &= -\beta\frac{SI}{N} + \nu I \\ \frac{dI}{dt} &= \beta\frac{SI}{N} - \nu I, \end{aligned} \tag{1.3.1}$$

## Steady States

Please note that $\frac{dS}{dt} + \frac{dI}{dt} = 0$ which means that the total population size is constant. now let $N = S + I \implies S = N - I$. The equilibrium solution of the above system is then

$$S^* = \frac{\nu}{\beta}N, \quad I^* = \frac{N}{\beta}(\beta - \nu)$$

*Basic Reproduction Number*

$$R_0 = \frac{\beta}{\nu} \tag{1.3.2}$$

Actually the system (1.3.1) can be reduced to one dimensional differential equation as:

$$\frac{dI}{dt} = (\beta - \nu - I)I$$

The disease free equilibrium, $i.e\ I = 0$. The solution when $I \neq 0$ and $I(t = 0) = I_0$ is given as

$$I(t) = \left(1 - \frac{1}{R_0}\right) \frac{F}{F + e^{-(\beta-\nu)t}}$$

where

$$F = \frac{\beta I_0}{\beta - \nu - \beta I_0}$$

.

On the long run we obtain

$$I(t) = (1 - \frac{1}{R_0}), \quad R_0 > 1$$

or

$$I(t) = I_0 e^{(\beta-\nu)t} \to 0, \quad R_0 < 1.$$


Figure 1.3: Flow diagram of the SIR model described in equation (1.3.3).

While the SIR model also assumes that there is a population of individuals and each one of these individuals is in one of these compartments, it describes the spread of infections that develop immunity permanently after recovery. Hence the name SIR stands for Susceptible,S, Infected, I and Recovered, R or removed (people who once contracted the disease and developed a permanent immunity against the disease after recovery). Once an individual is in this class he or she does not participate to the infection process. This model has been successfully applied to study and understand the behaviour of acute infections, that is fast growing diseases, in which the patient develops immune response very rapidly (days to weeks) to clear off the pathogen. Example of acute infections include distemper, influenza, rabies and rubella, and childhood diseases such as mumps, chickenpox and measles [4, 63].

The three couple differential equations describe the flux (rate of change) of the individuals in each compartment, the compartments are susceptible , infected class and recovered.

$N, \beta, \nu$ are as defined above.

$$\begin{aligned} \frac{dS}{dt} &= -\beta \frac{SI}{N} \\ \frac{dI}{dt} &= \beta \frac{SI}{N} - \nu I \\ \frac{dR}{dt} &= \nu I \end{aligned} \tag{1.3.3}$$

we assume that $S(0), I(0)$ and $R(0)$ are all greater than zero and that $S(0)+I(0)+R(0) = N$. It is easy to see that $\lim_{t\to\infty} I(t) = 0$ and that $S(t)$ and $I(t)$ are bounded above. The basic reproduction number is calculated as

$$R_0 = \frac{S(0)}{N}\frac{\beta}{\nu} \tag{1.3.4}$$

This number serves the same and the dynamics of the initial disease behaves the same as the one described above for the SIS model.

In (Figure 1.4), we display the simulated result of both models (1.3.1) and (1.3.3) but focused only the infected class (disease curve) because it enables us to quantify the number of patients/possible deaths throughout the pandemic. We have seen that in the SIS model depending of the parameters of the model, there is always a certain number of people who have the disease in the population. In the SIR model, there is an initial exponential growth, and then at some point the disease curve reaches its maximum. The disease curve then decays exponentially, because people become infected then recover and are removed from the infection process. In other words, the infection "runs out of gas" and eventually the number of infected individuals decreases.

## Transition Probabilities

To study the long term behaviour of the infectious disease mathematically, there are two approaches, namely the deterministic and the stochastic. The deterministic version has a threshold parameter call basic reproduction number $R_0 = 1$ defined in equation (1.3.2). If $R_0 > 1$, then the infection will become endemic, while the infection dies out if $R_0 < 1$. This fact does not hold in a stochastic version (with a birth and death process), as the disease dies out regardless of the value of $R_0$ [84]. Since our main goals is to study time to extinction and the quasi-stationary distribution of the stochastic SIS model as in [84], it is therefore necessary to integrate a stochastic process into our deterministic model (1.3.1). To do so, we first find and define the transition probabilities of each event. The following equations describe the probabilities of moving from one state to the other. Here, the state are infection and recovery.

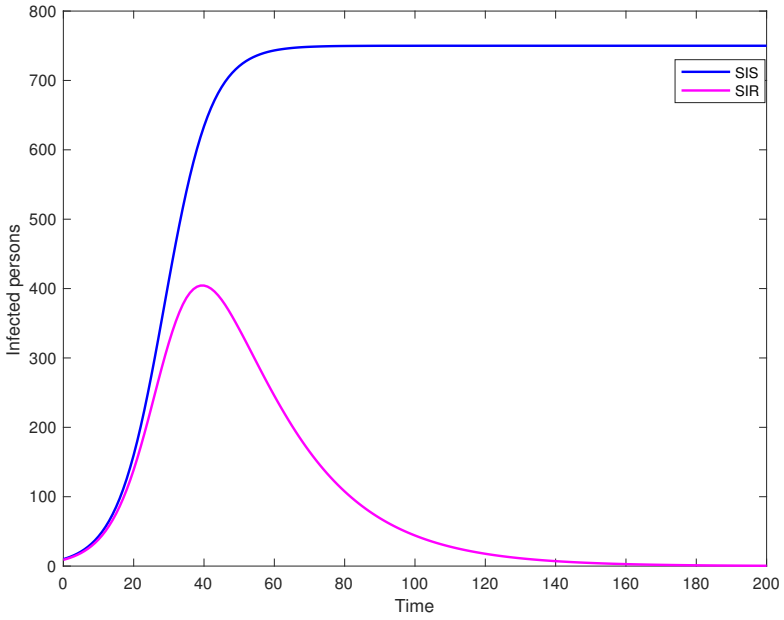


Figure 1.4: Number of infected people predicted by both SIS and SIR models (1.3.1, 1.3.3) respectively.

Table 1.1: Transitions rates for the model 1.3.1

| Type | Transition | Rate |
|---|---|---|
| Infection of $S$ by $I$ | $(S_t, I_t) \to (S_t - 1, I_t + 1)$ | $\beta \frac{SI}{N} \Delta t + o\Delta(t)$ |
| Recovery $I$ & replacement with $S$ | $(S_t, I_t) \to (S_t + 1, I_t - 1)$ | $\nu I \Delta t + o\Delta(t)$ |

### 1.3.1 Master equation

The master equation of the model 1.3.1 otherwise known as *Kolmogorov equation*, describes the deterministic evolution of the above transition probabilities. The master equation is also used to generate the generator matrix A. Because we are dealing with one dimensional system, the generator matrix is given in equation (1.3.8), as in [84, 33, 7].

$$\begin{aligned} \frac{\mathrm{d}p_{(i)}}{\mathrm{d}t} =& \frac{\beta}{N}(N - i + 1)(i - 1)p_{(i-1)} + \nu(i + 1)p_{(i+1)} \\ & - \left[\frac{\beta}{N}(N - i)i + \nu i\right] p_{(i)} \end{aligned} \tag{1.3.5}$$

Let

$$b_i = \frac{\beta}{N} i(N - i) \quad \text{and} \quad d_i = \nu i$$

then equation (1.3.5) can be written as

$$\frac{\mathrm{d}p_{(i)}}{\mathrm{d}t} = b_{i-1}p_{(i-1)} - [b_i + d_i]p_{(i)} + d_{(i+1)}p_{(i+1)} \tag{1.3.6}$$

for $i = 1, \ldots, N$ and $\frac{dp_0}{dt} = p_1 d_1$. In matrix form, the above equation (1.3.6) can be written as follows

$$\frac{\mathrm{d}p_{(i)}(t)}{\mathrm{d}t} = Ap(t) \tag{1.3.7}$$

where $p(t) = (p_0(t), \ldots, p_N(t))^T$ and the matrix $A$ known as infinitesimal generator matrix [106] defined as

$$A = \begin{pmatrix} 0 & d_1 & 0 & \ldots & 0 \\ 0 & -(d_1 + b_1) & d_2 & \ldots & 0 \\ 0 & b_1 & -(d_2 + b_2) & \ldots & 0 \\ 0 & 0 & b_2 & \ldots & 0 \\ & \ldots & \ldots & \ldots & 0 \\ 0 & 0 & 0 & \ldots & -d_N \end{pmatrix}, \tag{1.3.8}$$

defined another matrix $\hat{A}$ which is the same as matrix $A$ in equation (1.3.8) with first row and first column deleted. This is so because the matrix does not have a solution as the detail balance fails there. But the submatrix $\hat{A}$ of $A$ is singular [89], therefore eventually the absorption occurs. i.e $\lim_{t\to\infty} p(t) = (1, 0, 0; \ldots, 0)^T$)

$$\hat{A} = \begin{pmatrix} -(d_1 + b_1) & d_2 & \ldots & 0 \\ b_1 & -(d_2 + b_2) & \ldots & 0 \\ 0 & b_2 & \ldots & 0 \\ \ldots & \ldots & \ldots & 0 \\ 0 & 0 & \ldots & -d_N \end{pmatrix} \tag{1.3.9}$$

### 1.3.2 Quasistationary Stationary Distribution

In this section, we review the study of time to extinction and the quasi-stationary distribution of the stochastic SIS model as in [84]. The SIS model has two equilibrium states, namely disease free equilibrium and endemic equilibrium. In the stochastic process (Continuous Time Markov Chain (CTMC)), the disease free equilibrium is an absorbing state which means that the chain eventually visits this state. Indeed, as the states of the SIS stochastic model communicate with each other and the limiting conditional distribution is unique, see [33], the process ends in the disease free state. However, the two equilibria are far apart from each other with low probability to move between them. This is known as the quasi-stationary distribution. We define the limiting conditional distribution $\hat{p}^*$ by conditioning that the process is yet to reach its extinction state, this is to say that $\hat{p}^* = (\hat{p}_1^*, \ldots, \hat{p}_N^*)^T$ where $\hat{p}_i^*$ is the probability $I(t) = i$ given that $I(r) > 0$ for some $t > r$ (the CTMC is yet to reach its absorbing state). Mathematically it can be write as follows

$$\hat{p}_i^*(t) = \mathrm{Prob}\{I(t) = i | I(r) > 0, t > r, \}, \quad i = 1, 2, \ldots, N.$$

The fact that the zero state is an absorbing state, then the probability Prob = Prob$\{I(r) > 0, t > r, \} = 1 - p_0$, Therefore,

$$\hat{p}_i^*(t) = \frac{p_i(t)}{1 - p_0(t)}, \quad i = 1, 2, \ldots, N. \tag{1.3.10}$$

differential equation for $\hat{p}_i^*(t)$ similar to equation (1.3.5) can be obtained by differentiating equation (1.3.10) with respect to time $t$.

$$\frac{d\hat{p}_i^*(t)}{dt} = \frac{dp_i/dt}{1 - p_0} + d_1\hat{p}_1^*\frac{p_1}{1 - p_0}, \quad i = 1, 2, \ldots, N \tag{1.3.11}$$

where $\hat{p}^* = (\hat{p}_1^*, \ldots, \hat{p}_N^*)^T$ is known as the quasi-statinary distribution. In matrix form the differential equation in (1.3.11) can be written as follows

$$\frac{d\hat{p}^*}{dt} = \hat{A}\hat{p}^* + d_1\hat{p}_1^*\hat{p}^* \tag{1.3.12}$$

where $\hat{A}$ is defined in equation (1.3.9). The quasi-statinary stationary distribution $\hat{p}^* = (\hat{p}_1^*, \ldots, \hat{p}_N^*)^T$ is giving by the nonlinear eigenvalue problem which is the stationary solution of equation (1.3.12)

$$\hat{A}\hat{p}^* = -d_1\hat{p}_1^*\hat{p}^* \tag{1.3.13}$$

where $\hat{p}^*$ is the leading left eigenvector of the matrix $\hat{A}$ which is a sub-matrix of the infinitesimal generator (transition) matrix $A$ conditioned on the non zero state.

Note that equation (1.3.13) can not be solved explicitly, but several approximations exist (for more details see [84]). There are two shapes of the quasi-stationary distribution depending on the value of the basic reproduction number, $R_0$. If $R_0 > 1$ the shape of the distribution looks like a normal distribution with the center (mean) being the balance between the birth $\frac{\beta}{N}i(N - i)$ and death $\nu i$ rates ($\frac{\beta}{N}i(N - i) = \nu i$ see Fig 1.5). If $R_0 < 1$ the shape of the distribution is monotonically decreasing with $\hat{p}_1^*$ being the highest value. The trajectory of disease progress will eventually die out but can be constrained by the non-extinction and therefore the distribution has a mean around small population size (see Fig 1.6).

**The expected time to extinction** is given by

$$E(\text{time to extinction}) = 1/d_1\hat{p}_1^* = 1/\rho(\hat{A}), \quad \text{this so because } d_1\hat{p}_1^* \text{ is a perron eigenvalue of } \hat{A} \tag{1.3.14}$$

## 1.4 Simulations

To give some intuitive explanation and to verify the analytic result obtained above, we use numerical simulations as [84] and as performed later on in this thesis. We use the

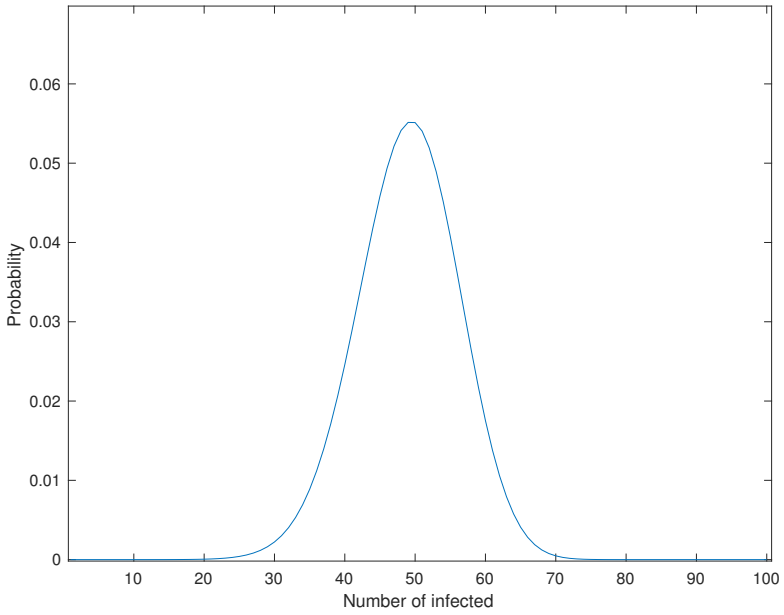


Figure 1.5: Quasistationary distribution of SIS stochastic epidemic model with $\beta = 2, \nu = 1$ and $N = 100$ .

Gillespie algorithm [37, 38]. It is used to generate stochastic realisations/sample paths of the birth and death processes described above. In other word, the algorithm is used to numerically compute the movement of the continuous time Markov chain CTMC from one state to the other. To use the algorithm two uniformly distributed random variables are required $u_1, u_2$. The first random variable $(u_1)$ is used to compute the time between events while the second variable $(u_2)$ is to determine which event happens. Generally speaking, consider $k$ events, the closed interval $[0, 1]$ is further subdivided according the probability $q$ of each event, $[0, q_1], (q_1, q_1 + q_2], (q_1 + q_2, q_1 + q_2 + q_3] \dots (q_1 + q_2 + \dots + q_{k-1}, 1]$, where $q_i, i = 1, \dots, k$ sums up to 1. If $u_2$ falls in the $rth$ subinterval, then the $rth$ event happens. The event and rate of each event is described in the transition probability above.

Due to the Markov property, the time between events $T$ are independent and identically distributed with an exponential Probability density function given as

$$T = f(t) = \lambda e^{-\lambda t}, \quad t > 0$$

where $\lambda$ is the total sum of the rates of the events. The cumulative distribution function is given as

$$\begin{aligned} F(t) &= \int_0^t f(\omega) d\omega \\ &= \int_0^t \lambda e^{-\lambda t} d\omega \end{aligned}$$

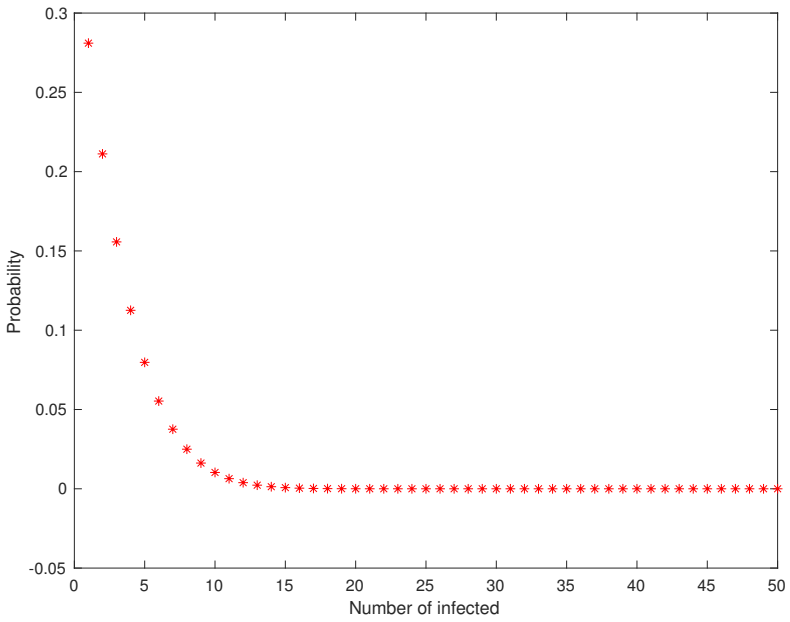


Figure 1.6: Quasistationary distribution of SIS stochastic epidemic model with $\beta = 1.6, \nu = 2$ and $N = 50$ .

$$= 1 - e^{-\lambda t}$$

let

$$u = 1 - e^{-\lambda t}$$
$$\implies t = -\frac{1}{\lambda} ln(1-u)$$
$$= -\frac{1}{\lambda} ln(u_1)$$

please observe that $1 - u = u_1$ have the same uniform distribution.

In words, we toss a coin and wait for the outcome, and depending on the value of the outcome, we then add one from the infected class and subtract one from the healthy class, or perform the reverse operation. We perform numerical simulations using Gillespie algorithm applied to the deterministic models (1.3.1), and the results are plotted in (Figure 1.9). Please note that the sample realisations of the stochastic SIS model fluctuate about the equilibrium trajectories of the deterministic SIS model.

## 1.5 Plan of the Thesis

After this introduction framing the reserach question and giving basics on the epidemiological models, I will now describe the content of this thesis. In chapter two, we extend the

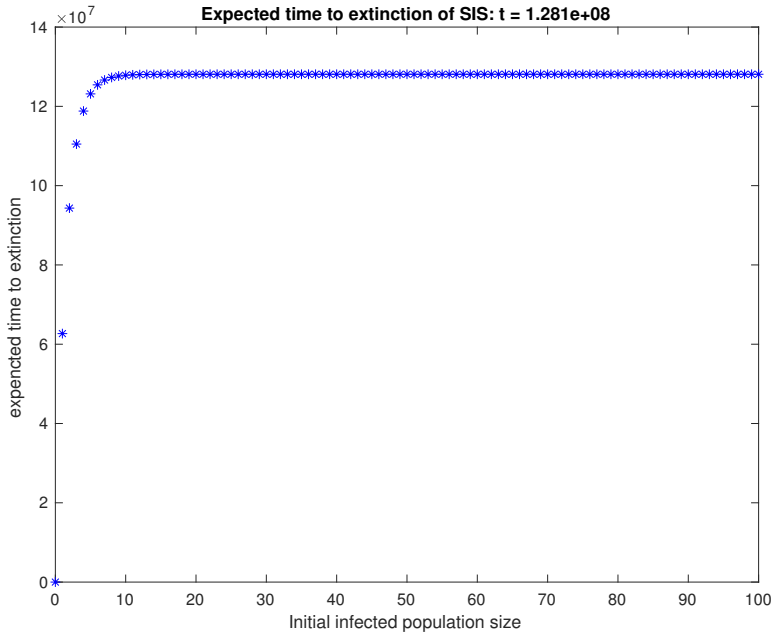


Figure 1.7: Expected time to extinction of the stochastic SIS model by using quasistationary distribution with $\beta = 2, \nu = 1$ and $N = 100$ .

SIS model by adding a quiescence phase. The extended model is call SIQS. Here, we want to understand the effect of quiescence/dormancy on the time to extinction and the effect of quiescence on the quasi-stationary distribution of the stochastic SIQS model. Therefore, we transform the deterministic model to include stochastic processes and we calculate the quasi-stationary solution of the process and obtain the time to extinction. We perform a comparative analysis between time to extinction of the SIS model and that of the SIQS model. In chapter 3, we build a multi strains model first without quiescence to understand the relationship between one host specie and two parasite species interactions since most parasite exists in multiple stains in a host population. The chapter makes a significant contribution towards understanding of the interactions in communities of living parasitic organisms, in which both competitive and trophic interactions are present at the same time. We later introduce a quiescence phase for one parasite type to the deterministic co-evolutionary model with two parasite types infecting one host type. We study analytically the local stability of the dynamical system. We develop a stochastic version of the model to study the influence of quiescence on stochasticity of the system dynamics. We compute the steady state distribution of the parasite types and obtained numerical solutions for the covariance matrix of the system under symmetric and asymmetric quiescence rates between parasite types. In chapter 4, we incorporate quiescence phase to a co-infection model (4.1.2) and end up with extended model (4.1.3) that captures the dynamics of the co-infections of two strains, one host type, in which one of the strains exhibits quiescence behaviour. The steady state solution is calculated and proceed to show that the endemic

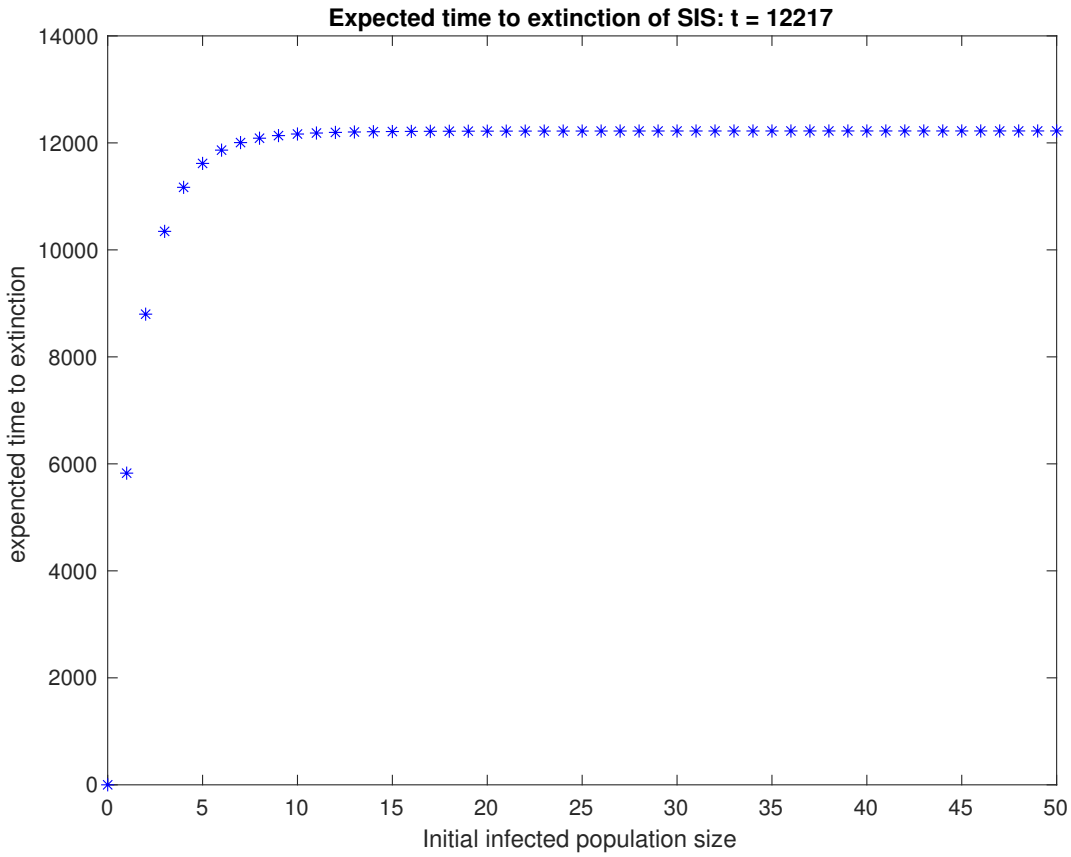


Figure 1.8: Expected time to extinction of the stochastic SIS model by using quasistationary distribution with $\beta = 2, \nu = 1$ and $N = 50$

equilibrium of the system is stable when $R_0 > 1$. We perform numerical computation using Gillespie's algorithm, and demonstrate that deterministic results and stochastic simulations are consistent. In such co-infection model, we observe a new behaviour, namely that quiescence affects the correlation between the presence and frequencies of the parasite strains. These results are important to show that quiescence has also an effect on interactions between parasite strains in a host population. We conclude this thesis in Chapter 5 by discussing the relevance of the research conducted for disease management, especially using data obtained for malaria infections in the Amazonian region of Brazil, where both *P. falciparum* and *P. vivax* are present.

## 1.6 Contributions

I have written all chapters. Chapter 2 is soon to be submitted to a peer-review journal. The model was developed by myself and Prof J. Müller. I have performed all analyses and

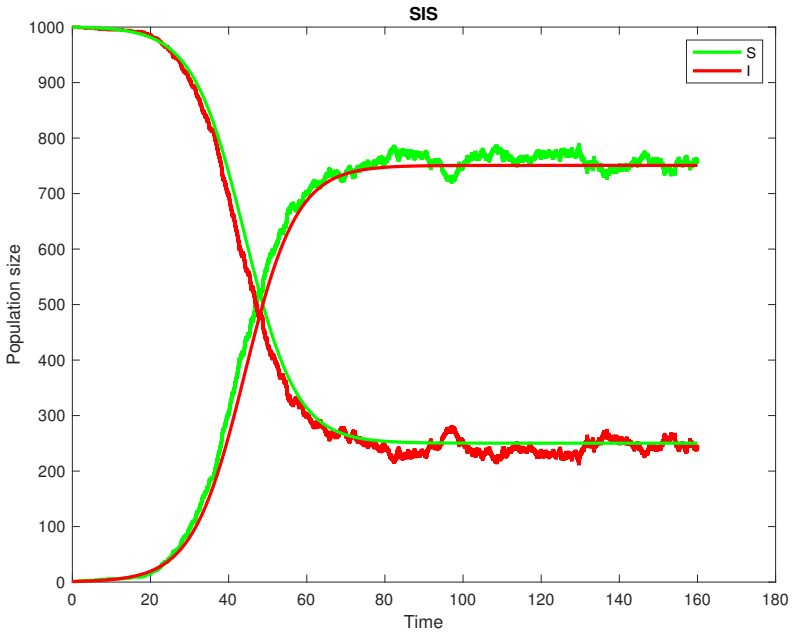


Figure 1.9: Numerical simulation of the deterministic SIS model compared with stochastic SIS simulation using Gillespie's algorithm; initial population size is $S = 1000$, $I = 1$. The parameters are $\beta = 0.2, \nu = 0.05$, the stochastic realisations fluctuate about the equilibrium of the deterministic trajectories.

simulations, and wrote the manuscript. For chapter 3, I have designed the model with Prof J. Müller, Dr S. John, and Prof A. Tellier, and I have performed all analyses and simulations myself. A large part of chapter 3 is published after peer-review in 2022 as Sanusi et al. Mathematics (MDPI2022) with URL: https://doi.org/10.3390/math10132289. The model of chapter 4 was conceived by myself, Prof A. Tellier and Dr E. Stadler. I have performed all analyses and simulations myself.

# Chapter 2

# Stochastic Time to Extinction of the SIQS Epidemic Models

## 2.1 Motivation

The aim of this research is to contribute towards the eradication and control of infectious diseases. However, as mentioned in Chapter 1, global eradication is hard to achieve. For example, while the eradication of polio was thought to be achieved, the virus started to come back into the population because of a decrease of vaccination coverage due to vaccine refusal and various societal issues. Note furthermore that while global eradication is hard to achieve, we do observe local extinction of diseases in real world data. In such cases, the disease re-appear later into the same population. We also observe that small populations of pathogens are always at high risk of becoming extinct. This type of dynamics is obviously not captured in the deterministic approach. It is therefore necessary to model the process by using stochastics, that is a birth and death process with a continuous time and discrete state-space. In (Figure 2.1), we observe the disease curve of dengue fever incidence in Thailand [30]. It shows that there are intermittent spikes of incidence with varying amplitudes. In between spikes, there are years with almost zero incidence, and the disease seem to re-appear later into the population. The same observation can be made from (Figure 2.2) for measles. On the other hand, another interesting feature of a disease epidemics, is that disease in small population is at high risk of becoming extinct.

## 2.2 Main goals

The main goals of this thesis chapter is to study the long term behaviour of the SIS model through studying its time to extinction and quasi-stationary distribution. We then incorporate a quiescence phase to the SIS model, so that the extended model is call SIQS, and we study the effect of quiescence on the time to extinction and the quasi-stationary

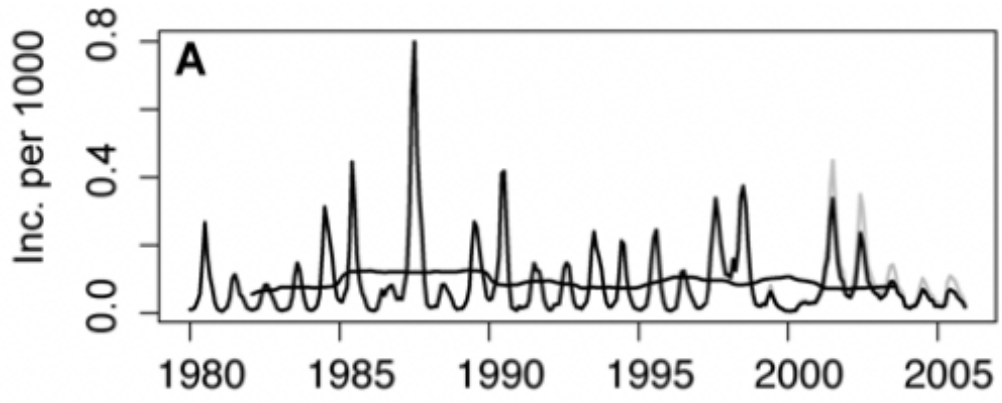


Figure 2.1: Extinction and re-introduction of Dengue incidence for Chaing Mai Province, Thailand; data was taken from [31]

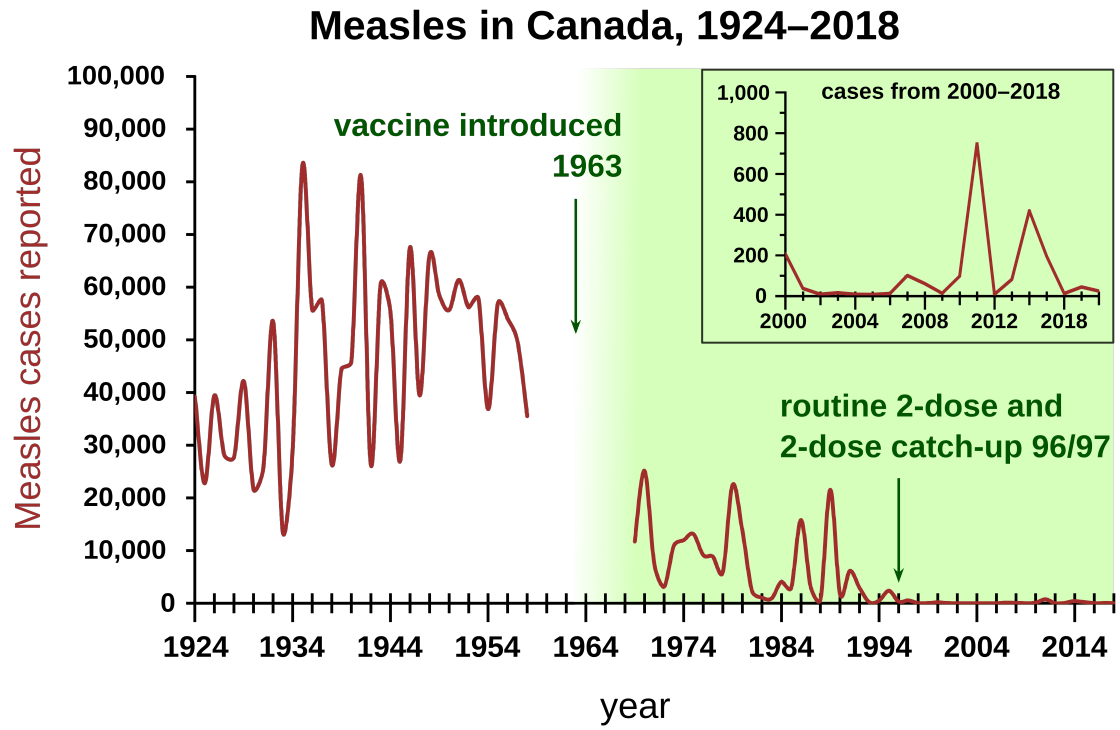


Figure 2.2: Number of cases of Measles in Canada from 1924-2018; Wikipedia; data was taken from [86]

distribution of the new SIQS model. We compare the shape of the SIS quasi-stationary distribution with that of the SIQS model to understand the influence of quiescence on the quasi-stationary distribution of SIS model [84]. It is well documented that the SIS quasi-stationary distribution has two shapes depending on the value of the basic reproduction number, $R_0$. When $R_0 < 1$, the quasi-stationary distribution decreases monotonically with

$\hat{p}_1^*$ being the maximal value, and the distribution is approximately normally distribution when $R_0 > 1$ [84, 82, 80]. We test if these predictions also hold in presence of quiescence in our SIQS model.

## Methods: the SIQS model

This section introduces the extended version of the SIS model that was described and analysed in [82, 113, 83]. In an SIS stochastic model, the disease free equilibrium is the zero state and an absorbing state. However, it is observed that just before the process reaches this equilibrium, the process first reaches an equilibrium (endemic, as the SIS model has two equilibrium solutions) that is different from the zeros state equilibrium. This equilibrium is called the quasi-stationary distribution, which was first studied in the late 1960s by Darroch [33]. The quasi-statinary distribution is obtained as the distribution conditioned on non-extinction of the continuous time Markov chain of the SIS stochastic model. This means that there is a condition on the distribution so that the stochastic process is yet to reach the disease free equilibrium [4].

We incorporate a quiescent stage to the standard SIS model, defining an SIQS model. The following system of ordinary differential equations (2.2.1) describes its dynamics. The name is derived from the dynamics of the population: at the beginning, the population is susceptible, then some individuals become infected, and amongst those, a portion of parasite enter the quiescence phase and can wake up later following a stochastic process, hence the name SIQS model.


Figure 2.3: Flow chart of the SIQS model

$$\begin{aligned} \frac{dS}{dt} &= -\beta\frac{SI}{N} + \nu I \\ \frac{dI}{dt} &= \beta\frac{SI}{N} - \rho I - \nu I + \zeta Q \\ \frac{dQ}{dt} &= \rho I - \zeta Q, \end{aligned} \tag{2.2.1}$$

where $Q$ is the number of individuals in quiescence stage, $\rho$ is the rate at which the infected individuals enter the quiescence stage and $\zeta$ is the rate at which the individuals in the

quiescence stage exit to become infected. The other parameters are as described in equation (1.3.1). We assume in the model that there is no birth nor death of hosts so that the total population is constant. The total population is divided into three mutually exclusive class, namely Susceptible, infected and Quiescence stage. Equation (2.2.1) describes the rate of change of individuals in each class.

let $N = S + I + Q$ then at the equilibrium, (2.2.1) has the following equilibrium solution

$$S^* = \frac{\nu}{\beta}N, \quad I^* = \frac{\zeta N(\beta - \nu)}{\beta(\zeta + \rho)}, \quad Q^* = \frac{\rho N(\beta - \nu)}{\beta(\zeta + \rho)}$$

## 2.3 Analytical results

### 2.3.1 Basic reproduction number

Next generation matrix

$$\mathcal{F} = \begin{bmatrix} \frac{\beta SI}{N} \\ 0 \end{bmatrix} \quad \text{and} \quad \mathcal{V} = \begin{bmatrix} (\rho + \nu)I - \zeta Q \\ -\rho I + \zeta Q \end{bmatrix}$$

let $(I, Q) = (x1, x2) = x$, then

$$\frac{dx}{dt} = \mathcal{F} - \mathcal{V} = \begin{bmatrix} \frac{\beta SI}{N} \\ 0 \end{bmatrix} - \begin{bmatrix} (\rho + \nu)I - \zeta Q \\ -\rho I + \zeta Q \end{bmatrix}$$

let

$$\mathrm{F} = \begin{bmatrix} \frac{\partial \mathcal{F}_1}{\partial x_1} & \frac{\partial \mathcal{F}_1}{\partial x_2} \\ \frac{\partial \mathcal{F}_2}{\partial x_1} & \frac{\partial \mathcal{F}_2}{\partial x_2} \end{bmatrix} = \begin{bmatrix} \beta & 0 \\ 0 & 0 \end{bmatrix}$$

$$\mathrm{V} = \begin{bmatrix} \frac{\partial \mathcal{V}_1}{\partial x_1} & \frac{\partial \mathcal{V}_1}{\partial x_2} \\ \frac{\partial \mathcal{V}_2}{\partial x_1} & \frac{\partial \mathcal{V}_2}{\partial x_2} \end{bmatrix} = \begin{bmatrix} \rho + \nu & -\zeta \\ -\rho & \zeta \end{bmatrix}$$

let

$$\kappa = \mathrm{F}\mathrm{V}^{-1} = \begin{bmatrix} \frac{\beta}{\nu} & \frac{\beta}{\nu} \\ 0 & 0 \end{bmatrix}$$

$$\therefore \quad \rho(\kappa) = \frac{\beta}{\nu}$$

### Transition Probabilities

Since our main goal is to study the time to extinction of the quasi-stationary distribution of the stochastic SIQS model, it is necessary to transform the deterministic model (2.2.1) into a stochastic process. In so doing, we have to first find the transition probabilities of each event. The following equations describe the probabilities of moving from one state to the other. Here, the states are infection, recovery, entering and exiting quiescence.

Table 2.1: Transitions rates for the model (2.2.1)

| Type | Transition | Rate |
|---|---|---|
| Infection of $S$ by $I$ | $(S_t, I_t, Q_t) \to (S_t - 1, I_t + 1, Q_t)$ | $\beta \frac{SI}{N} \Delta t + o\Delta(t)$ |
| Recovery $I$ & replacement with $S$ | $(S_t, I_t, Q_t) \to (S_t + 1, I_t - 1, Q_t)$ | $\nu I \Delta t + o\Delta(t)$ |
| Go quiescent $I$ & birth of $Q$ | $(S_t, I_t, Q_t) \to (S_t, I_t - 1, Q_t + 1))$ | $\rho I \Delta t + o\Delta(t)$ |
| Wake-up $Q$ & replacement with $I$ | $(S_t, I_t, Q_t) \to (S_t, I_t + 1, Q_t - 1))$ | $\zeta Q \Delta t + o\Delta(t)$ |

### 2.3.2 Master equation

The master equation otherwise known as the Kolmogorov equation, describes the deterministic evolution of the above transition probabilities. The master equation is also used to generate the generator matrix A. Because we are dealing with two dimensional system the generator matrix is rather complex.

let $S = N - I - Q$, then model (2.2.1) reduces two dimension and the master equation of the corresponding system can be written as follows

Let $p(i, j)(t) = \text{Prob}\{I = i, Q = j\}$, then

$$\begin{aligned}\frac{\mathrm{d}p_{(i,j)}}{\mathrm{d}t} =& \beta/N(N - i - j + 1)(i - 1)p_{(i-1,j)} + \nu(i + 1)p_{(i+1,j)} + \rho(i + 1)p_{(i+1,j-1)} \\ &+ \zeta(j + 1)p_{(i-1,j+1)} - [\beta/N(N - i - j)i + \nu i + \rho i + \zeta j]\, p_{(i,j,k)}.\end{aligned} \tag{2.3.1}$$

### 2.3.3 Quasi-stationary distribution of the SIQS model

$$\begin{aligned} b_i =& \frac{\beta}{N} i(N - i - j) \\ c_i =& \rho i \\ d_i =& \nu i \\ e_j =& \zeta j \end{aligned}$$

with this notation, then the above equation (2.3.1) can be rewritten in an increasing $i's$ as follows

$$\frac{\mathrm{d}p_{(i,j)}}{\mathrm{d}t} = b_{i-1}p_{(i-1,j)} - [b_i + c_i + d_i + e_j]p_{(i,j)} + c_{(i+1)}p_{(i+1,j-1)} + d_{(i+1)}p_{(i+1,j)} + e_{(j+1)}p_{(i-1,j+1)} \tag{2.3.2}$$

The above equation can be written more compactly as follows

$$\frac{dp_{(ji)}(t)}{dt} = \sum_l \sum_k b_{ji}^{lk} p_{(lk)} \quad \text{for} \quad i, j = 1, 2, \ldots N \tag{2.3.3}$$

Let

$$B = \sum_l \sum_k b_{ji}^{lk} \quad \text{for} \quad i, j = 1, 2, \ldots N \tag{2.3.4}$$

and defined

$$\tilde{B} = \sum_l \sum_k b_{ji}^{lk} \quad \text{for} \quad i, j = 2, \ldots N = B(2:N, 2:N) \tag{2.3.5}$$

Let $(X_t, Q_t)$ be random variables for the number of infected individuals and the individuals in quiescence stage respectively, then

$$p_{(ij)} = p_{(i,j)}(X_t = i, Q_t = j)$$

let also

$$\tilde{X}_t, \tilde{Q}_t = X_t, Q_t | (X_t, Q_t) \neq (0,0)$$
$$\tilde{p}_{(i,j)\neq(0,0)} = p_{(i,j)}(X_t = i, Q_t = j | (X_t, Q_t) \neq (0,0))$$

$$\frac{d\tilde{p_{(i,j)}}}{dt} = \frac{p_{(i,j)}(X_t = i, Q_t = j | (X_t, Q_t) \neq (0,0))}{p(X_t, Q_t \neq (0,0))}$$
$$= \frac{p_{(i,j)}(X_t = i, Q_t = j)}{1 - p(X_t = 0, Q_t = 0)} = \frac{p_{(ij)}}{1 - p_{(0,0)}}$$
$$\frac{d\tilde{p}_{(i,j)}}{dt} = \frac{d}{dt}\left(\frac{p_{(i,j)}}{1 - p_{(0,0)}}\right) = \frac{\dot{p}_{i,j}(t)}{1 - p_{(0,0)}} + \frac{p_{(i,j)}(t)}{(1 - p_{(0,0)})} \frac{\dot{p_{(0,0)}}}{(1 - p_{(0,0)})}$$

The equilibrium solution of the above equation known as quasi-stationary distribution is given as

$$\tilde{p}^*_{(i,j)}(t) = (\tilde{p}^*_{(1,1)}, \tilde{p}^*_{(1,2)}, \ldots, \tilde{p}^*_{(N,N)})^T$$
$$(\tilde{B} + d_1\tilde{p}_{(1,0)})\tilde{p}^*_{(i,j)} = 0$$
$$\tilde{B}\tilde{p}^*_{(i,j)} = -d_1\tilde{p}^*_{(1,0)}\tilde{p}^*_{(i,j)} \tag{2.3.6}$$

note that $p^*_{(i,j)}$ can not be solved explicitly from equation (2.3.6) .

## 2.4 Expected time to extinction

**Expected time to extinction**

**Theorem 1.** *The expected time to extinction is given by*

$$E(\textit{time to extinction}) = 1/d_1\tilde{p}^*_{(1,0)} = 1/\rho(\tilde{B})$$

*Proof.* Recall that

$$\frac{dp}{dt} = Bp, \qquad p_{(0,0)} = (0, \tilde{p}^*)$$

therefore,

$$\frac{d}{dt}p_{(0,0)} = d_1\tilde{p}^*_{(1,0)}$$

$$\frac{d}{dt}\tilde{p} = \tilde{B}\tilde{p}$$

since $\tilde{p}_{(0,0)} = \tilde{p}$ is an eigenvalue of $\tilde{B}$, we have $\tilde{p}(t) = e^{-d_1\tilde{p}^*_{(1,0)}t}\tilde{p}^*$.Thus,

$$\tilde{p}_{(0,0)}(t) = \int_0^\infty d_1(e^{-d_1\tilde{p}^*_{(1,0)}t}\tilde{p}^*_{(1,0)})dt = 1 - e^{-d_1\tilde{p}^*_{(1,0)}t}$$

$$E(\text{ time to extinction}) = \int_0^\infty t(-\frac{d}{dt}P(\text{ alive at time t})dt$$

$$= \int_0^\infty (1 - p_{(0,0)}(t))dt = \int_0^\infty e^{-d_1\tilde{p}_{(1,0)}t}dt = 1/d_1\tilde{p}^*_{(1,0)} = 1/\rho(\tilde{B})$$

□

**Theorem 2.** *The expected time to extinction increases linearly with the increase of the rate of entering quiescence phase, that is $\rho$.*

*Proof.* Matrix $B$ in equation (2.3.4) can be written as

$$B = A + \rho C$$

$$B(\epsilon) = A_0 + \epsilon C$$

let

$$X(\epsilon) : A(\epsilon)X(\epsilon) = \lambda(\epsilon)X(\epsilon)$$

and

$$Y(\epsilon) : A(\epsilon)Y(\epsilon) = \lambda(\epsilon)Y(\epsilon)$$

$$X(\epsilon) = X_0 + \epsilon X_1 + \dots$$

$$Y(\epsilon) = Y_0 + \epsilon Y_1 + \dots$$

$$\lambda(\epsilon) = \lambda_0 + \epsilon\lambda_1 + \dots$$

then

$$X(\epsilon)Y(\epsilon) = X_0Y_0 + \epsilon X_0Y_1 + \epsilon Y_0X_1 + o(\epsilon^2) = 1$$

$$B(\epsilon)X(\epsilon) = \lambda(\epsilon)X(\epsilon)$$

$$(B_0 + \epsilon B_1)(X_0 + \epsilon X_1) = (\lambda_0 + \epsilon\lambda_1)(X_0 + \epsilon X_1)$$

$$B_0X_0 = \lambda_0X_0$$

$$B_1X_0 + B_0X_1 = \lambda_1X_0 + \lambda_0X_1$$

$$Y_0B_1X_0 + Y_0B_0X_1 = \lambda_1Y_0X_0 + \lambda_0Y_0X_1$$

$$\lambda_1 = Y_0B_1X_0$$

$$(B_0 - \lambda_0I)X_1 = -B_1X_0 + (Y_0B_1X_0)X_0 = -(B_1 - Y_0B_1X_0I)X_0$$

$$Y_0(B_1 - Y_0B_1X_0I)X_0 = Y_0B_1X_0 - (Y_0B_1X_0)(Y_0IX_0) = Y_0B_1X_0 - Y_0B_1X_0 = 0.$$

This shows that $X_1$ has a solution.

$$(B_0 - \lambda_0I)X_1 = -(B_1 - Y_0B_1X_0I)X_0$$

$$\int_0^\infty e^{x(B_0-\lambda_0I)t}(B_0 - \lambda_0I)X_1dt = -\int_0^\infty e^{x(B_0-\lambda_0I)s}(B_1 - Y_0B_1X_0I)X_0ds$$

$$X_1 = -\int_0^\infty \bar{e}^T e^{x(B_0-\lambda_0I)s}(B_1 - Y_0B_1X_0I)X_0ds$$

we now need to show that the matrix is invertible

**Proposition 1.** *$C$ is an invertible matrix on positive complex plane $\implies$ $\int_0^\infty e^{-Cs}ds = C^{-1}$*

*Proof.* Assume that the eigenvectors of $C$ are $\bar{X_1}, \ldots, \bar{X_n}$ corresponding to the eigenvalues $\lambda_1, \ldots, \lambda_n \implies \int_0^\infty e^{-Cs}\bar{X_i}ds = \int_0^\infty e^{-\lambda_i s}\bar{X_i}ds = \frac{1}{\lambda}\bar{X_i} = C^{-1}\bar{X_i}$ □

□

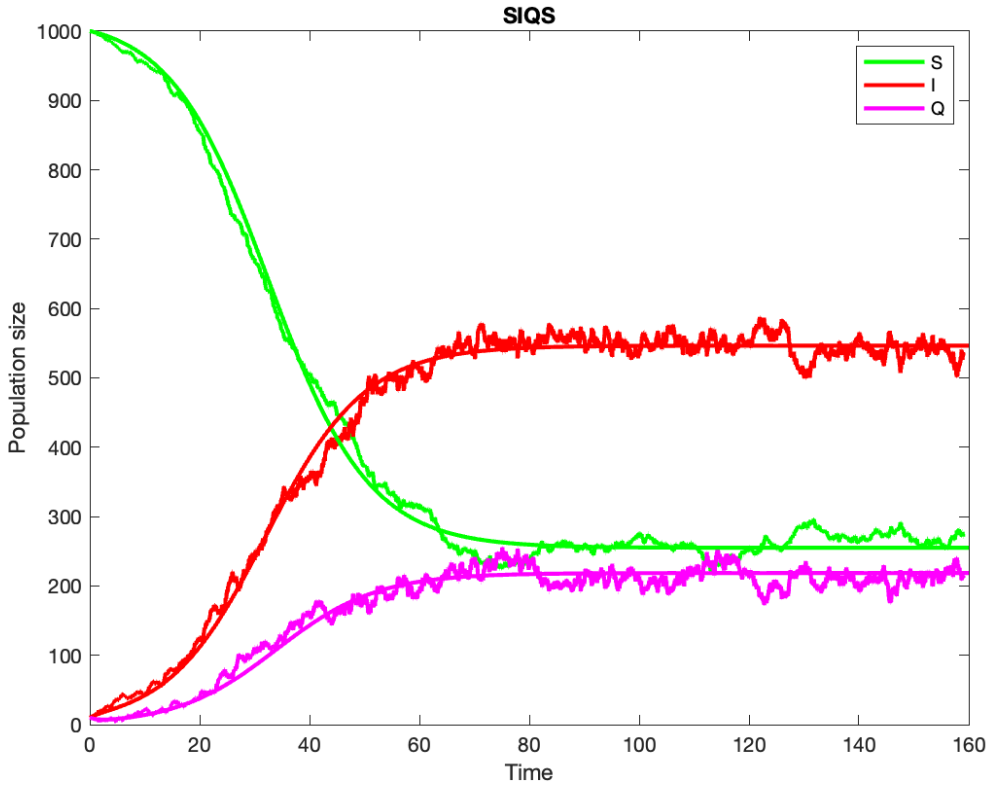


Figure 2.4: Numerical simulation of the deterministic SIQS model compared with stochastic SIQS simulation using Gillespie's algorithm; initial population size is $S = 1000$, $I = 1Q = 3$. The parameters are $\beta = 0.2, \nu = 0.05, \rho = 0.5, \zeta = 0.2$, the stochastic realisations fluctuate about the equilibrium of the deterministic trajectories.

## 2.5 Numerical results

We present here several stochastic simulations using the Gillespie's algorithm to provide some intuition and test the robustness of our analytical results.

We compute the time to extinction of both models (1.3.1 and 2.2.1) and find that the quiescence phase increases the time to extinction of the epidemics. This result is also confirmed by the simulations using Gillespie's algorithm. The results are shown in (Figure 2.6, 2.7 and 2.5). The time when the epidemic ends is much longer with the quiescence phase. We show that the time to extinction for SIS (1.3.1) is of an order of magnitude of four with the population size $N = 50$ and parameter $\beta = 2, \nu = 1$ (Figure 1.8) while the time to extinction for the SIQS model is of the order six with the population size $N = 50$ and parameter $\beta = 2, \nu = 1, \rho = 0.7, \zeta = 0.2$ (Figure 2.8). We also note that the shape of the quasi-stationary distribution exhibits a normal shape regardless of the value of $R_0$. This is to say that quiescence breaks one of the known shape of the quasi-

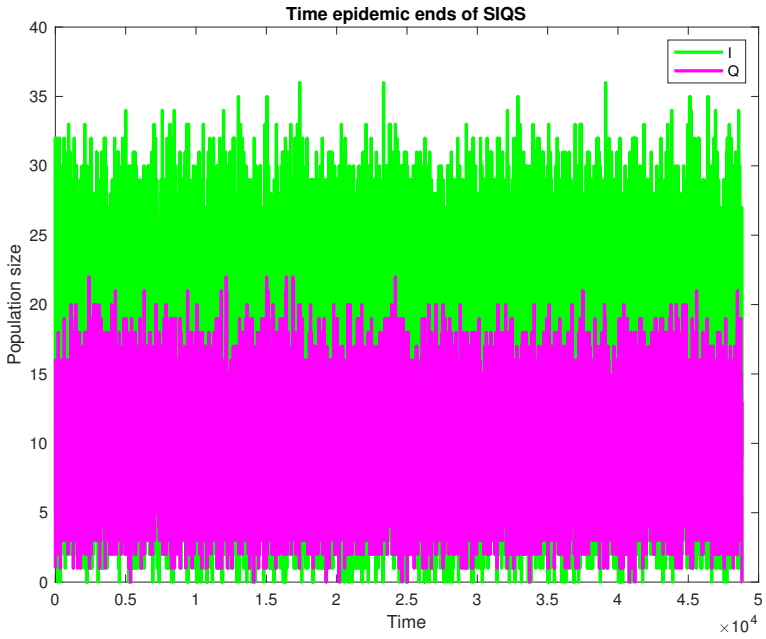


Figure 2.5: stochastic realisation of the stochastic SIQS model until both infected and quiescence individuals hit zero population size with total population $N = 50$ , $\beta = 2$ and $\nu = 1$ with the initial population size $I(0) = 5, Q(0) = 1$.

stationary state, namely the decreasing shape when $R_0 < 1$ (Figure 1.6). We also find analytically and by simulations, that the time to extinction increases linearly with the increase of the rate of entering quiescence ($\rho$) as seen in (Figures 2.9a) and (2.9b). Note that in (Figure 2.9a) the time to extinction is longer compared to (Figure 2.9b) because a larger proportion of individuals leave the quiescence phase in (Figure 2.9b) than in (Figure 2.9a). Furthermore, the time to extinction decays exponentially with the increase of the rate of exiting quiescence ($\zeta$) ( Figures 2.10a and 2.10b). Note that the time to extinction in (Figure 2.10a) decays faster than in (Figure 2.10b) because individuals enter the quiescence phase at higher proportion in (Figure 2.10b) than in (Figure 2.10a).

## 2.6 Conclusion

We extended the study of the time to extinction and the quasi-stationary solution of the stochastic SIS model which is a one dimensional structure to include quiescence phase which makes it a two dimensional structure. We approached the problem numerically where we came up with a block Infinitesimal generator matrix. We calculated the quasi-stationary solution of the stochastic SIQS model. Moreover, we learnt that quiescence affects one of the known shapes of the quasi-stationary distribution. Furthermore, the quiescence increases the time to extinction linearly with the increase of the rate of entering

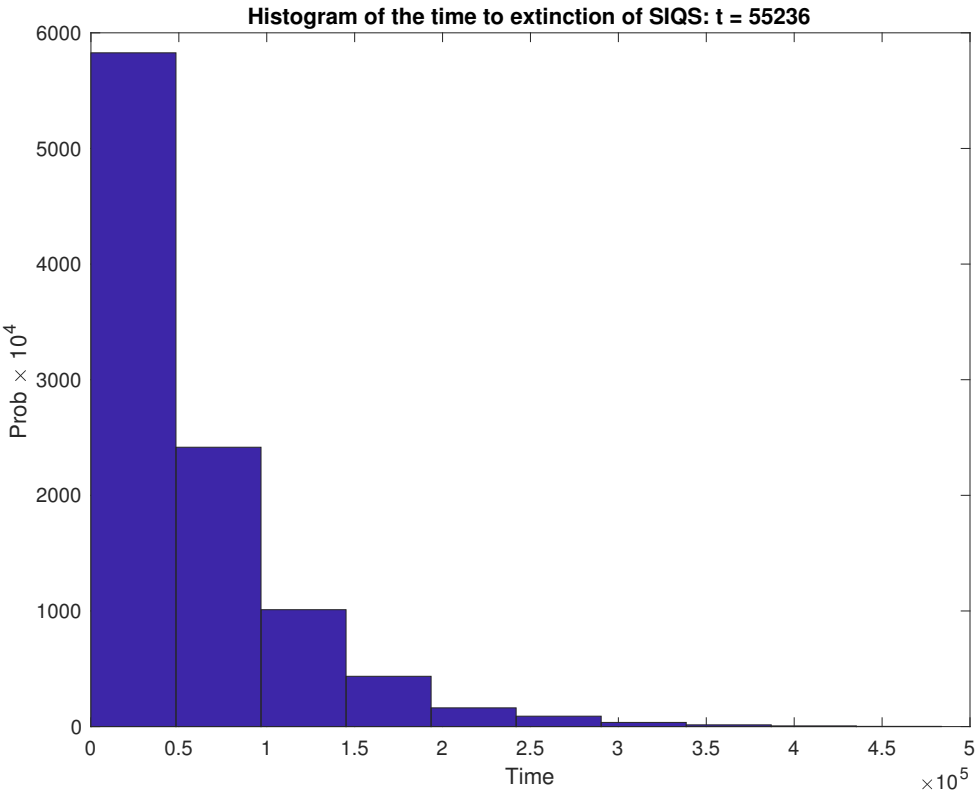


Figure 2.6: Histogram of the probability distribution of the time epidemic ends of the scholastic SIQS epidemic model generated from 1000 realisations/sample paths by using Gillespie's algorithm with $I(0) = 5, Q(0) = 1, N = 50, \beta = 2, \nu = 1, \rho = 0.7, \zeta = 0.2$, the mean of the distribution is 55236.

quiescence. We also learnt that the quiescence phase increases the time the pandemic ends. This is to say that quiescence is not only a bet-hedging strategy but makes the population of the parasite more stable in time and insensitive to the application of antibiotics.

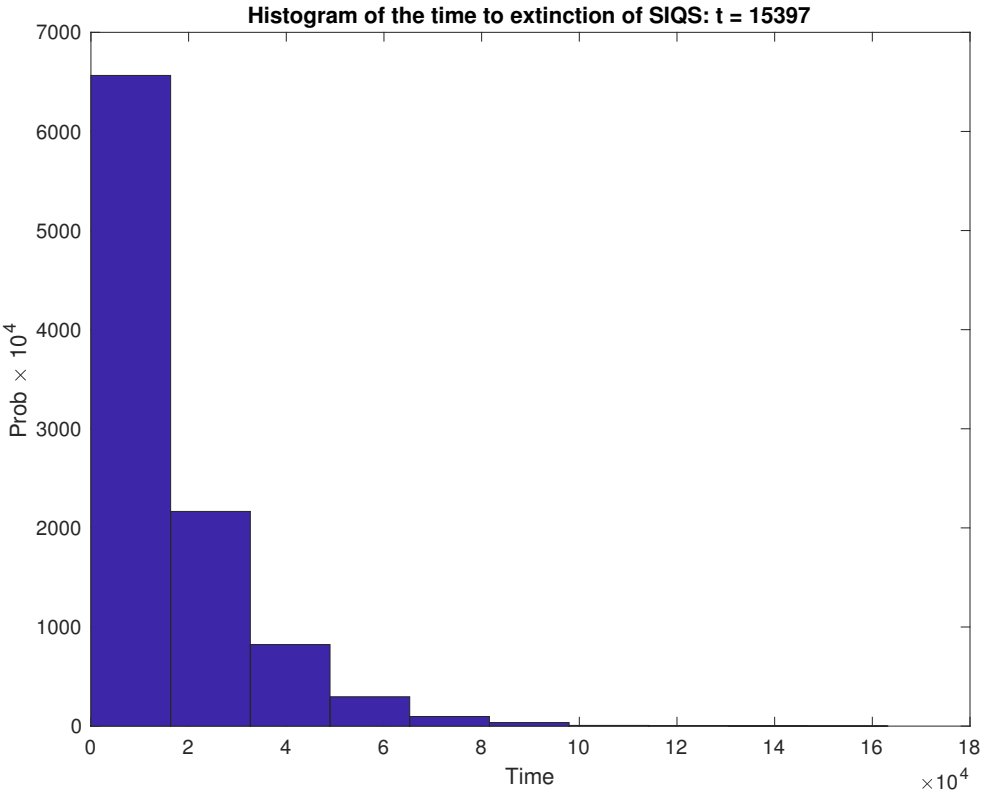


Figure 2.7: Histogram of the probability distribution of the time epidemic ends of the scholastic SIQS epidemic model generated from 1000 realisations/sample paths by using Gillespie's algorithm with $I(0) = 5, Q(0) = 1, N = 50, \beta = 2, \nu = 1, \rho = 0.2, \zeta = 0.7$, the mean of the distribution is 15397.

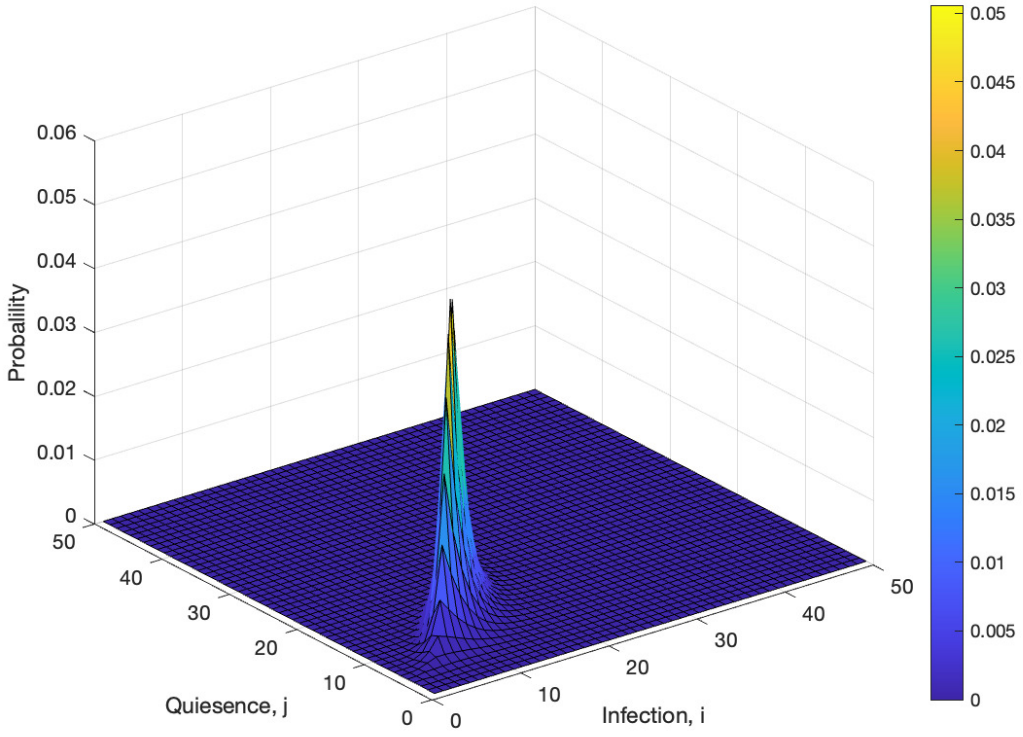


Figure 2.8: Bivariate quasi-stationary distribution of the SIQS model $N = 50, \beta = 2, \nu = 1, \rho = 0.7, \zeta = 0.2$, and the time to extinction is $7.5391e + 06$

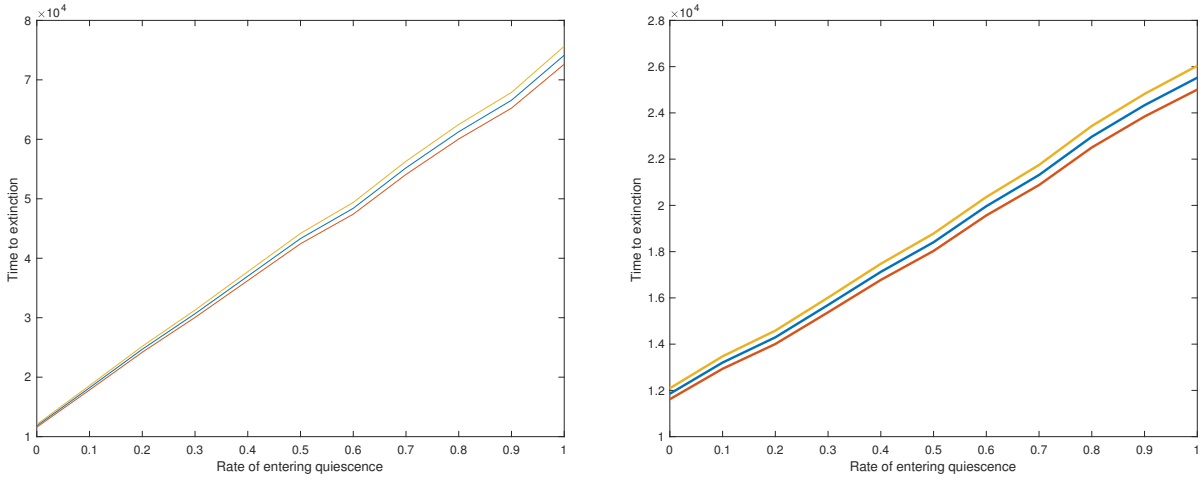


(a) (b)

Figure 2.9: **(a)** Confidence interval of the time epidemic ends as a function of $\rho$ of the scholastic SIQS epidemic model generated from 10000 realisations/sample paths by using Gillespie's algorithm with $I(0) = 5, Q(0) = 1, N = 50, \beta = 2, \nu = 1, \zeta = 0.7$. **(b)** Confidence interval of the time epidemic ends as a function of $\rho$ of the scholastic SIQS epidemic model generated from 10000 realisations/sample paths by using Gillespie's algorithm with $I(0) = 5, Q(0) = 1, N = 50, \beta = 2, \nu = 1, \zeta = 0.9$.

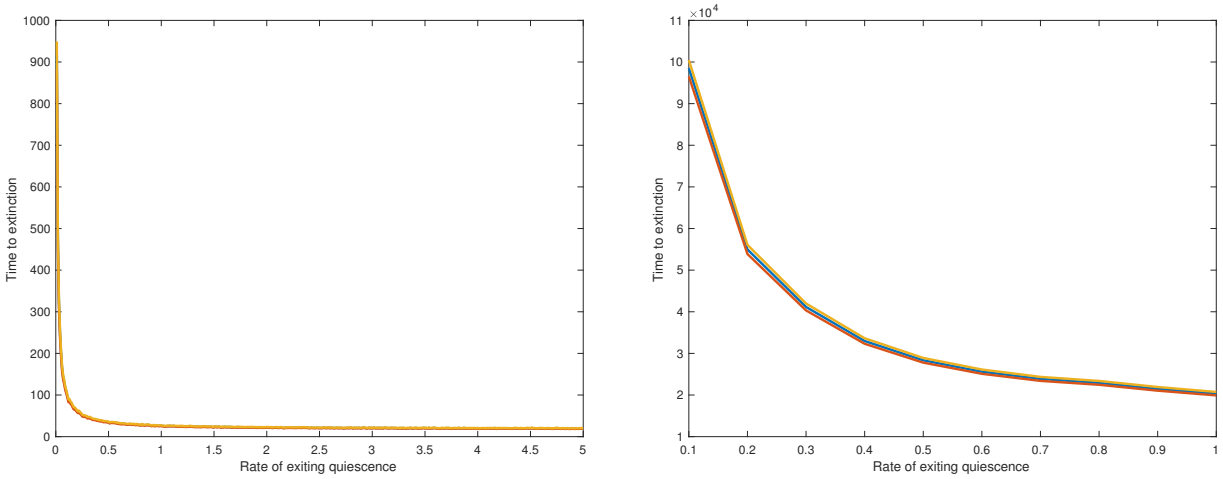


(a) (b)

Figure 2.10: **(a)** Confidence interval of the time epidemic ends as a function of $\zeta$ of the scholastic SIQS epidemic model generated from 1000 realisations/sample paths by using Gillespie's algorithm with $I(0) = 5, Q(0) = 1, N = 50, \beta = 0.2, \nu = 0.1, \rho = 0.4$. **( b)** Confidence interval of the time epidemic ends as a function of $\zeta$ of the scholastic SIQS epidemic model generated from 10000 realisations/sample paths by using Gillespie's algorithm with $I(0) = 5, Q(0) = 1, N = 50, \beta = 0.2, \nu = 0.1, \rho = 0.7$.

# Chapter 3

# Impact of Pathogen Quiescence on the Stochastic Model

## 3.1 Introduction

Dormancy or quiescence is a bet-hedging strategy common to many bacteria, fungi [76, 70], invertebrates [81], and plants which evolves to dampen off the effect of bad conditions and maximize the reproductive output under good conditions [98, 116, 19]. This bet-hedging in time occurs when the individual (bacteria, fungus, invertebrates) or the offspring of the individual (plants, invertebrates) enter dormancy with a low metabolic state for some period of time during which reproduction and evolution occurs in the active part of the population. The dormant individuals constitutes a reservoir, the so-called seed banks, and can re-enter the active population at a later time point. Dormancy (quiescence) evolves a bet-hedging strategy in response to unpredictable environments such as random variations of the abiotic conditions [52], competition under density-dependence regulation of the population [20], contact between a bacteria host and viruses [17], frequency- or density-dependent selection due to host-parasite coevolution [46] or prey-predator interactions.

Parasite quiescence is a strategy of microparasites (bacteria, fungi) becoming inactive inside an infected host for some period of time. During this period, the disease does not progress in the host and the host can express symptoms or be asymptomatic. Importantly, quiescent parasites do not contribute to the disease transmission. In the medical community, the infections in which the parasite is quiescent or inactive are referred to as silent or dormant, and in the virology literature they are referred to as covert [102]. Parasite quiescence has well known but yet under-appreciated consequences for disease management. During quiescence, the parasite are often resistant to the application of drugs, antibiotics or fungicides [27, 28, 122, 121]. Furthermore, applying antibiotics can trigger the switching of bacteria from active to the inactive (quiescent) state. *Plasmodium falciparum*, the main agent of malaria, has the ability to lurk in the hepatocytes of some patients, re-

maining inactive but being resistance to drug treatments, causing later on disease relapse [29, 121, 46]. *P. vivax*, another malarial agent, exhibits also the ability to become dormant in the liver of a host for some weeks, months even up to a year or more, which makes the task to eradicate the disease difficult [118, 105, 26]. Therefore, it is important to determine the 1) conditions for the evolution of parasite quiescence, and 2) influence of quiescence on the sustainability of parasite populations. A key theoretical study on the evolution of quiescence in animal parasites [102] shows that silent/covert infection is not likely to be the optimal strategy (trait value) for the parasite (so called Evolutionary Stable Strategy (ESS)) in an epidemiological model with one host and one parasite genotype. Parasite quiescence would only evolve if there were substantial fluctuations in the host population size or seasonal variations in transmission rates. Therefore, the authors state that their models predict low rates of covert infection, which does not reflect the consistent high levels that are found in some host parasite systems. Based on a modelling framework with fixed population sizes but two hosts and two parasite types, the host population can evolve dormancy as an optimal strategy (ESS) as a result of the parasite pressure and coevolutionary dynamics [116]. While more theoretical work is needed to decipher the conditions for the evolution of parasite quiescence/dormancy, likely involving a combination of temporally variable environmental and coevolutionary pressures, we focus in the present study on the consequence of quiescence for the stability and outcome of host parasite coevolutionary dynamics. As a first step in this direction, we consider here a model with one host and two parasite strains (or types).

Indeed, one host population under pressure by several parasite strains, or even several parasite species, is the rule rather than the exception [14, 115]. Considering the epidemiological dynamics under competition/co-infection between strains is important [52] to predict the evolution of parasite virulence, that is disease induced death rate of host [112]. We are interested here in understanding the epidemiological dynamics of a single host type infected by one of the two parasite strains exhibiting quiescence. We ask whether quiescence affects the parameters for which two strains can co-exist or competitively exclude one another. Furthermore, the maintenance of several strains, the persistence of disease as endemic or the persistence of the host population are affected by stochastic processes. Disease epidemics are subjected to stochasticity at various levels, the main one being in the transmission rate, and thus stochastic approaches are required to predict the outcome of epidemics. While the deterministic model of epidemiology successfully captures the behaviour when the size of host and parasite populations are large, stochasticity can affect the outcome of the dynamics for small sizes significantly [63, 11, 4, 7]. Quiescence affects the size of the parasite active population and thus possibly the epidemiological dynamics. We hereby hypothesize that quiescence may also affects the outcome of stochasticity on the co-existence of our two parasite strains epidemiological model.

In the first part we describe our epidemiological model with changes in the number of healthy and infected host individuals over time under quiescence of both parasite strains. We then derive a stability condition for the dynamical ODE system. In the second part of the study, we introduce stochasticity in disease transmission and derive a Fokker-Planck

equation of the Continuous Time Markov Chain model. Lastly, we perform some numerical study on the model behaviour under stochasticity. We show that for symmetric case i.e when the infected class are identical and quiescence phases are also identical, quiescence increases the variance, and decrease it when the rate of infection is small. For asymmetric case, that is when the infected class as well as the quiescence phases are not identical, quiescence has a major effect in reducing the intensity of the noise in the stochastic process, whenever the rate of entering (or exiting) quiescence differ between strains. By analogy, we term this phenomenon as moving average.

## 3.2 Deterministic model with quiescence

### 3.2.1 Model description

Our model is similar in essence to classic epidemiological models [49, 60, 52, 100, 10, 42]. Here we consider one host population and two parasite strains, thus the population is divided into five mutually exclusive compartments: one healthy susceptible host compartment $H$, two infected host, $I_1$ and $I_2$, infected by parasite of type 1 and 2 respectively, and two quiescence compartments $Q_1$ and $Q_2$, comprise the infected individuals $I_1$ and $I_2$ for which the parasite is in the quiescent state. We define the following system of ordinary differential equations describing the rate of change of the number of individuals in each compartment.

$$\begin{aligned}
\frac{dI_1}{dt} &= \beta_1 H I_1 - \rho_1 I_1 - dI_1 - \gamma_1 I_1 - \nu_1 I_1 + \zeta_1 Q_1 + \epsilon_1 \\
\frac{dI_2}{dt} &= \beta_2 H I_2 - \rho_2 I_2 - dI_2 - \gamma_2 I_2 - \nu_2 I_2 + \zeta_2 Q_2 + \epsilon_2 \\
\frac{dH}{dt} &= \Lambda - \beta_1 H I_1 - \beta_2 H I_2 - dH + \nu_1 I_1 + \nu_2 I_2 \\
\frac{dQ_1}{dt} &= \rho_1 I_1 - \zeta_1 Q_1 - dQ_1 \\
\frac{dQ_2}{dt} &= \rho_2 I_2 - \zeta_2 Q_2 - dQ_2
\end{aligned} \tag{3.2.1}$$

where $\Lambda$ is the constant birth rate of healthy host and $d$ to is the natural death rate, $\gamma_1$ and $\gamma_2$ are the disease induced death rate or (virulence) caused by parasite 1, and 2 respectively. Similarly all other parasite specific parameters such as disease transmission rate $\beta$, recovery rate $\nu$, rate at which parasite switches to quiescence $\rho$ and the switching back rate $\zeta$ are defined for each parasite strains separately. The parameters $\epsilon_1$ and $\epsilon_2$ are the rates of incoming migration of parasite 1 and 2 respectively from an outside compartment/population. These parameters are introduced to avoid the competitive exclusion principle, namely without the $\epsilon$'s, one parasite type necessarily excludes the other and there is no coexistence of both parasite types at the epidemic equilibrium, the same effect is expected if the migration of quiescent parasite would occur (not shown here). We assume 1) that the parasite lives and multiplies within its host, 2) the absence of multiple infection so that

strains 1 and 2 of the parasite are mutually exclusive on one host, and 3) no latency period for the parasite, hence, the infected persons are infectious immediately after infection. Note that the model reduces to a simple model of one susceptible host and two infected host types ($SI_1I_2S$, referred to as system without quiescence) when setting the quiescence parameters equal to zero (Appendix C). In the present study we are particularly interested in following the number of hosts infected by parasite 1 or 2 and to study conditions for which both types of parasites are maintained. We therefore assume constant birth rate, to ensure a non-explosive process when moving to the stochastic version of our model. We finally introduce the parameters $\epsilon_1$ and $\epsilon_2$ to promote the coexistence of both strains at the equilibrium and to guarantee a unique steady state solution in the continuous time Markov chain version of the model (see below, Stochastic model)

### 3.2.2 Steady state solutions

In this section we find the equilibrium solutions of the system. First, we analyse the system without inflow of new infection to the population ($\epsilon_1 = \epsilon_2 = 0$). This simple system generically has the three equilibrium states: 1) a disease free equilibrium in which both parasite strains die off and are removed from the system (yielding $I_1 = I_2 = Q_1 = Q_2 = 0$), 2) two-boundary equilibria at which a single parasite strain survive *i.e.* competitive exclusion when parameters of the model are non-symmetric (yielding in either $I_1 = Q_1 = 0$ or $I_2 = Q_2 = 0$). In the non-generic case that we have symmetric parameters, we have line of stationary solutions. By evaluating the Jacobian matrix of the system, one can evaluate the stability conditions for these equilibria. To ensure the existence of unique polymorphic equilibrium, we introduce two parameters for invasion/immigration rates namely, $\epsilon_1$ and $\epsilon_2$ which are greater than zero. The introduction of these two parameters results in moving the disease free as well as one of the boundary equilibria to the negative cone *i.e.* makes them to have negative values which is biologically meaningless. We are thereafter left with only one polymorphic equilibrium which is biologically meaningful. Henceforth, we focus on the analysis of the polymorphic equilibrium for which both parasite strains are maintained in the system. We show the existence and uniqueness of this endemic equilibrium under mild conditions (for more details, see Appendix A).

### 3.2.3 Stability analysis

An $n \times n$ Jacobian matrix $P$ is said to be stable, and thus an equilibrium being locally stable, if all its eigenvalues lie on the left half plane. As it may be impractical to determine the stability of a matrix analytically [49], by using the Lyapunov theorem to determine if the system is stable, it is easier to apply the Routh-Hurwitz criterion [49, 80, 66]. However, this criteria can be cumbersome if the matrix is of high dimension. In this section we therefore derive the stability condition for a generic $5 \times 5$ matrix $G$ with parasite quiescence by reducing our system to $3 \times 3$ which is more easily amenable to computation.

The Jacobian of system in equation (3.2.1) evaluated at equilibrium is given as follows

$$G = \begin{pmatrix} \beta_1 H^* - \rho_1 - \gamma_1 - \nu_1 - d & 0 & \beta_1 I_1^* & \zeta_1 & 0 \\ 0 & \beta_2 H^* - \rho_2 - \gamma_2 - \nu_2 - d & \beta_2 I_2^* & 0 & \zeta_2 \\ -\beta_1 H^* + \nu_1 & -\beta_2 H^* + \nu_2 & -\beta_1 I_1^* - \beta_2 I_2^* - d & 0 & 0 \\ \rho_1 & 0 & 0 & -\zeta_1 - d & 0 \\ 0 & \rho_2 & 0 & 0 & -\zeta_2 - d \end{pmatrix}.$$

Now we define a matrix

$$A \in ((a_{i,j})) \in \mathbb{R}^{3\times 3} \tag{3.2.2}$$

to be the Jacobian matrix evaluated at equilibrium of the system without quiescent described in appendix C. We introduce $B = G + dI$, such that the spectrum of $B$ is just the shifted spectrum of $G$. Indeed, the stability of $B$ implies stability of $G$.
Let

$$B = \begin{pmatrix} a_{11} - \rho_1 & a_{12} & a_{13} & \zeta_1 & 0 \\ a_{21} & a_{22} - \rho_2 & a_{23} & 0 & \zeta_2 \\ a_{31} & a_{32} & a_{33} & 0 & 0 \\ \rho_1 & 0 & 0 & -\zeta_1 & 0 \\ 0 & \rho_2 & 0 & 0 & -\zeta_2 \end{pmatrix}. \tag{3.2.3}$$

**Definition 3.2.1.** *Let $3 \times 3$ matrix $A$ be a Jacobian matrix of system without quiescence phase and we also define*

$$\begin{aligned} a_1 &= -tr(A) = -a_{11} - a_{22} - a_{33}, \\ a_2 &= a_{11}a_{22} + a_{11}a_{33} + a_{22}a_{33} - a_{23}a_{32} - a_{12}a_{21} - a_{13}a_{31}, \\ a_3 &= -det(A). \end{aligned} \tag{3.2.4}$$

*The matrix $A$ in 3.2.2 is stable if and only if*

$$tr(A) < 0, \quad det\ (A) < 0 \quad and \quad a_2 > 0. \tag{3.2.5}$$

The above proposition 1 is simply a reformulation of the Routh-Hurwitz criteria (see details in [49, 80, 66]). We now find a criteria for stability of $B$ under the following proposition.

**Proposition 2.** *The following three statements are equivalent for the matrix $B$ above:*

*Statement 1:*

*The matrix $B$ in 3.2.3 is stable for all $\rho_1, \rho_2, \zeta_1, \zeta_2 > 0$.*

*Statement 2 :*

$b_1 > 0, \quad b_2 > 0, \quad b_3 > 0, \quad b_4 > 0, \quad b_5 > 0, \quad b_1 b_2 b_3 > b_3^2 + b_1^2 b_4,$

$(b_1 b_4 - b_5)(b_1 b_2 b_3 - b_3^2 - b_1^2 b_4) > b_5(b_1 b_2 - b_3)^2 + b_1 b_5^2 \quad for\ all \quad \rho_1, \rho_2, \zeta_1, \zeta_2 > 0.$

*Statement 3:*

$det(A) < 0, \quad tr(A) \leq 0, \quad a_2 > 0, \quad a_{11} \leq 0, \quad a_{22} \leq 0, a_{33} \leq 0, \quad a_{13}a_{31} \leq a_{11}a_{33},$

$a_{23}a_{32} \leq a_{22}a_{33}.$

The above statements are technically equivalent in the sense that for the system in (3.2.1) to be stable it must satisfy the given statements. We prove that *statement 1* implies *statement 2*, *statement 2* implies *statement 3* and *statement 3* implies *statement 1*. This proposition is a generalisation of the theorem in [49] and we use the same method as in [49] (see Appendix B for the proof of the proposition 2 above, as we prove the stability of a generic matrix $B$ as defined in 3.2.3). The conditions in *statement 3* of the above proposition can be used to prove that the endemic equilibrium of (3.2.1) is locally asymptotically stable. Which means that if the system undergoes a perturbation (the system is set not too far away from its equilibrium) then the system eventually reaches its equilibrium. The local stability is not as strong as global stability, the latter meaning that the system returns to it equilibrium after whatever perturbation (without restriction). Note that we see the effect of local stability of the equilibrium solutions in the stochastic simulations using Gillespie's algorithm, as the realisations (sample paths) remain within the domain of attraction of the deterministic endemic equilibrium (Figures 3.2a and 3.2b).

As mentioned, the *statement 2* may sometimes be hard to apply, thus as an alternative, one can use *statement 3* to show that (3.2.1) is locally asymptotically stable. This is relatively easy as the dimension of the system is now reduced to $3 \times 3$, so that it is possible to compute the Jacobian matrix of the system without quiescence (A.3.1) described in Appendix C to obtain the matrix A in (3.2.2). Then one can test the conditions described in *statement 3* above. Once those conditions are satisfied then the larger system (3.2.1) is also locally asymptotically stable.

## 3.3 Stochastic Analysis

### 3.3.1 Transition probabilities

This section defines a stochastic version to the deterministic model as described in equation (3.2.1) of section 3.2.1. We add stochasticity occurring at any of the possible transition of individuals between classes (birth and death). The transition probabilities of jumping from one state (e.g. infected quiescent) to the another state (e.g. infected) are defined bellow. We choose $\Delta t$ very small so that during this time interval only one event occurs. The proportion of healthy population is $H$, the proportion of infected by parasite 1 population is $I_1$, the proportion of infected by parasite 2 population is $I_2$, the proportion of population in quiescence compartment infected by parasite 1 is $Q_1$ and the proportion of population in quiescence compartment infected by parasite 2 is $Q_2$. The possible changes are either $H+1, H-1, I_1+1, I_1-1, I_2+1, I_2-1, Q_1+1, Q_1-1, Q_2+1, Q_2-1$ or no change at all. Therefore, our stochastic process is a birth and death process. The one step transition probabilities are given in table 3.1:

Table 3.1: Transitions rates for the quiescence model 1.

| Type | Transition | Rate |
|---|---|---|
| Birth of healthy host $H$ | $(H_t, I_{1t}, I_{2t}, Q_{1t}, Q_{2t}) \to (H_t + 1, I_{1t}, I_{2t}, Q_{1t}, Q_{2t})$ | $\Lambda\Delta t + o\Delta(t)$ |
| Natural death of $H$ | $(H_t, I_{1t}, I_{2t}, Q_{1t}, Q_{2t}) \to (H_t - 1, I_{1t}, I_{2t}, Q_{1t}, Q_{2t})$ | $dH\Delta t + o\Delta(t)$ |
| Infection of $H$ by $I_1$ | $(H_t, I_{1t}, I_{2t}, Q_{1t}, Q_{2t}) \to (H_t - 1, I_{1t} + 1, I_{2t}, Q_{1t}, Q_{2t})$ | $\beta_1 H I_1 \Delta t + o\Delta(t)$ |
| Infection of $H$ by $I_2$ | $(H_t, I_{1t}, I_{2t}, Q_{1t}, Q_{2t}) \to (H_t - 1, I_{1t}, I_{2t} + 1, Q_{1t}, Q_{2t})$ | $\beta_2 H I_2 \Delta t + o\Delta(t)$ |
| Death of $I_1$ | $(H_t, I_{1t}, I_{2t}, Q_{1t}, Q_{2t}) \to (H_t, I_{1t} - 1, I_{2t}, Q_{1t}, Q_{2t})$ | $(d + \gamma_1) I_1 \Delta t + o\Delta(t)$ |
| Death of $I_2$ | $(H_t, I_{1t}, I_{2t}, Q_{1t}, Q_{2t}) \to (H_t, I_{1t}, I_{2t} - 1, Q_{1t}, Q_{2t})$ | $(d + \gamma_1) I_2 \Delta t + o\Delta(t)$ |
| Recovery $I_1$ & replacement with $H$ | $(H_t, I_{1t}, I_{2t}, Q_{1t}, Q_{2t}) \to (H_t + 1, I_{1t} - 1, I_{2t}, Q_{1t}, Q_{2t})$ | $\nu_1 I_1 \Delta t + o\Delta(t)$ |
| Recovery $I_2$ & replacement with $H$ | $(H_t, I_{1t}, I_{2t}, Q_{1t}, Q_{2t}) \to (H_t + 1, I_{1t}1, I_{2t} - 1, Q_{1t}, Q_{2t})$ | $\nu_2 I_2 \Delta t + o\Delta(t)$ |
| Immigration to $I_1$ | $(H_t, I_{1t}, I_{2t}, Q_{1t}, Q_{2t}) \to (H_t, I_{1t} + 1, I_{2t}, Q_{1t}, Q_{2t})$ | $\epsilon_1 \Delta t + o\Delta(t)$ |
| Immigration to $I_2$ | $(H_t, I_{1t}, I_{2t}, Q_{1t}, Q_{2t}) \to (H_t, I_{1t}, I_{2t} + 1, Q_{1t}, Q_{2t})$ | $\epsilon_2 \Delta t + o\Delta(t)$ |
| Go quiescent $I_1$ & birth of $Q_1$ | $(H_t, I_{1t}, I_{2t}, Q_{1t}, Q_{2t}) \to (H_t, I_{1t} - 1, I_{2t}, Q_{1t} + 1, Q_{2t})$ | $\rho_1 I_1 \Delta t + o\Delta(t)$ |
| Go quiescent $I_1$ & birth of $Q_1$ | $(H_t, I_{1t}, I_{2t}, Q_{1t}, Q_{2t}) \to (H_t, I_{1t}, I_{2t} - 1, Q_{1t}, Q_{2t} + 1)$ | $\rho_2 I_2 \Delta t + o\Delta(t)$ |
| Wake-up $Q_1$ & replacement with $I_1$ | $(H_t, I_{1t}, I_{2t}, Q_{1t}, Q_{2t}) \to (H_t, I_{1t} + 1, I_{2t}, Q_{1t} - 1, Q_{2t})$ | $\zeta_1 Q_1 \Delta t + o\Delta(t)$ |
| Wake-up $Q_2$ & replacement with $I_2$ | $(H_t, I_{1t}, I_{2t}, Q_{1t}, Q_{2t}) \to (H_t, I_{1t}, I_{2t} + 1, Q_{1t}, Q_{2t} - 1)$ | $\zeta_2 Q_2 \Delta t + o\Delta(t)$ |
| Natural death of $Q_1$ | $(H_t, I_{1t}, I_{2t}, Q_{1t}, Q_{2t}) \to (H_t, I_{1t}, I_{2t}, Q_{1t} - 1, Q_{2t})$ | $dQ_1 \Delta t + o\Delta(t)$ |
| Natural death of $Q_2$ | $(H_t, I_{1t}, I_{2t}, Q_{1t}, Q_{2t}) \to (H_t, I_{1t}, I_{2t}, Q_{1t}, Q_{2t} - 1)$ | $dQ_2 \Delta t + o\Delta(t)$ |

### 3.3.2 Stochastic simulations

In order to test the validity of our assumptions to analyse the stochastic system, we used Gillespie's algorithm [37, 38, 6] to generate stochastic realisations/sample paths of the birth and death processes (Figures 3.2a and 3.2b). In (Figures 3.2a and 3.2b), the stochastic trajectories fluctuate around the deterministic equilibrium as predicted by equation (3.2.1). Please note that in (Figure 3.2a) there are only three curves in the deterministic trajectories while there are five in the stochastic realisation. This is to due the fact that we chose symmetric parameter values of the model, so $I_1 = I_2$ and $Q_1 = Q_2$ in the deterministic setting, but not in the stochastic version.

### 3.3.3 Master equation

The forward Kolmogorov differential equation also known as Master Equation, describes the rate of change of these probabilities is given in table 3.1. The master equation describes the evolution of the disease individuals at the early times of the infection. To understand the long term dynamics, we need to derive its corresponding Fokker-Planck equation.
Let $p(i, j, k, l, m)(t) = \text{Prob}\{H(t) = i, I_1(t) = j, I_2(t) = k, Q_1(t) = l, Q_2(t) = m\}$, then

$$
\begin{aligned}
\frac{\mathrm{d}p_{(i,j,k,l,m)}}{\mathrm{d}t} =& \Lambda p_{(i-1,j,k,l,m)} + d(i+1)p_{(i+1,j,k,l,m)} + \beta_1(i+1)(j-1)p_{(i+1,j-1,k,l,m)} \\
&+ (d+\gamma_1)(j+1)p_{(i,j+1,k,l,m)} + \beta_2(i+1)(k-1)p_{(i+1,j,k-1,l,m)} \\
&+ (d+\gamma_2)(k+1)p_{(i,j,k+1,l,m)} + \nu_1(j+1)p_{(i-1,j+1,k,l,m)} + \nu_2(k+1)p_{(i-1,j,k+1,l,m)} \\
&+ \epsilon_1 p_{(i,j-1,k,l,m)} + \epsilon_2 p_{(i,j,k-1,l,m)} + \rho_1(j+1)p_{(i,j+1,k,l-1,m)} + \rho_2(k+1)p_{(i,j,k+1,l,m-1)} \\
&+ \zeta_1(l+1)p_{(i,j-1,k,l+1,m)} + \zeta_2(m+1)p_{(i,j,k-1,l,m+1)} \\
&+ d(l+1)p_{(i,j,k,l+1,m)} + d(m+1)p_{(i,j,k,l,m+1)} \\
&- \Big[\Lambda + di + \beta_1 ij + (d+\gamma_1)j + \beta_2 ik + (d+\gamma_2)k + \nu_1 j + \nu_2 k \\
&+ \epsilon_1 + \epsilon_2 + \rho_1 j + \rho_2 k + \zeta_1 l + \zeta_2 m + dl + dm\Big] p_{(i,j,k,l,m)}
\end{aligned}
\tag{3.3.1}
$$

This master equation (3.3.1) is then used to work out *Kramers-Moyal expansion* that led to the derivation of the *Fokker-Planck equation* below.

### 3.3.4 Fokker-Planck equation of the model

To understand the long term dynamics of the master equation (3.3.1), we need to derive the corresponding Fokker-Planck equation. The Fokker-Planck equation describes further the rate of change of transitions probabilities described in table 3.1. We can also find the long term distribution of variables.

Now, let

$$
p(i,j,k,l,m) = \int_{ih-\frac{h}{2}}^{ih+\frac{h}{2}} \int_{jh-\frac{h}{2}}^{jh+\frac{h}{2}} \int_{kh-\frac{h}{2}}^{kh+\frac{h}{2}} \int_{lh-\frac{h}{2}}^{lh+\frac{h}{2}} \int_{mh-\frac{h}{2}}^{mh+\frac{h}{2}} u(x_1,x_2,x_3,x_4,x_5)dx_1dx_2dx_3dx_4dx_5 + o(h^6),
$$

let also $x_1 = ih, x_2 = jh, x_3 = kh, x_4 = lh, x_5 = mh$ and $h = \frac{1}{N}$. We then performed *Kramers-*

*Moyal expansion* to derived the following Fokker-Planck equation which is given as follows.

$$\begin{aligned}
\partial_t u(x_1,\ldots,x_5,t) = & -\partial_{x_1}\{h\lambda - dx_1 - \beta_1 x_1 x_2 - \beta_2 x_1 x_3 + \nu_1 x_2 + \nu_2 x_3\}u(x_1,\ldots,x_5,t) \\
& -\partial_{x_2}\{\beta_1 x_1 x_2 - (d+\gamma_1)x_2 - \nu_1 x_2 - \rho_1 x_2 + \zeta_1 x_4 + \epsilon_1\}u(x_1,\ldots,x_5,t) \\
& -\partial_{x_3}\{\beta_2 x_1 x_3 - (d+\gamma_2)x_2 - \nu_2 x_2 - \rho_2 x_3 + \zeta_2 x_5 + \epsilon_2\}u(x_1,\ldots,x_5,t) \\
& -\partial_{x_4}\{\rho_1 x_2 - \zeta_1 x_4 - dx_4\}u(x_1,\ldots,x_5,t) \\
& -\partial_{x_5}\{\rho_2 x_3 - \zeta_2 x_5 - dx_5\}u(x_1,\ldots,x_5,t) \\
& +\frac{h}{2}\partial_{x_1x_1}\{h\lambda + dx_1 + \beta_1 x_1 x_2 + \beta_2 x_1 x_3 + \nu_1 x_2 + \nu_2 x_3\}u(x_1,\ldots,x_5,t) \\
& +\frac{h}{2}\partial_{x_2x_2}\{\beta_1 x_1 x_2 + (d+\gamma_1)x_2 + \nu_1 x_2 + \rho_1 x_2 + h\epsilon_1\}u(x_1,\ldots,x_5,t) \\
& +\frac{h}{2}\partial_{x_3x_3}\{\beta_2 x_1 x_3 + (d+\gamma_2)x_3 + \nu_2 x_3 + \rho_2 x_3 + h\epsilon_2\}u(x_1,\ldots,x_5,t) \\
& +\frac{h}{2}\partial_{x_4x_4}\{\rho_1 x_2 + \zeta_1 x_4 + dx_4\}u(x_1,\ldots,x_5,t) \\
& +\frac{h}{2}\partial_{x_5x_5}\{\rho_2 x_3 + \zeta_2 x_5 + dx_5\}u(x_1,\ldots,x_5,t) \\
& -h\partial_{x_1x_2}\{\beta_1 x_1 x_2 + \nu_1 x_2\}u(x_1,\ldots,x_5,t) \\
& -h\partial_{x_1x_3}\{\beta_2 x_1 x_3 + \nu_1 x_3\}u(x_1,\ldots,x_5,t) \\
& -h\partial_{x_2x_4}\{\rho_1 x_2 + \zeta_1 x_4\}u(x_1,\ldots,x_5,t) \\
& -h\partial_{x_3x_5}\{\rho_2 x_3 + \zeta_2 x_5\}u(x_1,\ldots,x_5,t)
\end{aligned} \tag{3.3.2}$$

### 3.3.5 Linear Transformation of the Fokker-Planck equation

In order to solve the above Fokker-Planck equation (3.3.2), we use the so-called asymptotic method (see for example [67]). The principle is to transform the multivariate Fokker-Planck equation to a linear Fokker-Planck equation which is linearised around the stationary state of the deterministic system (3.2.1). The solution of the linear Fokker-Planck is found to be normally distributed, the solution is given in the following two theorems (see chapter 8 of [114]). We numerically checked this results using our stochastic simulations and the comparison is shown in (Figure 3.3).

**Theorem 1.** *The linear multivariate Fokker-Planck of (3.3.2) can be written as follows*

$$\frac{\partial P(y,t)}{dt} = -\sum_{ij}^{5} M_{ij}\frac{\partial}{\partial y_i}y_i P(y,t) + \frac{1}{2}\sum_{ij}^{5} N_{ij}\frac{\partial^2}{\partial y_i \partial y_j}P(y,t) \tag{3.3.3}$$

*where* $y = (y_1,\ldots,y_5)$, $N_{ij}$ *is symmetric and positive definite, its solution is given as*

$$P(y,t) = (2\pi)^{\frac{1}{2}} det(\Sigma)^{\frac{1}{2}} exp(-\frac{1}{2}y\Sigma^{-1}y^T)$$

*with*

$$\Sigma^{-1} = 2\int_0^\infty e^{-Mt} N e^{-Mt} dt.$$

The matrices $N$ and $M$ are defined explicitly in Appendix D.

**Theorem 2.** *For every matrix $N$ which is symmetric and positive-definite, there a unique solution $\Sigma^{-1}$ to the following equation known as Lyapunov equation*

$$M\Sigma^{-1} + \Sigma^{-1}M^T = N$$

*where $\Sigma^{-1}$ is symmetric, positive-definite and equal to*

$$\Sigma^{-1} = \int_0^\infty e^{-Mt} N e^{-M^T t} dt.$$

Theorem 2 which known as Lyapunov equation [54] allows us to compute the covariance matrix as found in the normal distribution shown in theorem 1 fairly easily, this is due to the fact that matrices $A$ and $B$ are constant matrices, the only unknown is the $\Sigma^{-1}$ matrix. The covariance matrix is of dimension 5 and tells us the degree at which each compartments namely healthy, infected by strain 1 and 2 and quiescence class 1 and 2 go together *i.e.* the relationship between each class. We use MATLAB to perform numerical calculations for the analytical solutions of the covariance matrix $\Sigma^{-1}$ .

We also computed 10,000 independent stochastic realisations using Gillespie's algorithm. The probability histogram was plotted in (Figure 3.3) for the number of infected individuals by strain 1. This distribution is then compared with the probability density function of the normal distribution with mean and variance obtained from both Gilliespie's algorithm and the normal approximation method using linear multivariate Fokker-Planck equation (3.3.2). The results are consistent which further validates our analytical result obtained using linear Fokker-Planck.

## 3.4 Covariance matrix

In order to understand the effect of quiescence in our stochastic model, we need to compare the system with quiescence to that of the system without quiescence in terms of the number of infected by both parasites. To do the comparative study we need to collapse the covariance matrix for both models with and without quiescence so that we only have 2 covariance matrix of the infected individuals. For the model with quiescence, this is done by adding the number of individuals in the infected class and the number of individuals in the quiescence stage to obtain a total number of infected individuals (irrespective of their quiescence status). For the system without quiescence, it is straight forward, it is achieved by isolating the number of individuals in the infected compartment. This step is justified below, and the following results indicate how to compute the covariance matrix [61, 109]. The obtained covariance matrix is denoted as the collapsed covariance matrix.
Let $\mathbf{Y} \sim \mathbf{N}_r(\mu, \Sigma)$ be r-variate multivariate normal distribution with mean $\mu$ and variance $\Sigma$, where

$$\mathbf{Y} = \begin{bmatrix} Y_1 \\ Y_2 \\ \vdots \\ Y_r \end{bmatrix} \qquad \mu = \begin{bmatrix} \mu_1 \\ \mu_2 \\ \vdots \\ \mu_r \end{bmatrix} \qquad \Sigma = \begin{bmatrix} \sigma_{1,1} & \sigma_{1,2} & \cdots & \sigma_{1,r} \\ \sigma_{2,1} & \sigma_{2,2} & \cdots & \sigma_{2,r} \\ \vdots & \vdots & \ddots & \vdots \\ \sigma_{r,1} & \sigma_{m,2} & \cdots & \sigma_{r,r} \end{bmatrix}$$

Any q linear combination of the $Y_i$, say $\mathbf{A'Y}$, is (q-variate) multivariate normal. Let

$$\mathbf{A'Y} = \begin{bmatrix} a_{11}Y_1 + a_{12}Y_2 + \cdots + a_{1r}Y_r \\ \\ a_{21}Y_1 + a_{22}Y_2 + \cdots + a_{2r}Y_r \\ \\ \cdots + \cdots + \cdots + \ldots \\ \\ a_{q1}Y_1 + a_{q2}Y_2 + \cdots + a_{qr}Y_r \end{bmatrix},$$

then

$$\mathbf{A'Y} \sim N_q(\mathbf{A'}\mu, \mathbf{A'}\Sigma\mathbf{A}). \tag{3.4.1}$$

Numerical examples of the collapsed covariance matrix are shown for various parameter combinations. The collapsed covariance matrix of the model with quiescence is denoted as $E_q$ and the collapsed covariance matrix of the model without quiescence as $E_{wq}$. In an effort to understand the effect of quiescence on the stochastic process, we consider two different cases of parameter combinations: symmetric where the parameter values of stain 1 and 2 are exactly the same (examples 1, 2, and 3), and non-symmetric where the parameter values of stain 1 and 2 are different (for example $\rho_1 \neq \rho_2$, examples 4, 5, 6 and 7).

**Example 1** We fix the following parameter values: $\beta_1 = \beta_2 = 0.005, d = 0.5, \Lambda = 1000, \nu_1 = \nu_2 = 0.3, \rho_1 = \rho_2 = 0.7, \gamma_1 = \gamma_2 = 0.003, \zeta_1 = \zeta_2 = 0.1, \epsilon_1 = \epsilon_2 = 0.6$ and the initial population sizes are $H = 50,000$, $I_1 = 10,000, I_2 = 10,000, Q_1 = 5,000, Q_2 = 5,000, \text{time} = 300$. We obtain the following collapsed covariance matrices:

$$E_{q1} = \begin{pmatrix} 683,640 & -682,500 \\ -682,500 & 683,640 \end{pmatrix}, \qquad E_{wq1} = \begin{pmatrix} 298,630 & -297,560 \\ -297,560 & 298,630 \end{pmatrix}.$$

**Example 2** We use the same parameter values as in example 1 only with a lower quiescence rate $\rho_1 = \rho_2 = 0.4$

$$E_{q2} = \begin{pmatrix} 655,170 & -654,060 \\ -654,060 & 655,170 \end{pmatrix}, \qquad E_{wq2} = E_{wq1}$$

We show in example 1 that the model with quiescence exhibits a larger variance compared with the model without quiescence. When comparing example 1 and 2, we observe the effect of quiescence on reducing the variance of the number of infected individuals. When the rate of entering quiescence stage ($\rho$) decreases, the variance of the number of infected individuals decreases ($E_{q1}$ versus $E_{q2}$).

**Example 3** The parameter and initial values are identical to example 1 except that the disease transmission rates are now 10 times lower $\beta_1 = \beta_2 = 0.0005$:

$$E_{q3} = \begin{pmatrix} 14.81 & -0.0388 \\ -0.0388 & 14.81 \end{pmatrix}, \qquad E_{wq3} = \begin{pmatrix} 27,651 & -26,443 \\ -26,443 & 27,651 \end{pmatrix}.$$

In example 3, we observe the effect of decreasing the transmission rate in reducing the variance and covariance of the collapsed covariance matrix. In contrast to example 1, in example 3, we find that the model with quiescence has less variance compared to the model without quiescence.

We describe the effect of quiescence on variance by comparing example 1 and 3. In contrast to the absence of quiescence, quiescence generates two effects under low transmission rate: 1) a decrease of the number of infections, and 2) a decrease in the probability of extinction (in a small population stochasticity is important). Based on our simulations, it is indeed more likely for the parasite to go extinct in example 3 than in example 1. Therefore, both effects of quiescence in example 3 concur to reduce the variance compared to the absence of quiescence. In example 1, the population size of each parasite is high enough to be well approximated by a mean-field ODE, quiescence increases the number of infections and quiescence events produce additional randomness and simply inflate the variance (compared to the absence of quiescence).

**Example 4** We use the same parameter values as in example 1 only with asymmetric rates of quiescence $\rho_1 = 0.3, \rho_2 = 0.5$

$$E_{q4} = \begin{pmatrix} 2,251.9 & -57.42 \\ -57.42 & 64.35 \end{pmatrix}, \qquad E_{wq4} = E_{wq1}$$

Now that we use asymmetrical rates of entering quiescence between the two strains in example 4, the variance are much decreased compared to examples 1 and 2. This further reduction in variance occurs because of the competition amongst the two parasite types in the model with quiescence (which was absent because of symmetrical rates in examples 1-3). In other words, because the two parasite strains have different quiescence rates, there is also competition between them to infect host individuals. Furthermore, the strain with the largest rate of entering the quiescence stage ($\rho$) exhibits a smaller variance than the strain with a lower quiescent rate. By analogy, we call this phenomenon as moving average behaviour (see discussion).

**Example 5** We use the same parameter values as in example 1 only with asymmetric rates of entering $\rho_1 = 0.8, \rho_2 = 0.4$ and exiting $\zeta_1 = 0.4, \zeta_2 = 0.8$ quiescence.

$$E_{q5} = \begin{pmatrix} 19.17 & -15.07 \\ -15.07 & 2187.1 \end{pmatrix}, \qquad E_{wq5} = E_{wq1}.$$

In example 5, we investigate the influence of asymmetric rates of entering and exiting the quiescent stage on the variance in infected individuals. We set the rate of entering quiescence of strain 1 to be larger than rate of strain 2, while the rate of exiting quiescence of strain 1 is smaller than that of strain 2. We still observe the so-called moving average effect, that is, the strain with the largest rate of entering the quiescence has the smaller variance. This example shows that entering quiescence has significant effect in changing the dynamics of the system.

**Example 6** We use the same parameter values as in example 1 only with asymmetric rates of entering $\rho_1 = 0.8, \rho_2 = 0.4$ and exiting $\zeta_1 = 0.8, \zeta_2 = 0.4$ quiescence.

$$E_{q6} = \begin{pmatrix} 164.04 & -151.92 \\ -151.92 & 2332.6 \end{pmatrix}, \qquad E_{wq6} = E_{wq1}.$$

In example 6, we take the rate of entering and exiting quiescence to be the same for each strain,that is, $\rho_1 = 0.8 = \zeta_1 = 0.8, \rho_2 = 0.4 = \zeta_2 = 0.4$, to ascertain if the moving average is determined by the rate of entering quiescence or the longest quiescence time. This example confirms that the moving average is determined by the rate of entering quiescence. We note by this example that rate of exiting quiescence stage doesn't effect the dynamic significantly as far as the moving average is concern.

**Example 7** In example 7, we increase the disease transmission rates and decrease the birth and death rate (compared to example 1), while we assume asymmetric rates of entering quiescence (as in example 5) but symmetric rates of exiting quiescence as well as the immigration rate. The following values are used $\beta_1 = \beta_2 = 0.05, d = 0.4, \Lambda = 100, \nu_1 = 0.03, \nu_2 = 0.3, \rho_1 = 0.8, \rho_2 = 0.4, \gamma_1 = \gamma_2 = 0.03, \zeta_1 = \zeta_2 = 0.1, \epsilon_1 = \epsilon_2 = 0.6$ and the initial population sizes are as in example 1. We obtain the following collapsed covariance matrices:

$$E_{q6} = \begin{pmatrix} 967.63 & -927.22 \\ -927.22 & 1151.1 \end{pmatrix}, \qquad E_{wq6} = \begin{pmatrix} 245.56 & -3.6384 \\ -3.6384 & 5.8915 \end{pmatrix}.$$

From examples 7, here we use asymmetric values of parameters in both models, we see the influence of quiescence in reducing the variance of the collapsed covariance matrix whenever one of the rates of entering quiescence is high. In addition, we also see the effect of strain competition in the model without quiescence in reducing the variance of the number of infected individuals. In the model with quiescence we take the recovery rate of infected individuals by strain 1 to be 10 times smaller than those infected by strain 2, and observe our moving average effect.

As additional verification, we draw contour plots of the joint density of infected individuals by strain 1 and 2 in (Figure 3.4a) and (Figure 3.4b) which compare the variance in the number of infected individuals by both strains. We confirm that the joint distribution of the number of infected individuals by parasite strain 1 and 2 have a smaller surface area, that is with less variance, under the model with quiescence than the absence of quiescence. In all examples, the values of the covariance (off-diagonal elements) are negative, and we observe this effect also in the contours (Figures 3.4a, 3.4b) because the number of infected individuals by parasite 1 and 2 are negatively correlated. This negative correlation is a result of the competition between the parasite types. We finally analyse the change in variance (Figure 3.5a) and covariance (Figure 3.5b) of the collapsed covariance matrix as a function of $\rho_1$ and $\rho_2$ (rates of entering quiescence). The effect of the transmission rates $\beta_1$ and $\beta_2$ is here again visible: when $\beta_1 = \beta_2$ are low, high rates of entering quiescence depletes the infected compartments so that the number of infected drops down and the infection decreases, which in turn reduces the variance. When $\beta_1 = \beta_2$ are high, there are enough infected to keep the infection spreading despite the rate of quiescence, hence the increases in the variance (under a fixed values of $\zeta_1$ and $\zeta_2$ (Figures 3.5a,3.5b). The behaviour of the covariance is reversed as the infected classes are negatively correlated. Based on the examples above, increasing $\zeta_1$ and $\zeta_2$ would results in decreasing the difference between the variance (as well as for the covariance) for the different transmission rates $\beta_1$ and $\beta_2$.

## 3.5 Discussion

In this study we aim to understand the effect of quiescence on the spread of infectious disease and with competition between parasite strains. Our study shows that introducing the pathogens ability to switch between an active and inactive (quiescence) phase can significantly impact the stochasticity in the system. In our system, when the invasion/immigration rates are turned off, one of the parasite type becomes extinct. However, when the invasion/immigration rates are turned on, coexistence of host and both parasite types is possible. If both strains show equal rates of infection, transmission and quiescence, there is no real competition and the system behaves as if only one parasite would be present. On other hand, when the parasite types have different characteristics, there is competition between them which generates various epidemiological dynamics.

Our collapsed covariance measure quantifies the infection load at the steady state of the system with and without quiescence. We measure this infection load for various parameter combinations of interest to understand the impact of quiescence on the stochastic process. Under symmetric quiescence rates and high transmission rates, quiescence increases the variance in infected individuals, while the quiescence reduces the variance in infected when transmission rates are low. When considering asymmetry in quiescence rates between parasite strains, we uncover a special phenomenon which we call by analogy to the moving average behaviour. Namely, the strain with the high rate of entering quiescence serves as moving average for the whole parasite population and buffers the effect of the second less quiescent strain. In other words, the strain with the higher quiescence determines the intensity of the noise in the stochastic infection process determining the variance of the number of infected individuals (lower variance under low disease transmission, higher variance under high disease transmission). Moving average is a well known concept in sound, signal, and image processing. In sound processing for example, moving average also known as low pass filter, filters the frequencies so that only low frequencies can be heard. The sound of noisy wave or distorted signal, is being smoothens by applying a moving average processing function because it assumes the areas of high frequencies as noise. We are not aware of the use of moving average in the field of disease epidemiology, and hence introduce it here as a consequence of quiescence in parasite. When different strains of parasite do show different quiescent rates, the competition between them under a stochastic epidemiological process reduces the number of infected individuals, as well as the virulence of the disease (number of host death). We theoretically predict that under competition between parasite types, the strain with the lower rate of entering quiescence gets fixed, however, if coexistence can be maintained by influx of parasite strains from outside, quiescence has the beneficial effect to reduce the stochasticity of the system. An extension for our work is to investigate if quiescence itself can evolve in such epidemiological setup as a bet-hedging strategy reducing stochasticity in transmission rates.

Due to the difficulty in the existing methods to analyse the stability of $5 \times 5$ matrix, we developed here a criterion for the study of stability of the system with quiescence for the deterministic system. Proposition 2 is important because it reduces the dimension of the system from 5 to 3. It is well known that studying the stability of the system with higher dimension is hard, often times impossible. While system with low dimension is easy and straight forward to study its stability. Thus the reduction in proposition 2 is of significant importance that removes the difficulties of analysing matrix with high dimension.

We then extended our model to a stochastic version. We show that the analytic solution of the linear Fokker-Planck equation is normally distributed with mean around the equilibrium solution. We confirm this results by computing 10,000 independent stochastic realisations using Gillespie's algorithm (Figure 3.3). The probability histogram was plotted at a time equals to 300 generations. This distribution is then compared with the probability density function of the normal distribution with mean and variance as obtained from both Gilliespie's algorithm and the normal approximation method using linear multivariate Fokker-Planck equation (3.3.2). The results are consistent which further validates our analytical result obtained using the linear Fokker-Planck equation.

As revealed by a wealth of recent studies on plant or animal, microbiomes are composed of multiple species and multiple strains per species. The composition of species and/or strains is governed by antagonistic, mutualistic or neutral inter- and intra-specific interactions along with stochastic processes such as birth and death, extinction-recolonization and migration of strains/species [see [11, 34]]. We speculate that our results on quiescence should be affecting the dynamics in these multi-species systems. Moreover, many microbe, especially human parasites, enter quiescence stage as a mechanism of resistance against antibiotics [13]. This has important consequences for the management of infectious diseases. Furthermore, host bacteria can also enter quiescence upon contact with viruses [17], which can lead to changes in the expected population dynamics of the bacterial and virus populations [21]. It is therefore of paramount importance to understand the influence of the quiescence on the population of hosts and parasites, especially as coevolution between antagonistic species can drive the evolution of quiescence/dormancy [46].

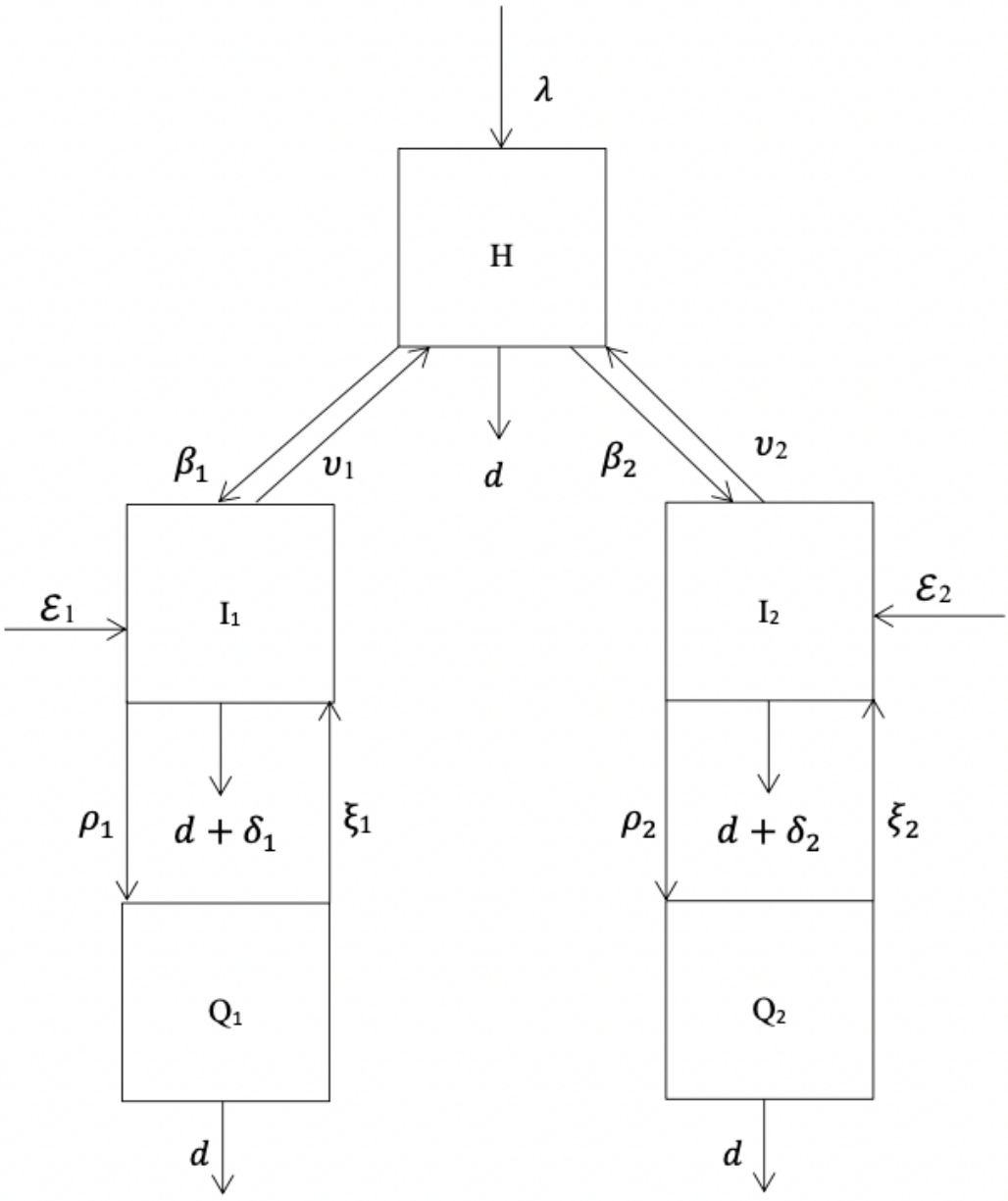


Figure 3.1: Flow chart of $SI_1I_2Q_1Q_2S$

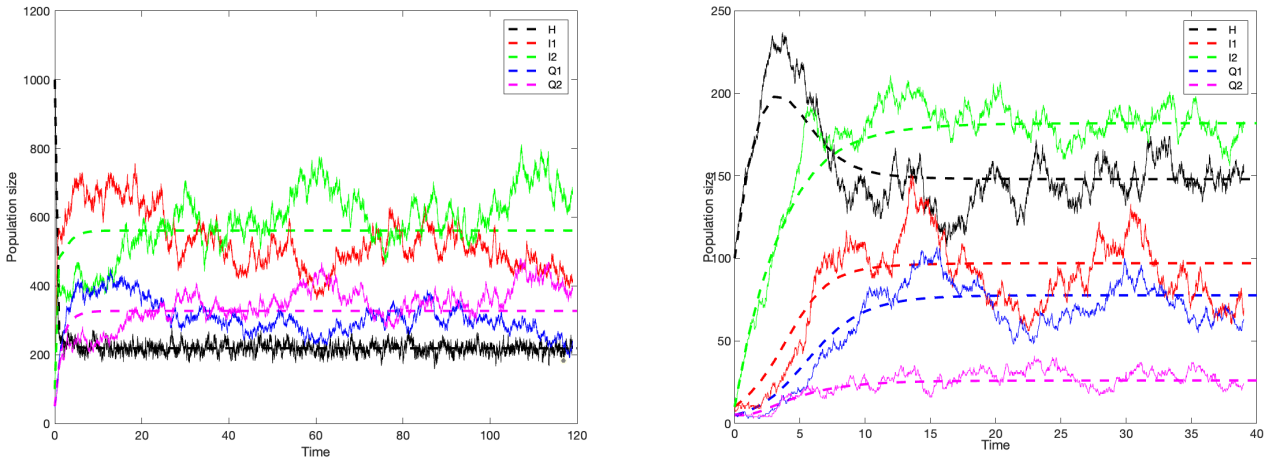


(a) (b)

Figure 3.2: **Numerical simulations of the deterministic model (3.2.1) compared with stochastic simulation using Gillespie's algorithm**. In (Figure 3.2a), the initial population size is $H = 1000$, $I_1 = 100, I_2 = 100, Q_1 = Q_2 = 50$. The values of the parameters are symmetrical; $\beta_1 = \beta_2 = 0.005, \Lambda = 1000, d = 0.5, \nu_1 = \nu_2 = 0.3, \gamma_1 = \gamma_2 = 0.003, \epsilon_1 = \epsilon_2 = 0.6, \zeta_1 = \zeta_2 = 0.7, \rho_1 = \rho_2 = 0.7$. While in (Figure 3.2b), the initial population size is $H = 100$, $I_1 = 10, I_2 = 10, Q_1 = Q_2 = 5$. The values of the parameters are asymmetrical; $\beta_1 = 0.005, \beta_2 = 0.0005, \Lambda = 100, d = 0.3, \nu_1 = 0.3, \nu_2 = 0.003, \gamma_1 = \gamma_2 = 0.003, \epsilon_1 = 10, \epsilon_2 = 50, \zeta_1 = 0.2, \zeta_2 = 0.4, \rho_1 = 0.4, \rho_2 = 0.1$.

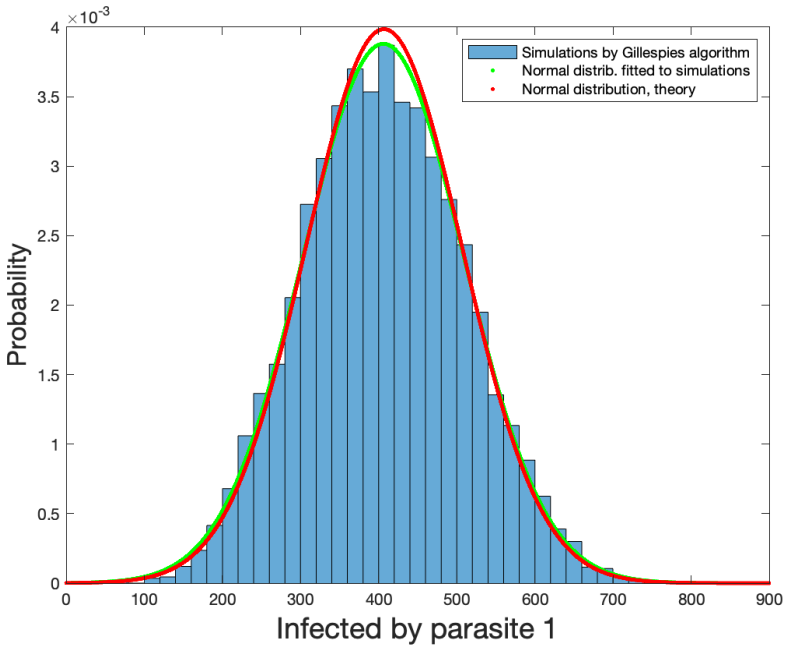


Figure 3.3: Histogram generated from simulations using Gillespie's algorithm is compared to the probability density with mean and variance obtained from simulation using Gillespie's algorithm and the probability density of normal distribution with mean and variance obtained from the theory of $I_1$, infected by parasite 1 compartment at time = 300 of the stochastic model with quiescence. The initial population sizes of the model are; $I_1 = 50000, I_2 = 10000, Q_1 = 5000, Q_2 = 5000$. The parameters of the model are $\beta_1 = \beta_2 = 0.05, \Lambda = 1000, d = 0.5, \nu_1 = \nu_2 = 0.3, \gamma_1 = \gamma_2 = 0.003, \zeta_1 = \zeta_2 = 0.1, \rho_1 = \rho_2 = 0.7, \epsilon_1 = \epsilon_2 = 10$.

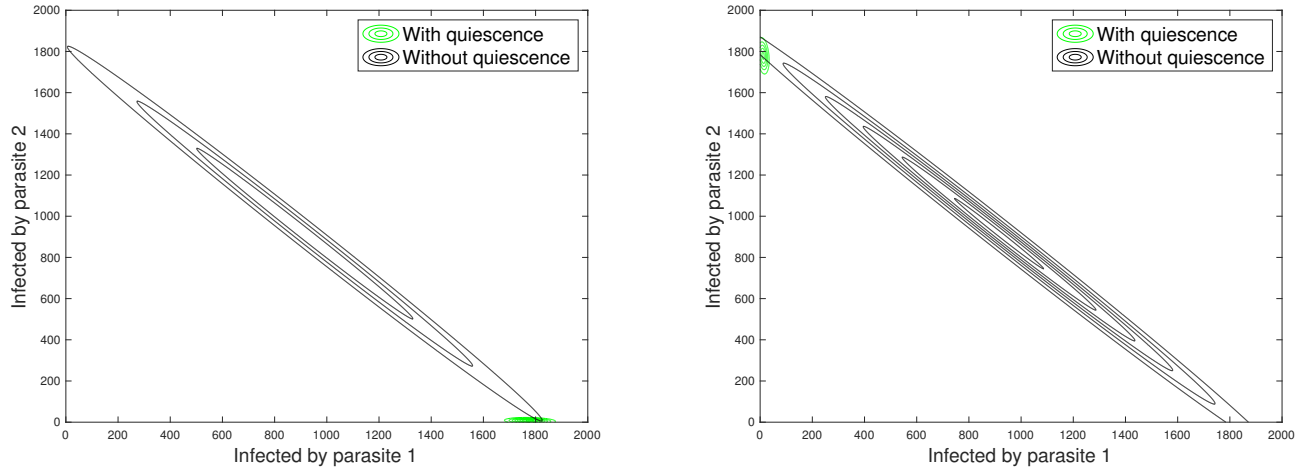


(a) (b)

Figure 3.4: Contour plots of the joint density of infected individuals by strain 1 and 2 based on simulations for **(a)** example 4, and **(b)** example 5 considered in the text. The x-axis is the number of infected individuals of strain 1 while the y-axis is the number of infected individuals by strain 2 based on the parameters stated in each example.

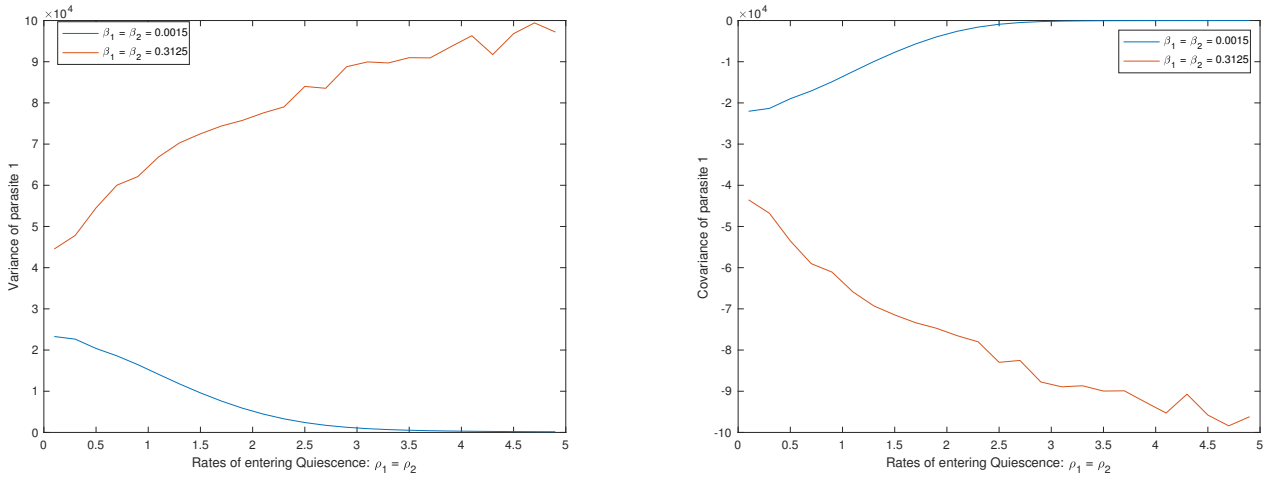


(a) (b)

Figure 3.5: Effect of quiescence, rates of entering the quiescence phase $\rho_1 = \rho_2$, and of transmission rates $\beta_1 = \beta_2$ on the **(a)** variance of parasite 1, and **(b)** covariance of parasite 1 of the collapsed covariance matrix. We use the following parameter values (symmetrical case): $d = 0.5, \Lambda = 1000, \nu_1 = \nu_2 = 0.3, \gamma_1 = \gamma_2 = 0.003, \zeta_1 = \zeta_2 = 0.1, \epsilon_1 = \epsilon_2 = 10$ and the initial population sizes are $H = 50,000$, $I_1 = 10,000, I_2 = 10,000, Q_1 = 5,000, Q_2 = 5,000, \text{time} = 300$. The blue line is for $\beta_1 = \beta_2 = 0.0015$, and the red line for $\beta_1 = \beta_2 = 0.3125$

.

# Chapter 4

# Quiescence and co-infection by two pathogen strains

## 4.1 Co-infection model without quiescence

In this introductory section, we review the work done in [52] in which the authors build mathematical epidemic model of non-interacting multiple strains that cause acute infection. Specifically, the authors develop novel statistical tools in order to correctly test for interactions between several pathogens that cause severe infections. The model assumes that two pathogen strains can be present in a host population, and that hosts can be infected by either strain or co-infected by both strains. In that sense the two strains are non-interacting with one another because there is no direct influence of the infection status by one strain on the probability of being infected by the other strain. The model challenges a very old assumption that non-interacting pathogens are statistically independent. The authors argue that the recovery of the co-infected individuals generates the net prevalence of individual pathogen to simultaneously decrease. Stochastic simulations reveal that the non-interacting pathogen are, as a result, positively correlated. Thus, a main results of this study is that the proportion of co-infected hosts is greater than the naively expected prevalence of co-infection obtained by multiplying the individual prevalence of both strains.

**Dynamics of individual pathogens.** The dynamics of individual parasites/pathogens is captured in the SIS model (1.3.1) discussed in chapter one. All previous mathematical analyses are still valid here.

### 4.1.1 Co-infection model

In recent times and with progress of DNA genotyping, epidemiologists/researchers have now well established that many infections often involve many strains/pathogens of the same species [115]. In fact, infection of one pathogen strain can trigger the subsequent infection by another strain [44, 90]. The co-infection affects the extend of symptoms and the degree of contagiousness of the infection, it also affects the duration and the severity of the infection [41]. Neutral, facilitative

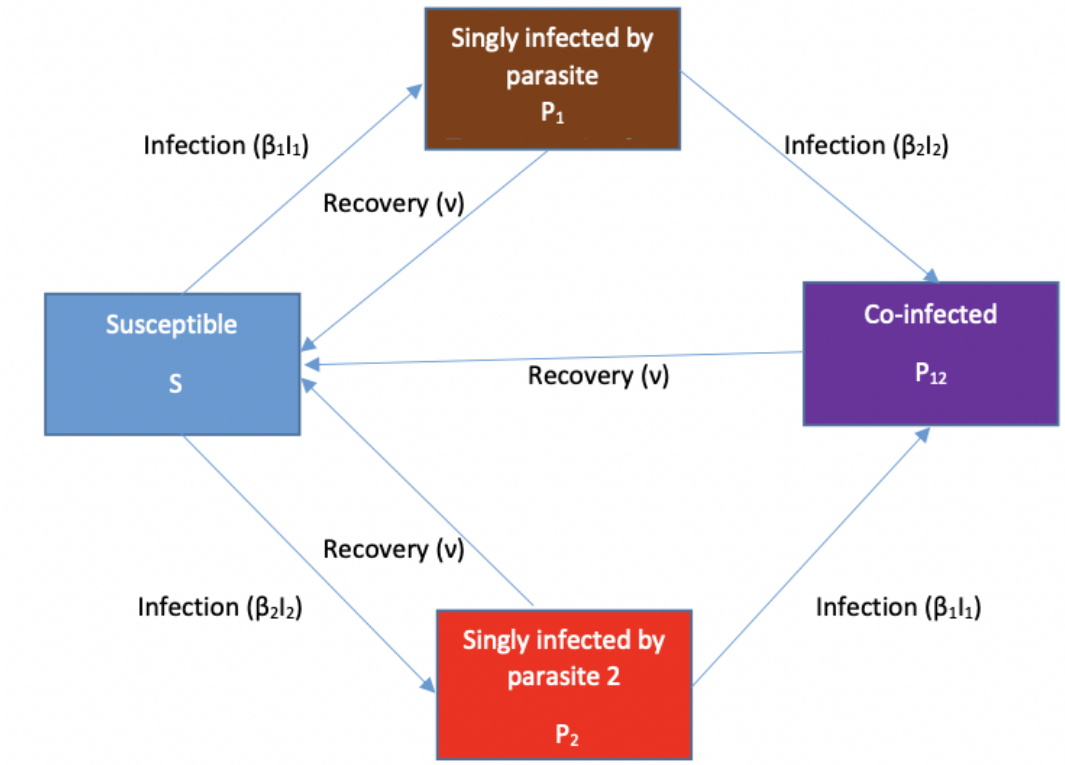


Figure 4.1: Flow diagram of the co-infection model

and antagonistic interactions are therefore possible [62, 93]. Neutral interaction is when one party of the interacting species benefits while the other remains unaffected (*e.g* bird nest and the tree), facilitative is which both parties of the interacting species benefit from each other (*e.g* plants and mycorrhizal fungi), antagonistic interaction is when one party of the interacting species benefits at the expense of the other (*e.g* hosts and pathogens) [107]. Thus, the occurrence of co-infection has a significant importance in disease management and optimal control strategy of the infections [103, 57, 3].

We now proceed to define the pathogen-specific net forces of infection as follows:

$$F_i = \beta_i I_i = \beta_i(P_i + P_{12}) \qquad \text{for} \quad i = 1, 2 \tag{4.1.1}$$

Here we have one host and two parasites, the proportions of individuals singly infected by parasite 1 and 2 are given by $P_1$ and $P_2$, respectively and the proportion of co-infected hosts is given as $P_{12}$, $\beta_1$ is the transmission rate of pathogen 1, $\beta_2$ is the transmission rate of pathogen 2 and $\nu$ is

the recovery rate. We define the model:

$$\begin{aligned}
\frac{dP_1}{dt} &= \beta_1 I_1 S - \beta_2 I_2 P_1 - \nu P_1 \\
\frac{dP_2}{dt} &= \beta_2 I_2 S - \beta_1 I_1 P_2 - \nu P_2 \\
\frac{dP_{12}}{dt} &= \beta_1 I_1 P_2 + \beta_2 I_2 P_1 - \nu P_{12} \\
S &= 1 - P_1 - P_2 - P_{12} \\
I_1 &= P_1 + P_{12} \\
I_2 &= P_2 + P_{12}
\end{aligned} \tag{4.1.2}$$

with the equilibrium solution given as

$$\tilde{P_{12}^*} = \Big(\frac{\beta_1 + \beta_2}{\beta_1 + \beta_2 - \nu}\Big)\tilde{I_1}^*\tilde{I_2}^* = \frac{(\beta_1 + \beta_2)(\beta_1 - \nu)(\nu - \beta_2)}{\beta_1\beta_2(\nu - \beta_1 - \beta_2)}$$

and

$$\tilde{P_1}^* = \tilde{I_1}^* - \tilde{P_{12}^*} = \frac{\nu(\nu - \beta_1)}{\beta_2(\nu - \beta_1 - \beta_2)}, \quad \tilde{P_2}^* = \tilde{I_2}^* - \tilde{P_{12}^*} = \frac{\nu(\nu - \beta_2)}{\beta_1(\nu - \beta_1 - \beta_2)},$$

where $\tilde{I_1}^*\tilde{I_2}^*$ are the equilibrium solutions of the SIS model (Chapter 1, 1.3.1). We present here two numerical simulations to exemplify the main results obtained in [52]. Basically it means that by computing the number of co-infected and infected by either strain, we can know if there is facilitation, antagonism or neutral interactions between strains.

### 4.1.2 Stability analysis

**Theorem 1.** *(Stability theorem) The endemic equilibrium solution of system (4.1.2) is locally asymptotically stable if*

$$\beta_i > \nu \quad for \quad i = 1, 2$$

*Proof.* The eigenvalues of the Jacobian matrix evaluated at this equilibrium state is given as

$$J = \begin{vmatrix} j_{11} & j_{12} & j_{13} \\ j_{21} & j_{22} & j_{23} \\ j_{31} & j_{32} & j_{33} \end{vmatrix}.$$

where

$$\begin{aligned}
j_{11} =& (1 - 2P_1 - P_2 - 2P_{12})\beta_1 - (P_2 + P_{12})\beta_2 - \nu, \\
j_{12} =& -(P_1 + P_{12})\beta_1 - \beta_2 P_1, \\
j_{13} =& (1 - 2P_1 - P_2 - 2P_{12})\beta_1 - P_1\beta_2, \\
j_{21} =& -(P_2 + P_{12})\beta_2 - \beta_1 P_2 \\
j_{22} =& (1 - P_1 - 2P_2 - 2P_{12})\beta_1 - (P_1 + P_{12})\beta_1 - \nu, \\
j_{23} =& (1 - P_1 - 2P_2 - 2P_{12})\beta_2 - P_2\beta_1, \\
j_{31} =& (P_2 + P_{12})\beta_2 + \beta_1 P_2, \\
j_{32} =& (P_1 + P_{12})\beta_1 + \beta_2 P_1, \\
j_{33} =& P_2\beta_1 + \beta_2 P_1 - \nu.
\end{aligned}$$

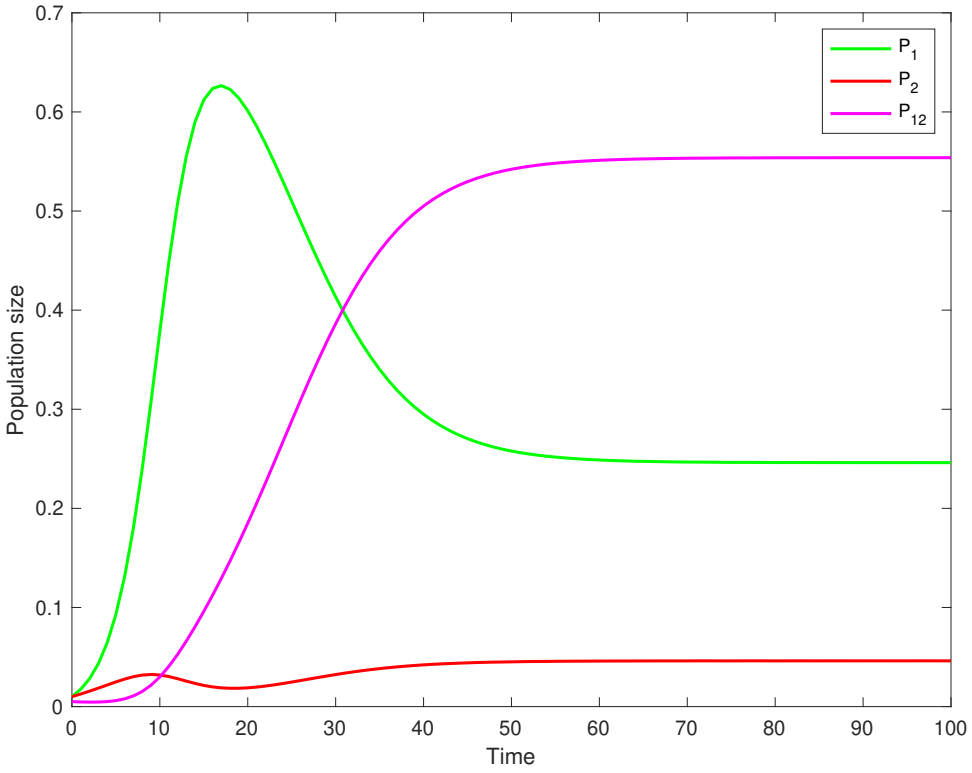


Figure 4.2: Deterministic simulation of the two-pathogens co-infection model without quiescence with $\beta_1 = 0.5, \beta_2 = 0.25$, and $\nu = 0.1$, $P_1(0) = P_2(0) = 0.01, P_{12} = 0.005, N = 1000$.

The eigenvalues are :

$$\nu - \beta_2,$$

$$\nu - \beta_1,$$

$$\nu - \beta_1 - \beta_1.$$

Please not that the eigenvalues lie on the left half plane once $\beta_1, \beta_2 > \nu$ which completes the proof. □

### 4.1.3 Co-Infection Model with Quiescence

In this section, we extend the model in system (4.1.2) to include quiescence compartment as this phenomenon is very common in parasites of humans, animals and plants. For example, one of the malaria parasites, call *P. vivax*, is known to have dormancy which can last for weeks, months and even years. However, not all malaria parasites are known to have dormancy [96]. There are numerous data that show co-infection between several malaria strains, and even malaria species ( for example see [15]). Therefore, it is important to consider the effect of quiescence on the

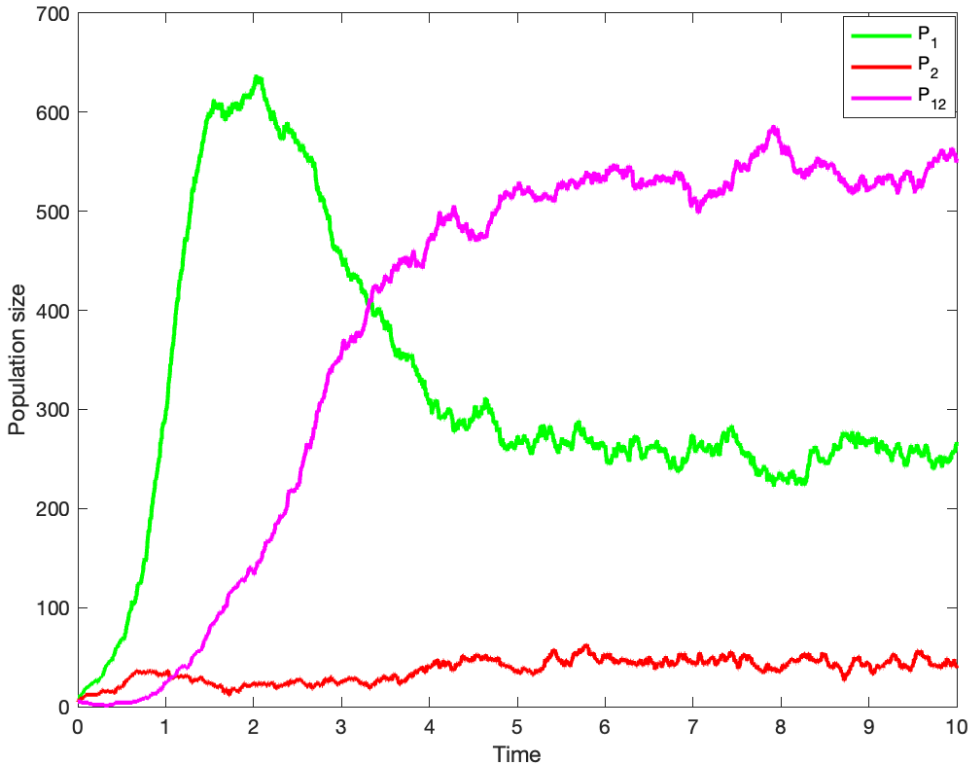


Figure 4.3: Stochastic simulation of the two-pathogens model without quiescence of the confection model with $\beta_1 = 5, \beta_2 = 2.5, \nu = 1$ (parameters have units of inverse time), the initial population sizes are $P_1(0) = P_2(0) = 10, P_{12} = Q(0) = 5, N = 1000$.

co-infection dynamics. Model (4.1.3) described below captures the dynamics of the system of co-infection with quiescence. The total population is divided into five mutually exclusive compartments, namely Susceptible compartment, Singly infected by parasite 1 compartment, Singly infected by parasite 2 compartment, Co-infected by both parasites compartment, Quiescence compartment of hosts singly infected by parasite 2. The first equation represents the rate of change of individuals singly infected by parasite 1, denoted by $P_1$. The second equation represents the rate of change of individuals singly infection by parasite 2, denoted by $P_2$. The second equation represents the rate of change of individuals that are co-infected by both parasites 1 and 2, denoted by $P_{12}$. While the last equation represents the rate of change of individuals infected by parasite 2 that are in quiescence stage, denoted by $Q_2$. The parameters $\rho$ and $\zeta$ are the rate of entering and exiting quiescence, respectively, the remaining of the parameters are as described in model (4.1.2) above. We assume that the total population size ($N$) is constant. The natural death rate is also neglected as we consider acute infections. Please note that this hypothesis may need to be revised for chronic infections which are common and underlie a large proportion of co-infections in animals and humans [40]. For plants, we note that when they are infected by many pathogens, they typically remain so throughout their lifetime [73]. The disease induced

death rate is also neglected.

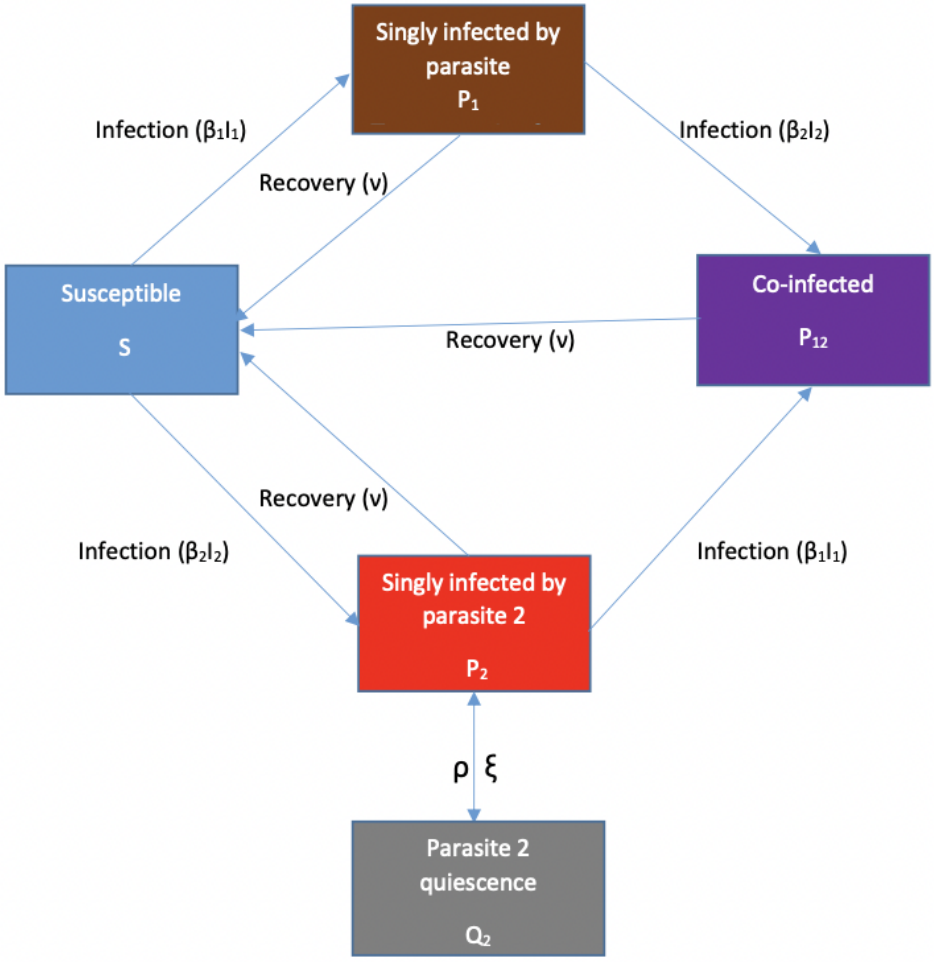


Figure 4.4: Flow diagram of the co-infection model with quiescence.

**Co-infection model with quiescence**

$$\begin{aligned}
\frac{dP_1}{dt} &= \beta_1 I_1 S - \beta_2 I_2 P_1 - \nu P_1 \\
\frac{dP_2}{dt} &= \beta_2 I_2 S - \beta_1 I_1 P_2 - \nu P_2 - \rho P_2 + \zeta Q_2 \\
\frac{dP_{12}}{dt} &= \beta_1 I_1 P_2 + \beta_2 I_2 P_1 - \nu P_{12} \\
\frac{dQ_2}{dt} &= \rho P_2 - \zeta Q_2 \\
S &= 1 - P_1 - P_2 - P_{12} - Q_2 \\
I_1 &= P_1 + P_{12} \\
I_2 &= P_2 + P_{12}
\end{aligned} \tag{4.1.3}$$

### 4.1.4 Equilibrium Solutions and Stability of the system

The following equations are the equilibrium solutions of the co-infection model (4.1.3)

- $P_1 = P_2 = P_{12} = Q_2 = 0$,
- $P_1 = P_{12} = 0, P_2 = \frac{\zeta(\beta_2-\nu)}{\beta_2(\zeta+\rho)}, Q_2 = \frac{\rho(\beta_2-\nu)}{\beta_2(\zeta+\rho)}$,
- $P_1 = 1 - \frac{\nu}{\beta_1}, P_2 = P_{12} = Q_2 = 0$,
- the co-existence equilibrium occurs when $P_1, P_2, P_{12}, Q_2 \neq 0$.

The co-existence equilibrium solution can be expressed in an implicit form as follows:

$$P_1^* = \frac{\beta_1 I_1 S}{\nu + \beta_2 I_2}, \quad P_2^* = \frac{\beta_2 I_2 S}{\nu + \beta_1 I_1}, \quad P_{12}^* = \frac{\beta_1 I_1 \beta_2 I_2 S(\beta_1 I_1 + 2\nu + \beta_2 I_2)}{\nu(\nu^2 + \nu\beta_2 I_2 + \nu\beta_1 I_1 + \beta_1 I_1 \beta_2 I_2)}, \quad Q_2^* = \frac{\rho\beta_1 I_1 S}{\zeta\nu + \beta_2 I_2}.$$

Please observe that

$$I_i^* = P_i^* + P_{12}^* = \tilde{I_i}^* - Q_2^* = 1 - \frac{\nu}{\beta_i} - Q_2^* \quad \text{for} \quad i = 1, 2 \tag{4.1.4}$$

This co-infection model (4.1.3) has three equilibrium solutions: (1) disease free equilibrium in which all the pathogens dies out and are cleared off from the population (yielding the result as stated in the first item above), (2) two solutions in which one single pathogen survives and the other pathogen strain dies off and is removed from the population (yielding the solution as obtained in the second or third item above). In the event where solution in the second item occurs then the system with co-infection model collapses to the *SIQS model, (2.2.1)* discussed in chapter 2 above (that is only the singly infected pathogen 2 and the quiescence pathogen 2 are found). Whereas if the solution in the third item above occurs when only single infected pathogen 1 survives and all other pathogens are cleared off from the system, in this case the co-infection model collapses to the SIS model (1.3.1) that is only pathogen 1 remains in the population. Finally, for (3) is a co-existence solution at which all the pathogens co-exist and become persistent in the population, the solution is given above.

**Theorem 2.** *(Stability theorem) The equilibrium solution of system (4.1.2) in which* $P_1 = P_{12} = 0, P_2, Q_2 \neq 0$ *is locally asymptotically stable if*

$$\beta_2 > \nu$$

*Proof.* The eigenvalues of the Jacobian matrix evaluated at this equilibrium state is given as

$$J = \begin{vmatrix} (1 - P_2 - Q_2)\beta_2 - P_2\beta_2 - \nu - \rho & -\beta_2 P_2 + \zeta \\ \rho & \zeta \end{vmatrix}.$$

The eigenvalues are :

$$-(\zeta + \rho),$$
$$\frac{\zeta(\nu - \beta_2)}{\zeta + \rho}.$$

Please not that the eigenvalues lie on the left half plane once $\beta_2 > \nu$, hence the proof. □

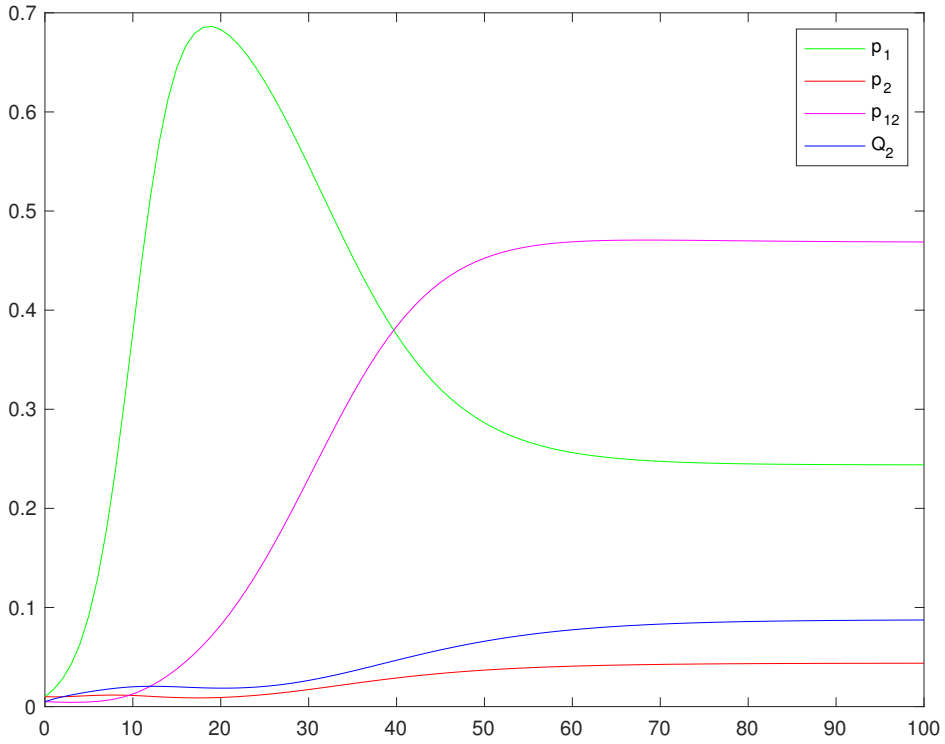


Figure 4.5: Deterministic simulation of the two-pathogens model with quiescence and co-infection, the parameters are $\beta_1 = 0.5, \beta_2 = 0.25, \nu = 0.1, \rho = 0.4$ and $\zeta = 0.2$ and the initial population sizes are $P_1(0) = P_2(0) = 0.01, P_{12} = Q(0) = 0.005, N = 1000$

## 4.2 Stochastic analysis

### 4.2.1 Transition probabilities

This section defines a stochastic version of the deterministic model as described in equation (4.1.3). We add stochasticity occurring at any of the possible transition of individuals between classes (birth and death). The transition probabilities of jumping from one state (*e.g.* infected quiescent) to the another state (*e.g.* infected) are defined below. We choose $\Delta t$ very small so that during this time interval only one event occurs. The number of individuals who are susceptible is $S$, the number of singly infected by parasite 1 is $P_1$, the number of singly infected by parasite 2 population is $P_2$, the number of co-infected by both parasites is $P_{12}$, the number of individual in quiescence compartment singly infected by parasite 2 is $Q_2$. The possible changes over time are either $S_t + 1, S_t - 1, P_{1t} + 1, P_{1t} - 1, P_{2t} + 1, P_{2t} - 1, P_{12t} + 1, P_{12t} - 1, Q_{2t} + 1, Q_{2t} - 1$. Therefore, our stochastic process is a birth and death process. The one step transition probabilities are given in table 4.1:

We performed stochastic simulation using Gillespie's algorithm to generate 10,000 realisations.

Table 4.1: Transitions rates for the co-infection model with quiescence 4.1.3.

| Type | Transition | Rate |
|---|---|---|
| Infection of $S$ by $P_1$ | $(S_t, P_{1t}, P_{2t}, P_{12t}, Q_{2t}) \to (S_t - 1, P_{1t} + 1, P_{2t}, P_{12t}, Q_{2t})$ | $\beta_1 \frac{S(P_1+P_{12})}{N} \Delta t + o\Delta(t)$ |
| Infection of $S$ by $P_2$ | $(S_t, P_{1t}, P_{2t}, P_{12t}, Q_{2t}) \to (S_t - 1, P_{1t}, P_{2t} + 1, P_{12t}, Q_{2t})$ | $\beta_2 \frac{S(P_2+P_{12})}{N} \Delta t + o\Delta(t)$ |
| Infection of $P_1$ by $P_2$ | $(S_t, P_{1t}, P_{2t}, P_{12t}, Q_{2t}) \to (S_t, P_{1t} - 1, P_{2t}, P_{12t} + 1, Q_{2t})$ | $\beta_2 \frac{P_1(P_2+P_{12})}{N} \Delta t + o\Delta(t)$ |
| Infection of $P_2$ by $P_1$ | $(S_t, P_{1t}, P_{2t}, P_{12t}, Q_{2t}) \to (S_t, P_{1t}, P_{2t} - 1, P_{12t} + 1, Q_{2t})$ | $\beta_1 \frac{P_2(P_1+P_{12})}{N} \Delta t + o\Delta(t)$ |
| Recovery $P_1$ & replacement with $S$ | $(S_t, P_{1t}, P_{2t}, P_{12t}, Q_{2t}) \to (S_t + 1, P_{1t} - 1, P_{2t}, P_{12t}, Q_{2t})$ | $\nu P_1 \Delta t + o\Delta(t)$ |
| Recovery $P_2$ & replacement with $S$ | $(S_t, P_{1t}, P_{2t}, P_{12t}, Q_{2t}) \to (S_t + 1, P_{1t}, P_{2t} - 1, P_{12t}, Q_{2t})$ | $\nu P_2 \Delta t + o\Delta(t)$ |
| Recovery $P_{12}$ & replacement with $S$ | $(S_t, P_{1t}, P_{2t}, P_{12t}, Q_{2t}) \to (S_t + 1, P_{1t}, P_{2t}, P_{12t} - 1, Q_{2t})$ | $\nu P_{12} \Delta t + o\Delta(t)$ |
| Go quiescent $P_2$ & birth of $Q_2$ | $(S_t, P_{1t}, P_{2t}, P_{12t}, Q_{2t}) \to (S_t, P_{1t}, P_{2t} - 2, P_{12t}, Q_{2t} + 1)$ | $\rho P_2 \Delta t + o\Delta(t)$ |
| Wake-up $Q_2$ & replacement with $P_2$ | $(S_t, P_{1t}, P_{2t}, P_{12t}, Q_{2t}) \to (S_t, P_{1t}, P_{2t} + 2, P_{12t}, Q_{2t} - 1)$ | $\zeta Q_2 \Delta t + o\Delta(t)$ |

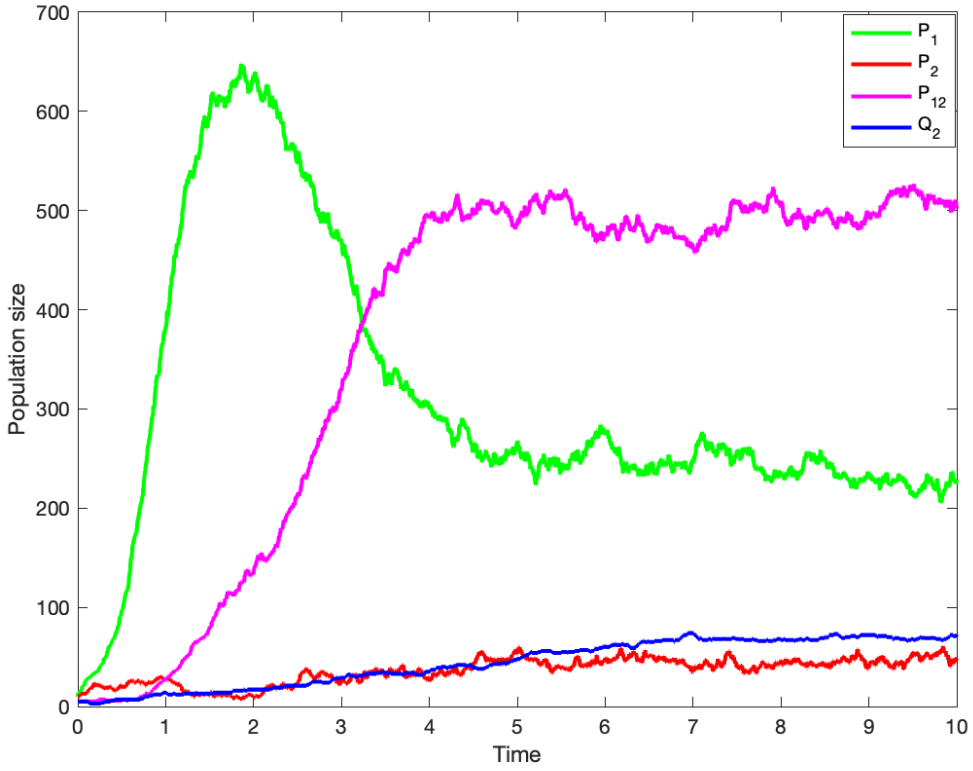


Figure 4.6: Stochastic simulation of the two-pathogens model with quiescence of the co-infection model with $\beta_1 = 5, \beta_2 = 2.5, \nu = 1, \rho = 0.4, \zeta = 0.2$ and the initial population sizes are $P_1(0) = P_2(0) = 10, P_{12} = Q(0) = 5, N = 1000$

The value of each realisation at time $t = 25$ is stored and graphic produced as shown in (Figures 4.7a, 4.7b, 4.8a, 4.8b and others). Here, when computing the number of hosts infected by strain 2, we add the hosts that are in the quiescence stage. We assess the existence of a statistical correlation between the number of infected by parasite 1 and those by parasite 2 by means of a linear correlation (using Matlab build in function, *fitlm*). The value of the $R^2$ is informative on the degree of variance explained by the correlation.

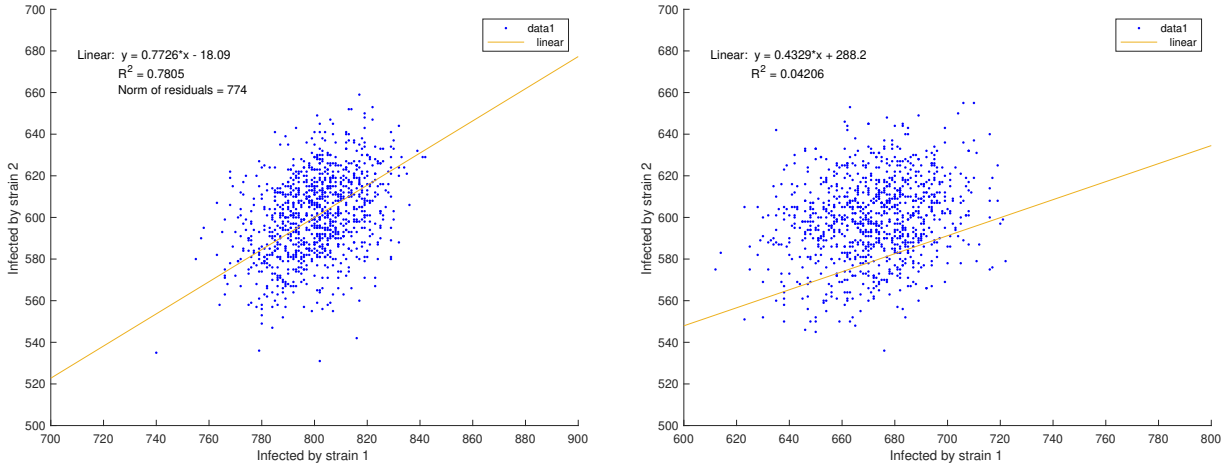


(a) (b)

Figure 4.7: **(a)** Positive correlation between number of parasites 1 and 2 in the stochastic co-infections epidemic model. The observations are generated from $1,000$ realisations/sample paths by using Gillespie's algorithm at time $t = 25$ with $P_1(0) =, P_2(0) = 10, P_{12} = 5, N = 1,000, \beta_1 = 5, \beta_2 = 2.5, \nu = 1$. **(b)** Quiescence breaks the positive correlation between number of parasites 1 and 2 in the stochastic co-infections epidemic model. The observations are generated from $1,000$ realisations/sample paths by using Gillespie's algorithm at time $t = 25$ with $P_1(0) = P_2(0) = 10, P_{12} = 5, Q(0) = 10, N = 1,000, \beta_1 = 5, \beta_2 = 2.5, \nu = 1, \rho = 1.2, \zeta = 0.4$.

## 4.3 Discussion

We incorporate quiescence phase into model (4.1.2) and build the extended model (4.1.3) that captures the dynamics of the co-infections of two strains in which one of the strains exhibits the quiescence behaviour. Note that the two strains are here non-interacting directly with one another. There is a need to build up a mathematical model that properly mimics the quiescence behaviour and its effect on disease dynamics to improve disease management. We show that the the model without quiescence is stable when both infection rates are greater than the recovery rate. We also show that the equilibrium of the co-infection model with quiescence in which the system collapses to the SIQS model is as well stable once infection rate is greater then the recovery rate. Regarding the stability of the co-infection model with quiescence, we already knew from Chapter 3 that quiescence does change the stability properties of the system [50, 48]. In fact the quiescence makes it more stable. Thus, the stability of the co-infection model without quiescence implies the stability of the system with quiescence. We then perform numerical computation using the Gillespie's algorithm and the results are shown in (Figures 4.3 and 4.6). The deterministic and stochastic simulations are consistent in their behaviour and convergence towards the steady state. However, it has been observed in the stochastic simulations that quiescence affects the correlation between the number of infected individuals by the two strains. We can describe the set of results of numerical simulations and number of infected hosts by parasite 1 and 2 as an

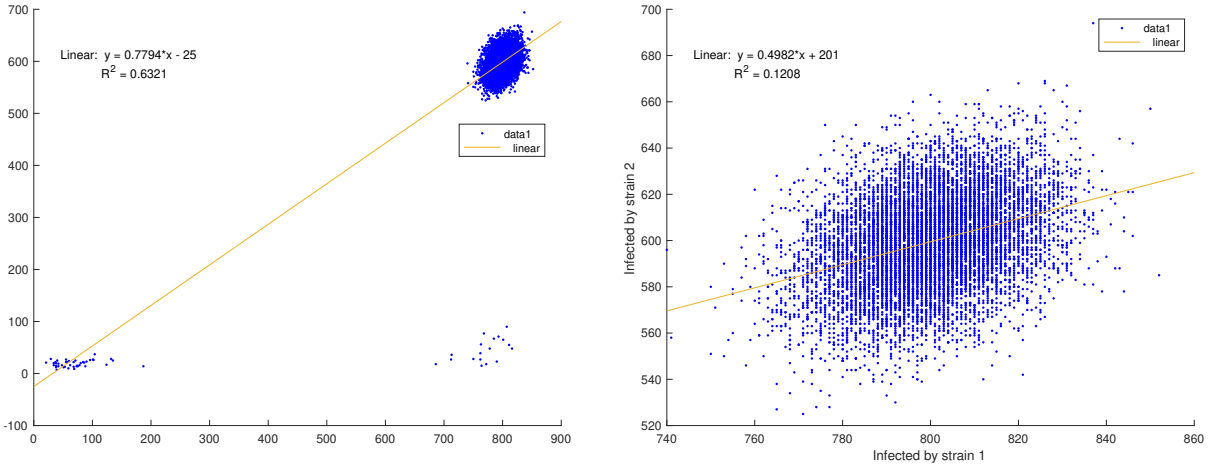


(a) (b)

Figure 4.8: **(a)** Positive correlation between number of parasites 1 and 2 of the stochastic co-infections epidemic model without quiescence. The observations are generated from $10,000$ realisations/sample paths by using Gillespie's algorithm at time $t = 25$ with $P_1(0) =$ , $P_2(0) = 10, P_{12} = 5, N = 1,000, \beta_1 = 5, \beta_2 = 2.5, \nu = 1$. **(b)** The truncated positive correlation between number of parasites 1 and 2 in the stochastic co-infections epidemic model without quiescence. The observations are generated from $10,000$ realisations/sample paths by using Gillespie's algorithm at time $t = 25$ with $P_1(0) = P_2(0) = 10, P_{12} = 5, Q(0) = 10, N = 1000, \beta_1 = 5, \beta_2 = 2.5, \nu = 1$.

ellipse of realized points in the plot of $I_1$ versus $I_2$ (as in [52]). When quiescence is added, this ellipse become rather circular whenever the rate of entering quiescence is greater then the rate of exiting the quiescence, *i.e.* when the fraction $\frac{\rho}{\zeta} > 1$. Therefore, we conclude that with quiescence, pathogen strains in co-infection are statistically independent based on the number of infected hosts infected by single strains, as opposed to the claim made in [52] without quiescence. This is due to the fact that when the rate of entering quiescence is strong then the number of those singly infected with active parasite 2 decreases, which in turn decreases the number of co-infected individuals. Basically quiescence delays further infection with parasite strain 1, and we can interpret our results as quiescence generating some indirect interaction between the two strains in the epidemiological dynamics.

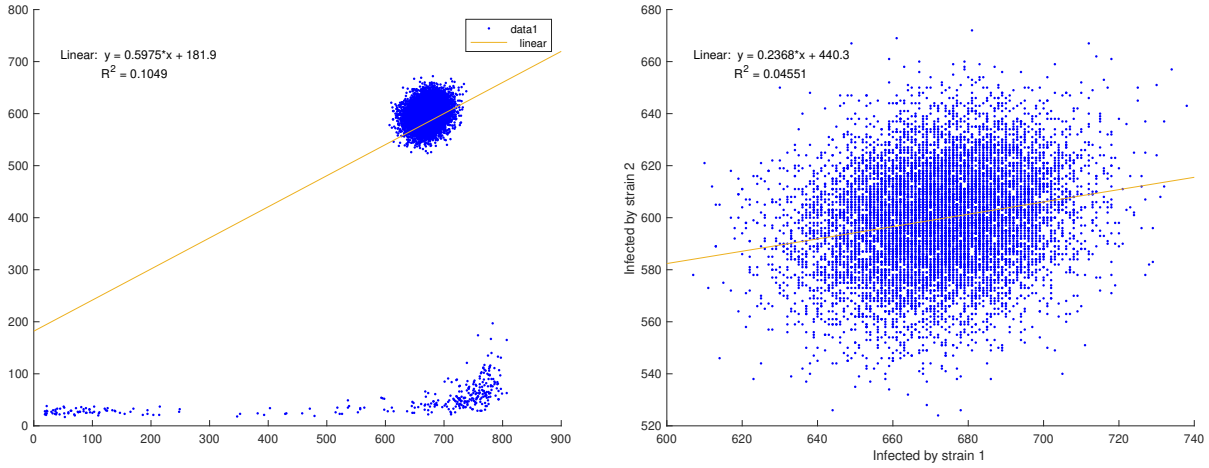


(a) (b)

Figure 4.9: **(a)** Quiescence breaks the positive correlation between number of parasites 1 and 2 of the stochastic co-infections epidemic model. The observations are generated from $10,000$ realisations/sample paths by using Gillespie's algorithm at time $t = 25$ with $P_1(0) =$ , $P_2(0) = 10, P_{12} = 5, N = 1000, \beta_1 = 5, \beta_2 = 2.5, \nu = 1, \rho = 1.2, \zeta = 0.4$. **(b)** Truncated set of high infection values in which quiescence breaks the positive correlation between number of parasites 1 and 2 in the stochastic co-infections epidemic model. The observations are generated from $10,000$ realisations/sample paths by using Gillespie's algorithm at time $t = 25$ with $P_1(0) = P_2(0) = 10, P_{12} = 5, Q(0) = 10, N = 1000, \beta_1 = 5, \beta_2 = 2.5, \nu = 1, \rho = 1.2, \zeta = 0.4$.

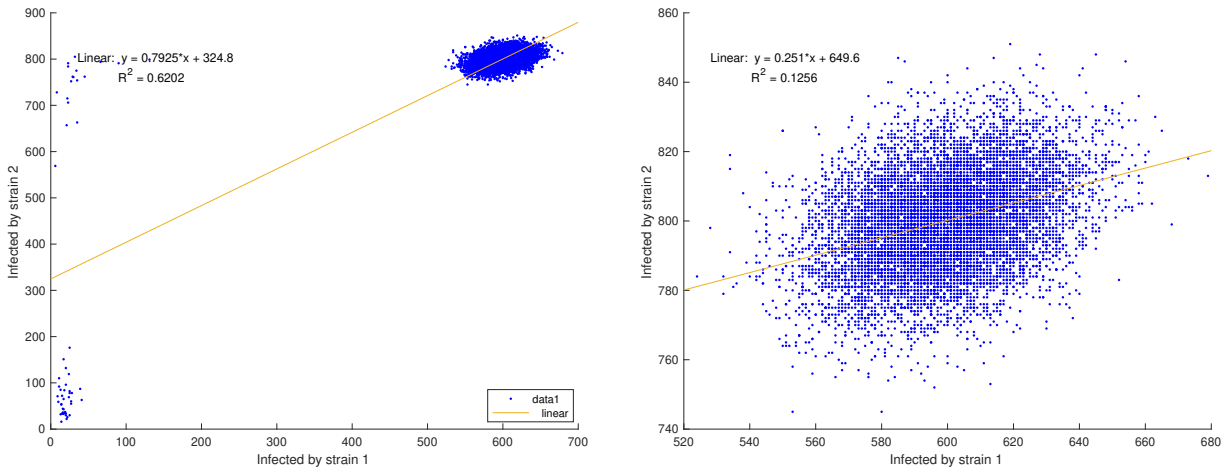


(a) (b)

Figure 4.10: **(a)** Positive correlation between number of parasites 1 and 2 of the stochastic co-infections epidemic model without quiescence. The observations are generated from $10,000$ realisations/sample paths by using Gillespie's algorithm at time $t = 25$ with $P_1(0) = , P_2(0) = 10, P_{12} = 5, N = 1000, \beta_1 = 2.5, \beta_2 = 5, \nu = 1$. **(b)** Truncated set of high values with positive correlation between number of parasites 1 and 2 in the stochastic co-infections epidemic model without quiescence. The observations are generated from $10,000$ realisations/sample paths by using Gillespie's algorithm at time $t = 25$ with $P_1(0) = P_2(0) = 10, P_{12} = 5, Q(0) = 10, N = 1000, \beta_1 = 5, \beta_2 = 2.5, \nu = 1$.

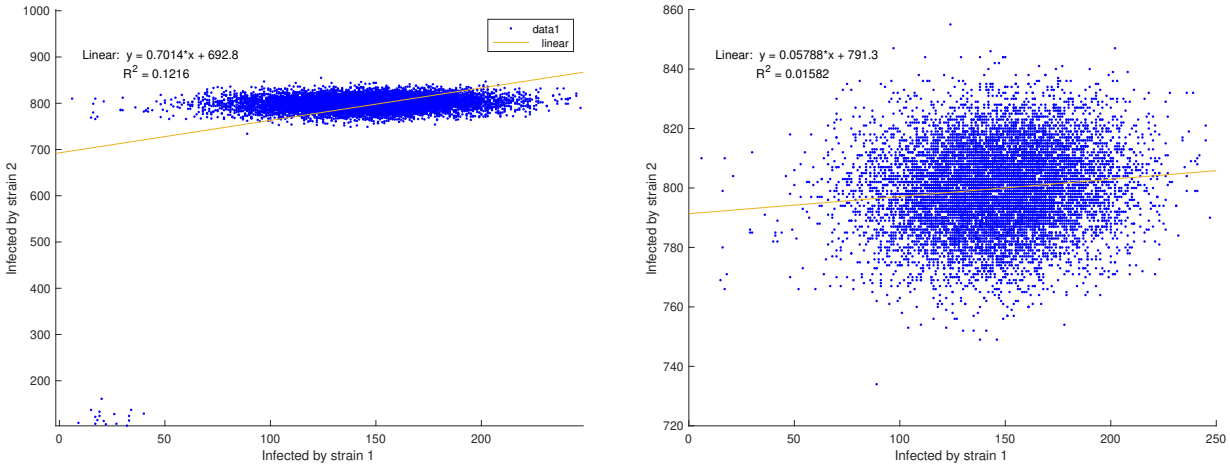


(a) (b)

Figure 4.11: **(a)** Quiescence breaks the positive correlation between number of parasites 1 and 2 of the stochastic co-infections epidemic model. The observations are generated from $10,000$ realisations/sample paths by using Gillespie's algorithm at time $t = 25$ with $P_1(0) =$ , $P_2(0) = 10, P_{12} = 5, N = 1000, \beta_1 = 2.5, \beta_2 = 5, \nu = 1, \nu = 1, \rho = 2, \zeta = 1$. **(b)** Truncated set of high values with quiescence breaking the positive correlation between number of parasites 1 and 2 in the stochastic co-infections epidemic model. The observations are generated from $10,000$ realisations/sample paths by using Gillespie's algorithm at time $t = 25$ with $P_1(0) = P_2(0) = 10, P_{12} = 5, Q(0) = 10, N = 1000, \beta_1 = 2.5, \beta_2 = 5, \nu = 1, \rho = 2, \zeta = 1$.

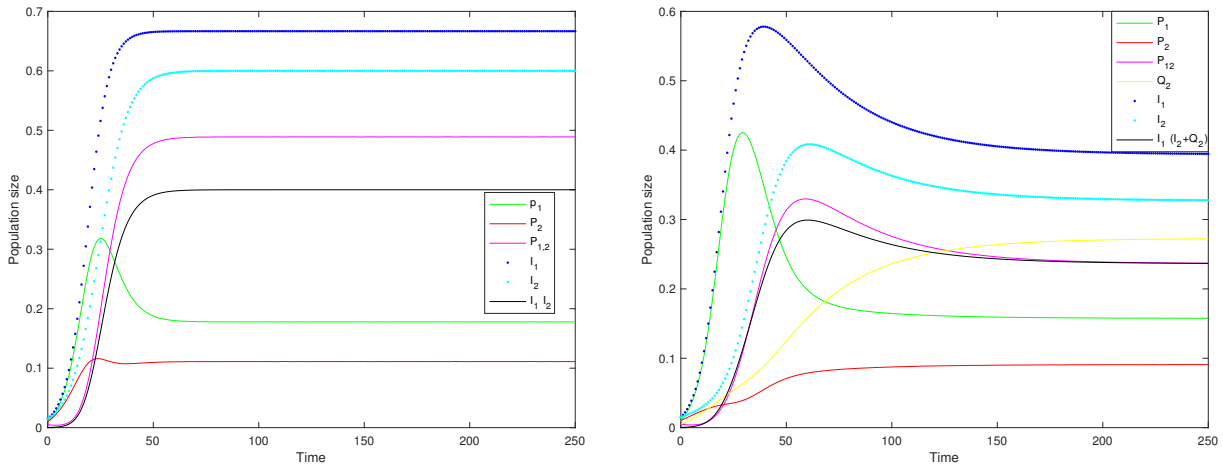


(a) (b)

Figure 4.12: Simulation of the deterministic co-infection models 4.1.2 and 4.1.3. **(a)** The proportion of co-infected individuals is higher than the proportion of product of parasites 1 and 2, with $P_1(0) = P_2(0) = 0.01, P_{12} = 0.005, N = 1000, \beta_1 = 0.3, \beta_2 = 0.25, \nu = 0.1$. **(b)** The proportion of co-infected individuals is equal to the proportion obtained by multiplying parasites 1 and 2, with $P_1(0) = P_2(0) = 0.01, P_{12} = Q(0) = 0.005, N = 1000, \beta_1 = 0.3, \beta_2 = 0.25, \nu = 0.1.\rho = 0.12, \zeta = 0.04$.

# Chapter 5

# Discussion

## 5.0.1 Discussion

### 5.0.1.1 Overview of results

Mathematical models are tools used to understand the behaviour of natural phenomenon. In my thesis, epidemiological models are built to understand the effect of quiescence on the infection process. We have seen that quiescence increases the time to extinction of the stochastic infection process of acute infections. Additionally, Quiescence affects the long term behaviour of the epidemics, that is to say, the quiescence increases the time at which the epidemic ends. We show in our study that quiescence mitigates stochasticity and reduces the noise under strain competition and generates a phenomenon equivalent to a moving average. This principle is general enough and the same idea could be investigated for a model of bacteria submitted to stochasticity of antibiotic treatment. We speculate that quiescence is not only a bet-hedging strategy, but also influences the stochasticity of the population behaviour. Namely the population size of bacteria may become more stable in time and insensitive to antibiotic treatment. Our results also call for more in depth investigations of the quiescence behaviour upon infection, of the length and determinants of the quiescent stages and the effect of quiescence on stochastic disease transmission in human diseases. We have also observed that the quiescence affects the correlation of two non-interacting pathogen strains. A correlation between number of parasites of strains 1, 2 and number of co-infected hosts decreases and vanishes whenever the rate of entering quiescence is greater than the rate of exiting quiescence. Quiescence decreases the prevalence of co-infections and thus generates the pathogen strains to be at statistical independent. Therefore, it is important to know the life-cycle of pathogens, that is if one strain undertakes quiescence, in order to predict if strains can show facilitation, antagonism or neutral interactions during co-infection.

## 5.0.2 Small case study: malaria and co-infections in Brazil

Malaria is one of the most severe disease in the world, infecting around 200,000 people annually in Brazil [15]. The Brazilian legal Amazon Malaria data contains information about the number of individuals infected by the three (3) malaria species, namely *P. falciparum, P. vivax, P. malarie* and possible co-infections. However, in this study we concentrate on the number of infected by

either *P. falciparum, P. vivax* and co-infections by both to test the predictions of our models. We therefore intend to perform comparative study/ data analysis based on the malaria infections by *P. falciparum* and/or *P. vivax* obtained in Brazil from the year 2009 to 20019. We want to see whether the model that we developed in chapter 4 can explain correlation or absence thereof in the data.

#### 5.0.2.1 Material and methods

The dataset is obtained from the Malaria Epidemiological Surveillance Information System (SivepMalaria). It is a malaria monitoring system in Brazilian legal Amazon which consists of nine Brazilian states and it is the area where malaria in endemic in the country contributing more then 90% of the number of malaria cases in Brazil [88]. The dataset consists of all medical records of individuals who were tested for malaria in the region from 2009 to 2019. It has 40 attributes and more than 22 million records of suspected malaria cases. The attributes consist of data regarding the examinations, notifications, as well as patient information [120, 15]. All suspected as well as confirmed case of infection by malaria is notified and registered in SivepMalaria [71]. All information in SivepMalaria are recorded yearly and arranged locally based on county. Therefore Sivepmalaria is a very crucial tool that can be used to study and understand the distribution of malaria to improve disease management [119].

#### 5.0.2.2 Overview of results: SivepMalaria Data

We first present an overview of the data of infections based on patient characteristics. (Figure 5.1) shows the association between patients' occupation and the infection by malaria parasites. There are slightly small variations in the patients' occupation and the percentage of infections by *P. falciparum, P. vivax* and the co-infections. The panning workers have high rate of co-infections followed by those that are working in mining. Whereas the other categories have almost the same percentage of co-infections. (Figure 5.2) shows the association of patients' education and the proportion of malaria infections. Those that do not complete their primary education have the highest percentage of infections by both *P. falciparum* and *P. vivax*. Then the second highest amount of infections are those that did not complete their secondary school education also by both species. These two categories of individual that came first and second by the infection of individual parasite have the highest count of co-infection. Individuals that have already completed their college education have low proportion of infection by both *P. falcifarum and P. vivax* as well as co-infections. In general, in this data, the higher the level of education, the lower are the infection and co-infection levels. In (Figure 5.3), there is no significant difference for infection levels as far as the gender is concerned. Generally speaking, we can say that female have a slightly lower proportion of infection.

(Figure 5.4) shows that the malaria infection by ethnicity. Basically, there is no significant difference in infection based on ethnicity. White and indigenous have slightly higher proportion of infection by *P. vivax* while black and mixed race have slightly higher percentage of infection by *P. falciparum* and co-infections are at similar level across ethnicities. (Figure 5.5) shows that few people infected by the malaria parasites, including the co-infections, do not show symptoms while the majority of the infected people show symptoms.

(Figure 5.6) shows that majority of the examination to detect malaria cases are thick and thin

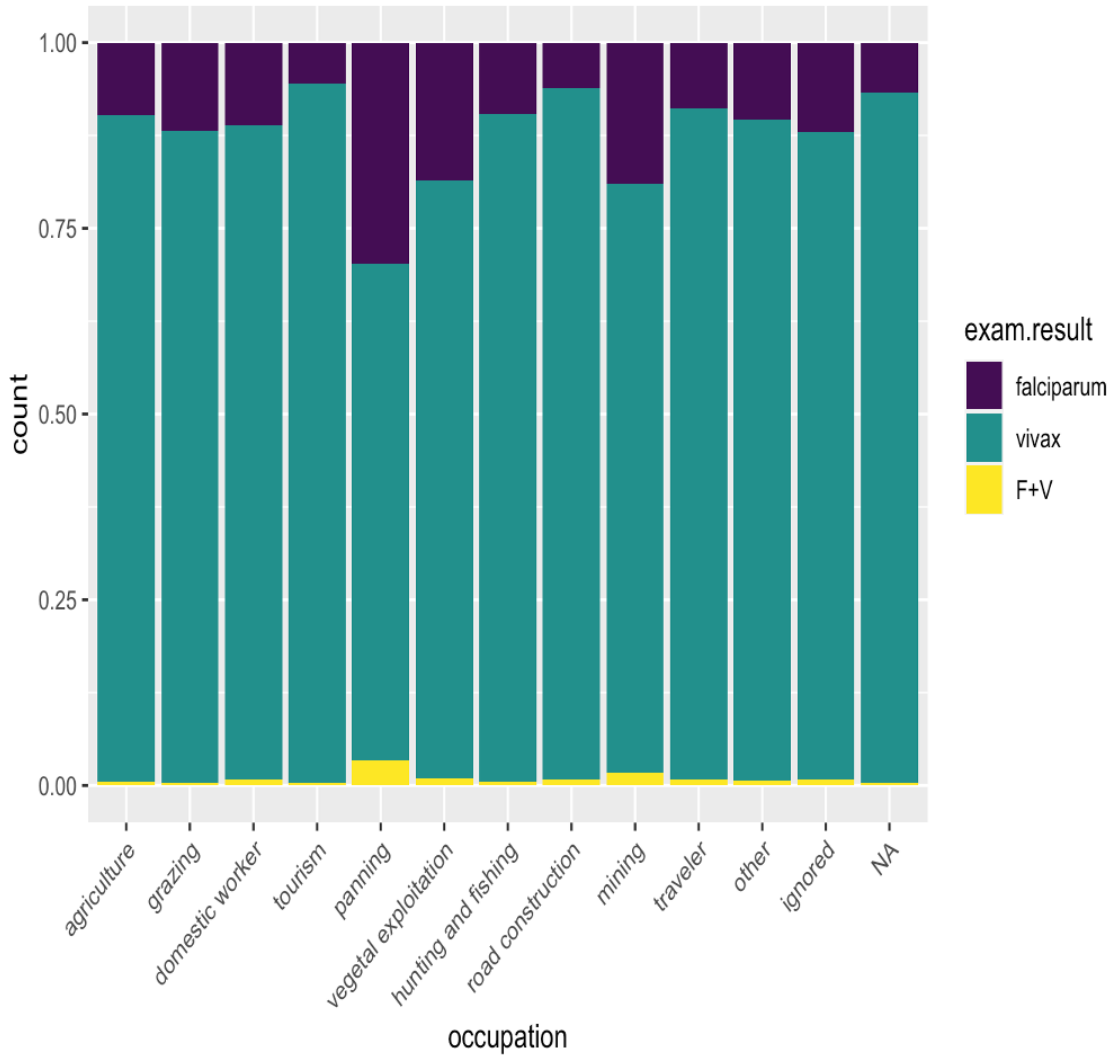


Figure 5.1: The relationship between patients' occupation and the relative proportion of malaria cases for *P. falciparum, P. vivax and co-infections.*

blood smears. Co-infections are chiefly found by rapid diagnostic test.

In (Figures 5.7a, 5.7b, 5.8a and 5.8b), we compute the correlations of the SIVEPMalaria data for the years $2019, 2010, 2015$ and $2019$ with $p-values$ and $R^2$. The value of $R^2$ tells us the degree of the correlation while $p-value$ tells us whether to accept or reject the null hypothesis $H_0$ are as well computed and are shown on the graph. If $p-value < 0.05$, we reject the $H_0$ hypothesis (no correlation) and accept the $H_1$ hypothesis (there is a correlation) and if $p-values > 0.05$, we accept the $H_0$ hypothesis (no correlation) and reject the $H_1$ hypothesis (there is a correlation) .

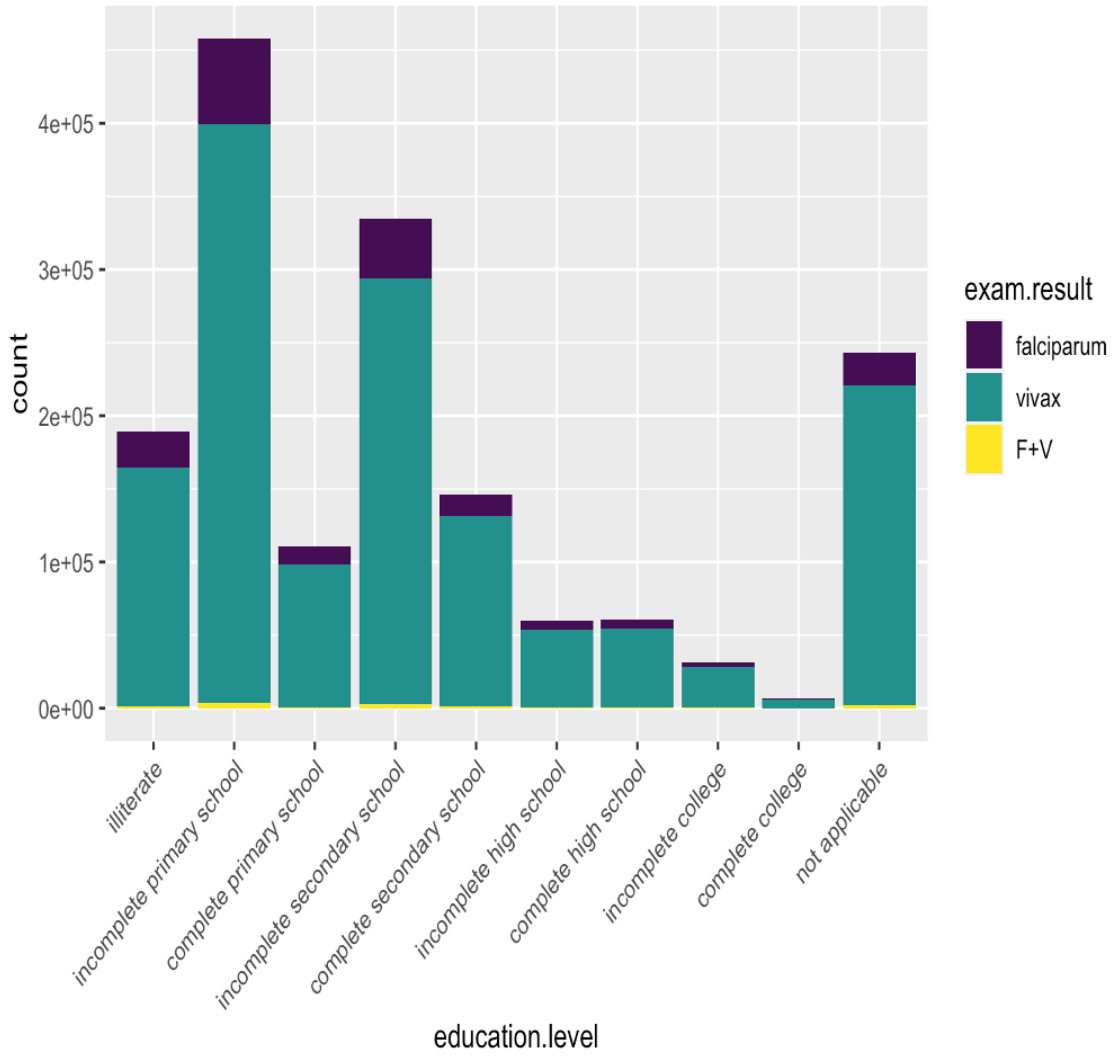


Figure 5.2: The relationship between a patients' education and the relative proportion of malaria cases for *Plasmodium falciparum, Plasmodium vivax and co-infections.*

#### 5.0.2.3 Conclusions

Based on the data analysis performed and the results obtained, it appears that the two species of malaria show a correlation in their infection process. We have predicted the opposite in our model with quiescence in chapter 4. The results agree with the predictions of the co-infection model without quiescence that the species infections are positively correlated. Our possible explanations include that 1) quiescence in *P. vivax* is not strong enough to influence the correlation and co-infections, 2) our model is too naive and misses some other assumptions to generate the correlation under quiescence, or 3) the number of infection data are too few to capture the lack of correlation introduced by quiescence.

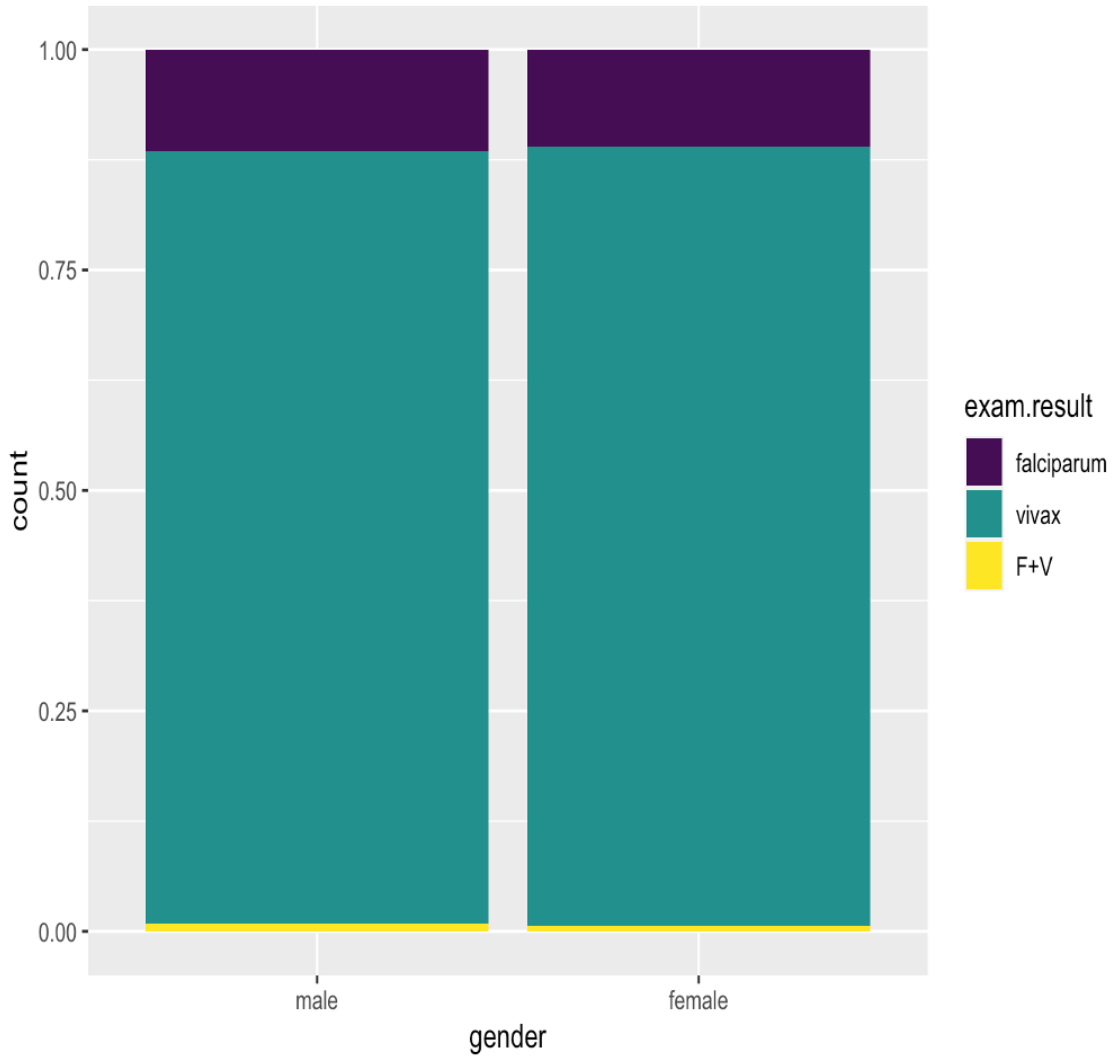


Figure 5.3: The relationship between a patients' gender and the relative proportion of malaria cases for *Plasmodium falciparum, Plasmodium vivax and simultaneous infections.*

### 5.0.3 Discussion on assumptions of our models

Models are simplified representation of reality, meaning that we believe our predictions are robust but may present limitations. In this research, we make simplifying assumptions regarding the spatial structure of populations and on the mechanism of quiescence. 1) We neglect the spatial structure, namely a subdivision of populations according to geographical location. We assume here a homogeneous mixing population, and our model does not capture the heterogeneity of the population for disease transmission. This is a very important factor as we consider malaria burden that affects whole continents. In reality the world population, and even within continents, is heterogeneous meaning that each location in the world has its own rate of disease transmission and recovery [22]. For example the climate change/ condition (which may affect the parameters of the disease process) differs from one geographical location to the other. The severity and mortality

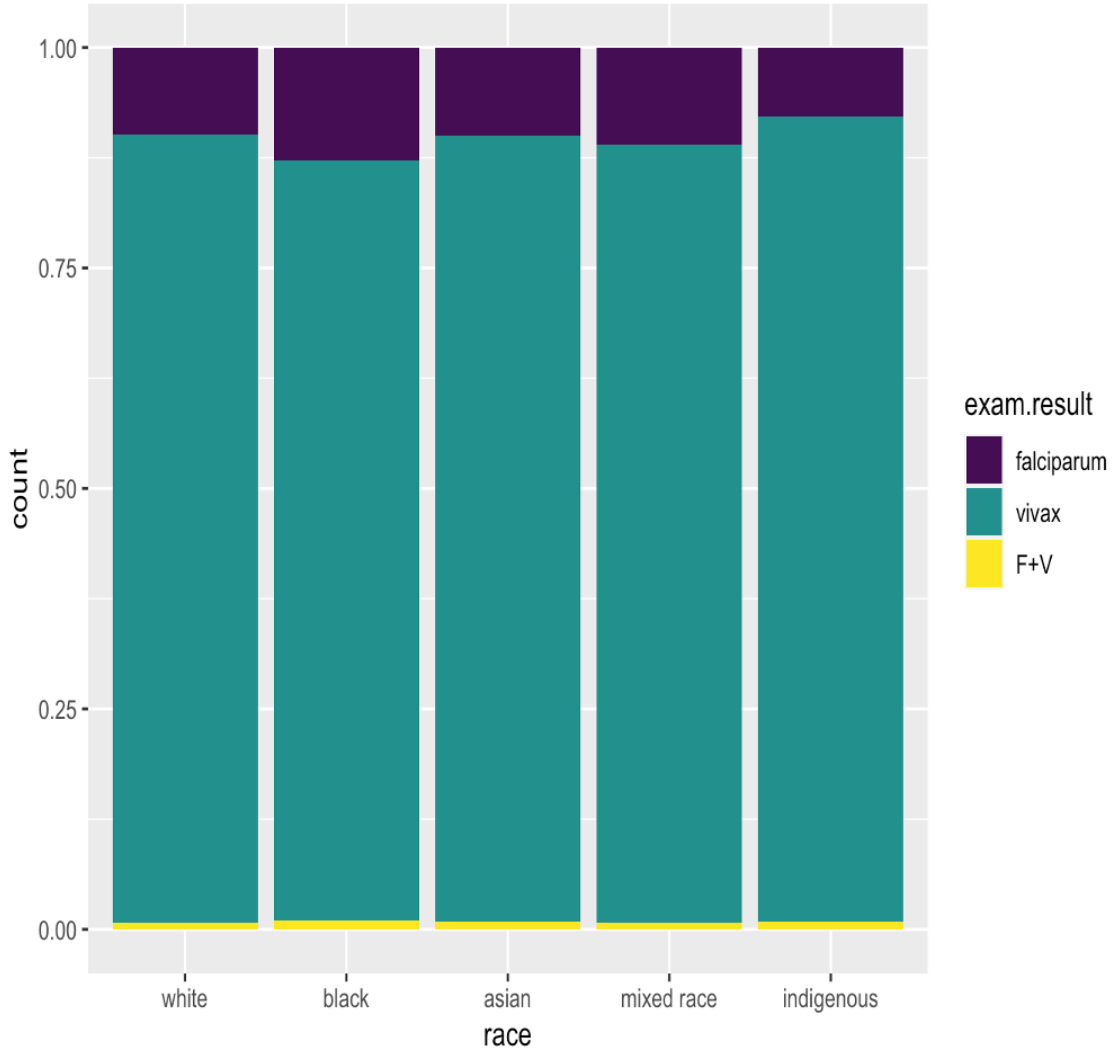


Figure 5.4: The relationship between a patients' race and the relative proportion of malaria cases for *Plasmodium falciparum, Plasmodium vivax and simultaneous infections.*

rates of malaria infection is also not evenly distributed across the globe. With the underlying homogeneity of parameters across different locations, our deterministic model predicts the same solution at different location of the world. For application of our models, specific adaptation of the relevant parameters should be done. We have also note that malaria transmission is seasonal which heavenly depends on the particular location of the world. The distribution of malaria species is also not evenly distributed across the world, as the distribution of *Plasmodium falciparum* is very much centred in Africa where malaria is endemic, while the distribution of *Plasmodium vivax* is centred in Africa but also common in Asia, India, South-America. Furthermore, an additional level of heterogeneity is found across individuals. For example for malaria, individuals are heterogeneous with respect of their naturally acquired immunity, their genetic resistance level, number of co-morbidities, and the drug treatment they take in order to clear off the disease [53,

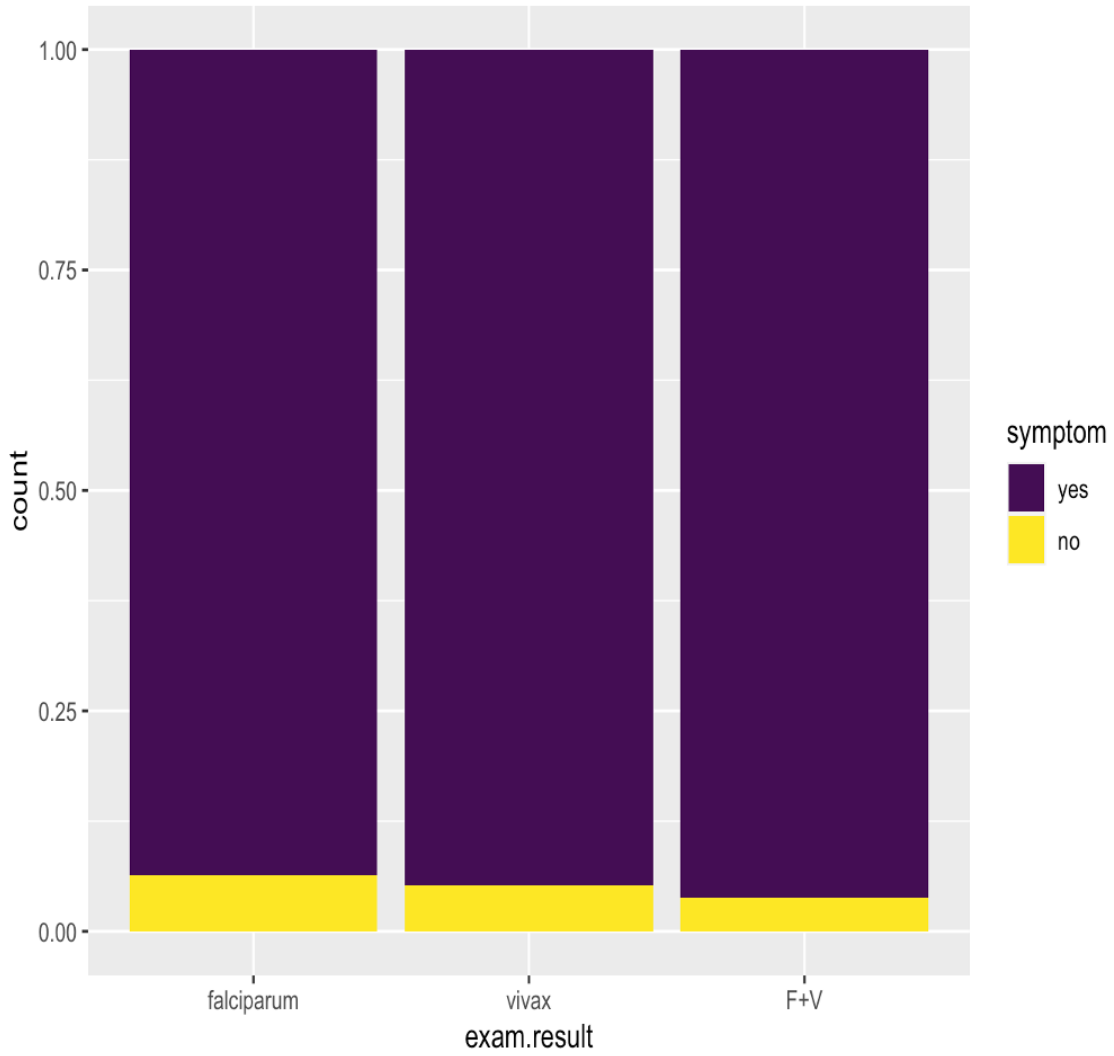


Figure 5.5: The relationship between a patients' symptoms and the relative proportion of malaria cases.

39]. 2) Another main assumption is that parasite becomes dormant after infecting an individual. The transmission of infectious disease is characterised by the level / amount of pathogens present within the host. In order to infect a new host, the pathogen load has to reach a certain amount of infectious propagules to enable the disease transmission. After becoming infected with the parasite/pathogen, instead of growing, under quiescence the parasites stops growing inside the host for some period of time. In this research we assume that a single individual becomes infectious, and we then follow the fate of infection from that individual to assess if the disease persists or becomes pandemic.

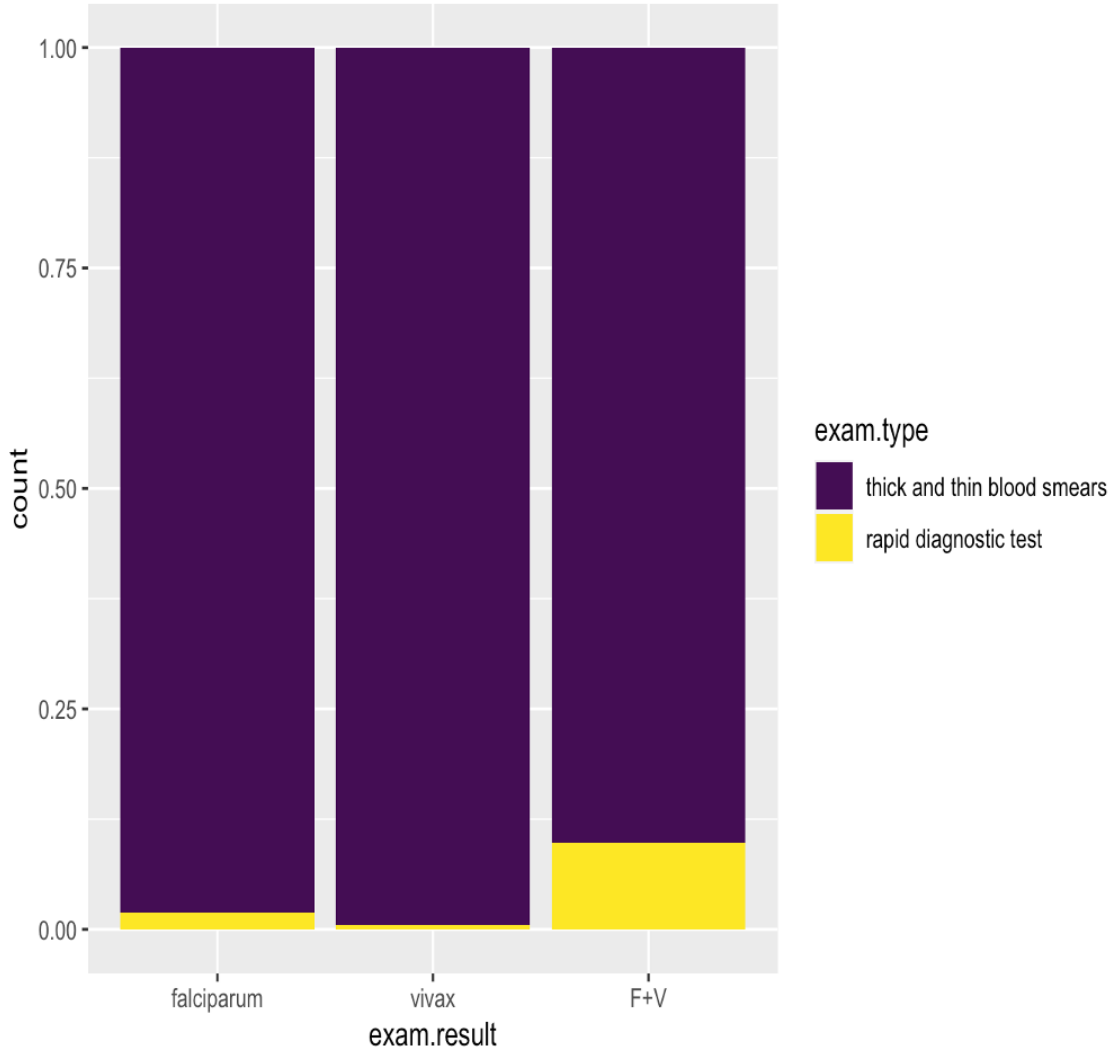


Figure 5.6: The relationship between a patients' exam and the relative proportion of malaria cases.

### 5.0.4 Outlooks: Future direction

Our results call for more investigation of the advantage of quiescence for human/animal/plant parasites. The classic assumption is that quiescence is a bet hedging strategy [102] and may evolve in very peculiar conditions. First, the question that I want to address in future is for example what is the disadvantage for parasite of doing quiescence? In this thesis we studied the effect of parasite quiescence/dormancy, once it is established as an evolutionary strategy. As quiescence affects disease dynamics, the length and severity of epidemics, it is of importance to find out effective disease management strategies for example against dormant malaria parasites. Secondly, my work in the future may consider investigating in more depth the influence of quiescence on the prevalence of co-infections, of the length and the determinants of the quiescence stage and the effect of quiescence on the stochastic disease transmission in human diseases. For example, it is

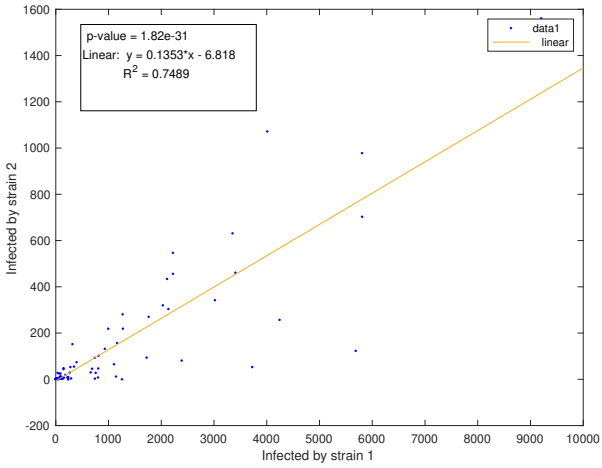


(a)

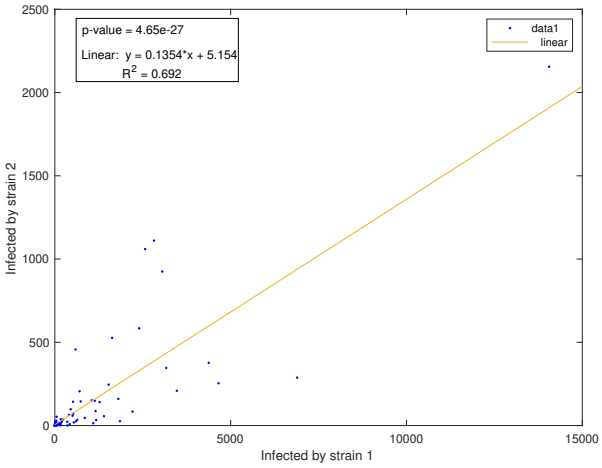


(b)

Figure 5.7: **(a)** Correlation between number of infected of parasites 1 and 2 of the SIVEP-Malaria data for the year 2009. **(b)** Correlation between number of infected of parasites 1 and 2 of the SIVEPMalaria data for the year 2010.

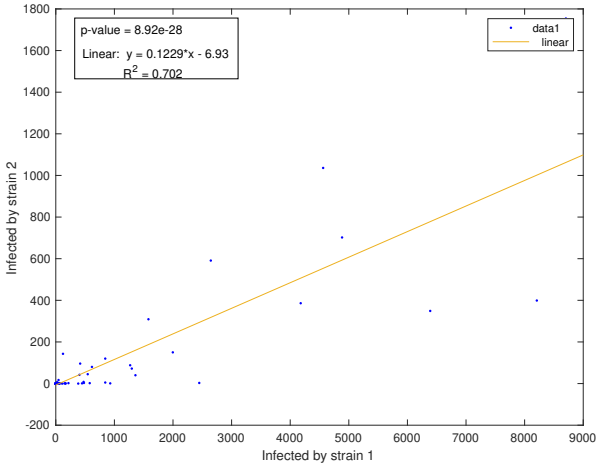


(a)

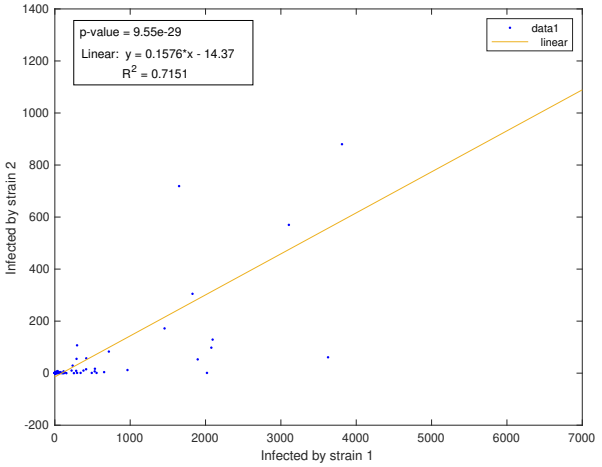


(b)

Figure 5.8: **(a)** Correlation between number of infected of parasites 1 and 2 of the SIVEP-Malaria data for the year 2015. **(b)** Correlation between number of infected of parasites 1 and 2 of the SIVEPMalaria data for the year 2019.

unclear whether co-infections between strains may be facilitated or antagonized by the presence of quiescence, namely what is the role of quiescence in triggering/slowing down the host immune system when exposed to a second strain. Third, a topic of interest is the evolution of parasite virulence. It is well documented in the literature that under co-infection, there is evolution of

more virulent strains by competition between new variants than the resident strain. A direction of future work may thus investigate and predict how parasite virulence is affected under the influence of quiescence.

# Appendix A

# Appendix

## A.1 Equilibrium Solution of the Model with Quiescent

From equations 5 and 4 of system (3.2.1), the quiescence compartments, we find the equilibrium solutions and is given as follows

$$Q_1^* = \frac{\rho_1 I_1}{\zeta_1 + d,}, Q_2^* = \frac{\rho_2 I_2}{\zeta_2 + d}. \quad \text{Let} \quad c_1 = \frac{\rho_1}{\zeta_1 + d}, c_2 = \frac{\rho_2}{\zeta_2 + d},$$

then the equilibrium solutions of the infected compartment (equations 1 and 2 of system (3.2.1) are given by

$$I_1^* = \frac{\epsilon_1}{d + \gamma_1 + \nu_1 + \rho_1 - \zeta_1 c_{11} - \beta_1 H^*}, I_2^* = \frac{\epsilon_2}{d + \gamma_2 + \nu_2 + \rho_2 - \zeta_2 c_{12} - \beta_2 H^*}.$$

Now we need to calculate the equilibrium solution in the healthy compartment, to do so we need the following propositions.

**Proposition 1.** *For $\epsilon_1, \epsilon_2 > 0$, there is at least one non-negative equilibrium solution in the healthy compartment.*

*Proof.* Substituting the equilibrium solutions of the quiescence and infected compartments as calculated above in the first equation of the system (3.2.1), we have

$$P(H) = \Lambda(d + \gamma_1 + \nu_1 + \rho_1 - \zeta_1 c_1 - \beta_1 H)(d + \gamma_2 + \nu_2 + \rho_2 - \zeta_2 c_2 - \beta_2 H) - \beta_1 H \epsilon_1 (d + \gamma_2 + \nu_2 + \rho_2 - \zeta_2 c_2 - \beta_2 H) - \beta_2 H \epsilon_2 (d + \gamma_1 + \nu_1 + \rho_1 - \zeta_1 c_1 - \beta_1 H) - dH(d + \gamma_1 + \nu_1 + \rho_1 - \zeta_1 c_1 - \beta_1 H)(d + \gamma_2 + \nu_2 + \rho_2 - \zeta_2 c_2 - \beta_2 H) + \nu_1 \epsilon_1 (d + \gamma_2 + \nu_2 + \rho_2 - \zeta_2 c_2 - \beta_2 H) + \nu_2 \epsilon_2 (d + \gamma_1 + \nu_1 + \rho_1 - \zeta_1 c_1 - \beta_1 H),$$

then

$$P(0) = \Lambda(d + \gamma_1 + \nu_1 + \rho_1 - \zeta_1 c_1)(d + \gamma_2 + \nu_2 + \rho_1 - \zeta_1 c_1) + \nu_1 \epsilon_1 (d + \gamma_2 + \nu_2 + \rho_2 -$$

$\zeta_2 c_2) + \nu_2\epsilon_2(d + \gamma_1 + \nu_1 + \rho_1 - \zeta_1 c_1) > 0,$

because the terms inside brackets are all positive, and $P(H) \to -\infty$, then by intermediary value theorem there exist $H^*$ such that

$$P(H^*) = 0, H^* > 0$$

Please observe that other compartments $(I_1^*, I_2^*, Q_1^*, Q_2^*)$ for $H^*$ are non-negative, since

$$P\Big(\frac{d + \gamma_1 + \nu_1 + \rho_1 - \zeta_1 c_1}{\beta_1}\Big) < 0, \implies H^* \leq \frac{d + \gamma_1 + \nu_1 + \rho_1 - \zeta_1 c_1}{\beta_1} \implies I_1^* \geq 0,$$

by the same argument, we show that $I_2^* > 0$. Since $I_1^*, I_2^* > 0$, then $Q_1^*, Q_2^* > 0$ □

In the above proposition 1, we find a polynomial of degree three in which we use intermediate value theorem to show that the polynomial has a solution.

**Uniqueness of The Equilibrium Solution**
We introduce the terms $a, b, c, e$ defined bellow, with this notation, we obtain the following proposition —

**Proposition 2.** *If $b^2 < 3ac$ , then there is a unique non-negative equilibrium solution of $P(H)$.*

*Proof.* Let

$$P(H) = aH^3 + bH^2 + cH + e = 0,$$
$$\frac{dP}{dH} = 3aH^2 + 2bH^2 + c = 0. \tag{A.1.1}$$

The solution of quadratic equation (A.1.1) is

$$H = \frac{-(2b) \pm \sqrt{(2b)^2 - 4(3a)c}}{2(3a)} \tag{A.1.2}$$

where

$$a = -3\beta_1\beta_2 d,$$

$b = 2d\beta_1\rho_2 + 2d\beta_2\rho_1 + 2d\beta_1\nu_2 + 2d\beta_1\nu_1 - 2c_{12}d\beta_1\zeta_2 - 2c_{11}d\beta_2\zeta_1 + 2\beta_1\beta_2\epsilon_2 + 2\beta_1\beta_2\epsilon_1 + 2d\beta_1\gamma_2 + 2d\beta_1\gamma_1 + 2\Lambda\beta_1\beta_2 + 2d^2\beta_2 + 2d^2\beta_1,$

$c = -\beta_1\epsilon_1\nu_2 - \Lambda\beta_1\nu_2 - \beta_2\epsilon_1\nu_1 - \Lambda\beta_2\nu_1 - d\rho_1\rho_2 - d\nu_1\rho_2 + c_{11}d\zeta_1\rho_2 - \beta_1\epsilon_1\rho_2 - d\gamma_1\rho_2 - \Lambda\beta_1\rho_2 - d^2\rho_2 - d\nu_2\rho_1 + c_{12}d\zeta_2\rho_1 - \beta_2\epsilon_2\rho_1 - d\gamma_2\rho_1 - \Lambda\beta_2\rho_1 - d^2\rho_1 - d\nu_1\nu_2 + c_{11}d\zeta_1\nu_2 - \beta_1\epsilon_2\nu_2 - d^2\nu_2 + c_{12}d\zeta_2\nu_1 - \beta_2\epsilon_2\nu_1 - d\gamma_2\nu_1 - d^2\nu_1 - c_{11}c_{12}d\zeta_1\zeta_2 + c_{12}\beta_1\epsilon_1\zeta_2 + c_{12}d\gamma_1\zeta_2 + c_{12}\Lambda\beta_1\zeta_2 + c_{12}d^2\zeta_2 + c_{11}\beta_2\epsilon_2\zeta_1 + c_{11}d\gamma_2\zeta_1 + c_{11}\Lambda\beta_2\zeta_1 + c_{11}d^2\zeta_1 - \beta_2\gamma_1\epsilon_2 - d\beta_2\epsilon_2 - \beta_1\gamma_2\epsilon_1 - d\beta_1\epsilon_1 - d\gamma_1\gamma_2 - \Lambda\beta_1\gamma_2 - d^2\gamma_2 - \Lambda\beta_2\gamma_1 - d^2\gamma_1 - \Lambda d\beta_1 - d^3,$

$e = \epsilon_1\nu_1\nu_2 + \Lambda\nu_1\nu_2 + \gamma_2\epsilon_1\nu_1 + \Lambda\gamma_1\nu_2 + d\epsilon_1\nu_1 + \Lambda\gamma_2\nu_1 + d\Lambda\nu_1 + \epsilon_2\nu_1\nu_2 + \gamma_1\epsilon_2\nu_2 + d\epsilon_2\nu_2 + \Lambda\gamma_1\gamma_2 + d\Lambda\gamma_1,$

choose parameter values so that

$$b^2 < 3ac,$$

then the quadratic equation (A.1.2) does not have real solution. □

In the above proof, we use calculus to find the maximum value of the polynomial. The analysis shows that the polynomial does not have a maximum or minimum value at the specified interval. This shows that the polynomial has only one root by proposition 1 (existence of a solution) above.

## A.2 Proof of Theorem 2 stated in Chapter 3

We now proof Theorem 2 stated in Chapter 3 above regarding the stability of the matrix $B$ defined in (3.2.3).

*Proof.* The characteristics polynomial of $B$ is given by

$$\lambda^5 + b_1\lambda^4 + b_2\lambda^3 + b_3\lambda^2 + b_4\lambda + b_5 = 0$$

where

$$b_1 = \rho_1 + \rho_2 + \zeta_1 + \zeta_2 - \mathrm{tr(A)}$$

$$b_2 = \rho_1\rho_2 + \rho_1\zeta_1 + \rho_2\zeta_1 + \zeta_1\zeta_2 - \zeta_1\mathrm{tr(A)} - \zeta_2\mathrm{tr(A)} - (a_{11} + a_{33})\rho_2 - (a_{22} + a_{33})\rho_1 + a_2$$

$$b_3 = \zeta_1 a_2 + \zeta_2 a_2 + (a_{11}a_{33} - a_{13}a_{31})\rho_2 + (a_{22}a_{33} - a_{23}a_{32})\rho_1 - \det(\mathrm{A}) - \zeta_1\zeta_2\mathrm{tr(A)}$$

$$- (a_{22} + a_{33})\rho_1\zeta_2 - a_{33}\rho_1\rho_2 - a_{33}\rho_2\zeta_1 - a_{11}\rho_2\zeta_1$$

$$b_4 = \zeta_1\zeta_2 a_2 + (a_{22}a_{33} - a_{23}a_{32})\rho_1\zeta_2 + (a_{11}a_{33} - a_{13}a_{31})\rho_2\zeta_1 - (\zeta_1 + \zeta_2)\det(\mathrm{A})$$

$$b_5 = -\zeta_1\zeta_2\det(\mathrm{A})$$

*Step 1:*

By Routh-Hurwitz Criterion [49, 80, 66] , the matrix $B$ is stable if and only if the following conditions hold:

- $b_i > 0 \quad (i = 1, \ldots, 5)$
- $b_1 b_2 b_3 > b_3^2 + b_1^2 b_4$
- $(b_1 b_4 - b_5)(b_1 b_2 b_3 - b_3^2 - b_1^2 b_4) > b_5(b_1 b_2 - b_3)^2 + b_1 b_5^2$

  *Step 2*

Suppose that for all $\rho_1, \rho_2, \zeta_1, \zeta_2 > 0$

- $b_1 > 0$

  $= \rho_1 + \rho_2 + \zeta_1 + \zeta_2 - \text{tr(A)} > 0 \implies \text{tr(A)} \leq 0$

- $b_2 > 0$

  $= \rho_1\rho_2 + \rho_1\zeta_1 + \rho_2\zeta_1 + \zeta_1\zeta_2 - \zeta_1\text{tr(A)} - \zeta_2\text{tr(A)} - (a_{11} + a_{33})\rho_2 - (a_{22} + a_{33})\rho_1 + a_2 > 0$

  $\implies \text{tr(A)} \leq 0, \quad a_{11} \leq 0, \quad a_{22} \leq 0, \quad \text{and} \quad a_{33} \leq 0$

- $b_3 > 0$

  $= \zeta_1 a_2 + \zeta_2 a_2 + (a_{11}a_{33} - a_{13}a_{31})\rho_2 + (a_{22}a_{33} - a_{23}a_{32})\rho_1 - \det\text{(A)} - \zeta_1\zeta_2\text{tr(A)}$

  $- (a_{22} + a_{33})\rho_1\zeta_2 - a_{33}\rho_1\rho_2 - a_{33}\rho_2\zeta_1 - a_{11}\rho_2\zeta_1 > 0$

  $\implies \det\text{(A)} < 0, \quad \text{tr(A)} \leq 0, \quad a_{11} \leq 0, \quad a_{22} \leq 0,$

  $a_{33} \leq 0, \quad a_{13}a_{31} \leq a_{11}a_{33}, \quad \text{and} \quad a_{23}a_{32} \leq a_{22}a_{33}$

- $b_4 > 0$

  $\implies \zeta_1\zeta_2 a_2 + (a_{22}a_{33} - a_{23}a_{32})\rho_1\zeta_2 + (a_{11}a_{33} - a_{13}a_{31})\rho_2\zeta_1 > (\zeta_1 + \zeta_2)\det\text{(A)}$

  $\implies \det\text{(A)} < 0, \quad a_{13}a_{31} \leq a_{11}a_{33}, \quad \text{and} \quad a_{23}a_{32} \leq a_{22}a_{33}$

- $b_5 > 0$

  $= -\zeta_1\zeta_2\det\text{(A)} > 0 \implies \det\text{(A)} < 0$

  *Step 3:*

  Assume that $\det\text{(A)} < 0, \quad \text{tr(A)} \leq 0, \quad a_2 > 0, \quad a_{11} \leq 0, \quad a_{22} \leq 0, \quad a_{33} \leq 0,$

  $a_{13}a_{31} \leq a_{11}a_{33}, \quad a_{23}a_{32} \leq a_{22}a_{33}$. then for all $\rho_1, \rho_2, \zeta_1, \zeta_2 > 0$, we have

- $\rho_1 + \rho_2 + \zeta_1 + \zeta_2 - \mathrm{tr(A)} = b_1 > 0$

- $\rho_1\rho_2 + \rho_1\zeta_1 + \rho_2\zeta_1 + \zeta_1\zeta_2 - \zeta_1\mathrm{tr(A)} - \zeta_2\mathrm{tr(A)} - (a_{11} + a_{33})\rho_2 - (a_{22} + a_{33})\rho_1 + a_2 = b_2 > 0$

- $\zeta_1 a_2 + \zeta_2 a_2 + (a_{11}a_{33} - a_{13}a_{31})\rho_2 + (a_{22}a_{33} - a_{23}a_{32})\rho_1 - \det(\mathrm{A}) - \zeta_1\zeta_2\mathrm{tr(A)} - (a_{22} + a_{33})\rho_1\zeta_2 - a_{33}\rho_1\rho_2 - a_{33}\rho_2\zeta_1 - a_{11}\rho_2\zeta_1 = b_3 > 0$

- $\zeta_1\zeta_2 a_2 + (a_{22}a_{33} - a_{23}a_{32})\rho_1\zeta_2 + (a_{11}a_{33} - a_{13}a_{31})\rho_2\zeta_1 - (\zeta_1 + \zeta_2)\det(\mathrm{A}) = b_4 > 0$

- $-\zeta_1\zeta_2\det(\mathrm{A}) = b_5 > 0$

- $$\begin{aligned}
&(\rho_1 + \rho_2 + \zeta_1 + \zeta_2 - \mathrm{tr(A)})(\rho_1\rho_2 + \rho_1\zeta_1 + \rho_2\zeta_1 + \zeta_1\zeta_2 - \zeta_1\mathrm{tr(A)} - \zeta_2\mathrm{tr(A)} \\
&- (a_{11} + a_{33})\rho_2 - (a_{22} + a_{33})\rho_1 + a_2)(-\det(\mathrm{A}) + \zeta_1 a_2 + \zeta_2 a_2 + (a_{11}a_{33} - a_{13}a_{31})\rho_2 \\
&+ (a_{22}a_{33} - a_{23}a_{32})\rho_1 - (a_{22} + a_{33})\rho_1\zeta_2 - a_{33}\rho_1\rho_2 - a_{33}\rho_2\zeta_1 - a_{11}\rho_2\zeta_1 - \zeta_1\zeta_2\mathrm{tr(A)}) \\
&- (-\det(\mathrm{A}) + \zeta_1 a_2 + \zeta_2 a_2 + (a_{11}a_{33} - a_{13}a_{31})\rho_2 + (a_{22}a_{33} - a_{23}a_{32})\rho_1 - (a_{22} + a_{33})\rho_1\zeta_2 \\
&- a_{33}\rho_1\rho_2 - a_{33}\rho_2\zeta_1 - a_{11}\rho_2\zeta_1 - \zeta_1\zeta_2\mathrm{tr(A)})^2 - (\rho_1 + \rho_2 + \zeta_1 + \zeta_2 - \mathrm{tr(A)})^2(-\zeta_1\det(\mathrm{A}) \\
&- \zeta_2\det(\mathrm{A}) + \zeta_1\zeta_2 a_2 + (a_{22}a_{33} - a_{23}a_{32})\rho_1\zeta_2 + (a_{11}a_{33} - a_{13}a_{31})\rho_2\zeta_1) \\
&= b_1 b_2 b_3 - b_3^2 - b_1^2 b_4 > 0 \\
&\implies b_1 b_2 b_3 > b_3^2 + b_1^2 b_4.
\end{aligned} \tag{A.2.1}$$

  For the full expansion of equation (A.2.1) for all $\rho_1 > 0, \rho_2 > 0, \zeta_1 > 0, \zeta_2 > 0$, see the wxMaxima output (as online available notebook).

•

$$\Big((\rho_1+\rho_2+\zeta_1+\zeta_2-\mathrm{tr(A)})(-\zeta_1\mathrm{det(A)}-\zeta_2\mathrm{det(A)}+\zeta_1\zeta_2a_2+(a_{22}a_{33}-a_{23}a_{32})\rho_1\zeta_2$$

$$+(a_{11}a_{33}-a_{13}a_{31})\rho_2\zeta_1)-(\zeta_1\zeta_2\mathrm{det(A)})\Big)\Big((\rho_1+\rho_2+\zeta_1+\zeta_2-\mathrm{tr(A)})(\rho_1\rho_2+\rho_1\zeta_1$$

$$+\rho_2\zeta_1+\zeta_1\zeta_2-\zeta_1\mathrm{tr(A)}-\zeta_2\mathrm{tr(A)}-(a_{11}+a_{33})\rho_2-(a_{22}+a_{33})\rho_1+a_2)$$

$$(-\mathrm{det(A)}+\zeta_1a_2+\zeta_2a_2+(a_{11}a_{33}-a_{13}a_{31})\rho_2$$

$$+(a_{22}a_{33}-a_{23}a_{32})\rho_1-(a_{22}+a_{33})\rho_1\zeta_2-a_{33}\rho_1\rho_2-a_{33}\rho_2\zeta_1-a_{11}\rho_2\zeta_1-\zeta_1\zeta_2\mathrm{tr(A)})$$

$$-(-\mathrm{det(A)}+\zeta_1a_2+\zeta_2a_2+(a_{11}a_{33}-a_{13}a_{31})\rho_2+(a_{22}a_{33}-a_{23}a_{32})\rho_1-(a_{22}+a_{33})\rho_1\zeta_2$$

$$-a_{33}\rho_1\rho_2-a_{33}\rho_2\zeta_1-a_{11}\rho_2\zeta_1-\zeta_1\zeta_2\mathrm{tr(A)}))^2-(\rho_1+\rho_2+\zeta_1+\zeta_2-\mathrm{tr(A)})^2$$

$$-(\rho_1+\rho_2+\zeta_1+\zeta_2-\mathrm{tr(A)})(-\zeta_1\mathrm{det(A)}-\zeta_2\mathrm{det(A)}+\zeta_1\zeta_2a_2+(a_{22}a_{33}-a_{23}a_{32})\rho_1\zeta_2$$

$$+(a_{11}a_{33}-a_{13}a_{31})\rho_2\zeta_1)\Big)$$

$$-(\zeta_1\zeta_2\mathrm{det(A)})\Big((\rho_1+\rho_2+\zeta_1+\zeta_2-\mathrm{tr(A)})(\rho_1\rho_2+\rho_1\rho_1+\rho_2\zeta_1+\zeta_1\zeta_2-\zeta_1\mathrm{tr(A)}-\zeta_2\mathrm{tr(A)}$$

$$-(a_{11}+a_{33})\rho_2-(a_{22}+a_{33})\rho_1+a_2)-(-\mathrm{det(A)}+\zeta_1a_2+\zeta_2a_2+(a_{11}a_{33}-a_{13}a_{31})\rho_2$$

$$+(a_{22}a_{33}-a_{23}a_{32})\rho_1-(a_{22}+a_{33})\rho_1\zeta_2-a_{33}\rho_1\rho_2-a_{33}\rho_2\zeta_1-a_{11}\rho_2\zeta_1-\zeta_1\zeta_2\mathrm{tr(A)})\Big)^2$$

$$-(\rho_1+\rho_2+\zeta_1+\zeta_2-\mathrm{tr(A)})(-\zeta_1\zeta_2\mathrm{det(A)})^2>0$$

$$=(b_1b_4-b_5)(b_1b_2b_3-b_3^2-b_1^2b_4)-b_5(b_1b_2-b_3)^2-b_1b_5^2>0 \tag{A.2.2}$$

$$\implies (b_1b_4-b_5)(b_1b_2b_3-b_3^2-b_1^2b_4)>b_5(b_1b_2-b_3)^2+b_1b_5^2$$

For the full expansion of equation (A.2.2) for all $\rho_1>0,\rho_2>0,\zeta_1>0,\zeta_2>0$, see the wxMaxima output (as online available notebook).

□

## A.3 Description of the model without quiescence

In this section we will develop a mathematical model that describes the evolution of single Host-two parasites with constant recruitment rate. The model without quiescence is given by these set (system) of ordinary differential equations:

$$\begin{aligned}
\frac{dI_1}{dt} &= \beta_1 H I_1 - dI_1 - \gamma_1 I_1 - \nu_1 I_1 + \epsilon_1 \\
\frac{dI_2}{dt} &= \beta_2 H I_2 - dI_2 - \gamma_2 I_2 - \nu_2 I_2 + \epsilon_2 \\
\frac{dH}{dt} &= \Lambda - \beta_1 H I_1 - \beta_2 H I_2 - dH + \nu_1 I_1 + \nu_2 I_2
\end{aligned} \tag{A.3.1}$$

**Steady State Solution of the System**

The analysis of steady state of the the system without quiescence (A.3.1) has the same steps and similar results as for the system with quiescence.

**Transition Probabilities**

Table A.1: Transitions rates of the model without quiescence A.3.1

| Type | Transition | Rate |
|---|---|---|
| birth of healthy host $H$ | $(H_t, I_{1t}, I_{2t}) \to (H_t + 1, I_{1t}, I_{2t})$ | $\Lambda\Delta t + o\Delta(t)$ |
| natural death of $H$ | $(H_t, I_{1t}, I_{2t}) \to (H_t - 1, I_{1t}, I_{2t})$ | $dH\Delta t + o\Delta(t)$ |
| infection of $H$ by $I_1$ | $(H_t, I_{1t}, I_{2t}) \to (H_t - 1, I_{1t} + 1, I_{2t})$ | $\beta_1 H I_1 \Delta t + o\Delta(t)$ |
| infection of $H$ by $I_2$ | $(H_t, I_{1t}, I_{2t}) \to (H_t - 1, I_{1t}, I_{2t} + 1)$ | $\beta_2 H I_2 \Delta t + o\Delta(t)$ |
| death of $I_1$ | $(H_t, I_{1t}, I_{2t}) \to (H_t, I_{1t} - 1, I_{2t})$ | $(d + \gamma_1) I_1 \Delta t + o\Delta(t)$ |
| death of $I_2$ | $(H_t, I_{1t}, I_{2t}) \to (H_t, I_{1t}, I_{2t} - 1)$ | $(d + \gamma_1) I_2 \Delta t + o\Delta(t)$ |
| recovery $I_1$ & replacement $H$ | $(H_t, I_{1t}, I_{2t}) \to (H_t + 1, I_{1t} - 1, I_{2t})$ | $\nu_1 I_1 \Delta t + o\Delta(t)$ |
| recovery $I_2$ & replacement $H$ | $(H_t, I_{1t}, I_{2t}) \to (H_t + 1, I_{1t} 1, I_{2t} - 1)$ | $\nu_2 I_2 \Delta t + o\Delta(t)$ |
| immigration to $I_1$ | $(H_t, I_{1t}, I_{2t}) \to (H_t, I_{1t} + 1, I_{2t})$ | $\epsilon_1 \Delta t + o\Delta(t)$ |
| immigration to $I_2$ | $(H_t, I_{1t}, I_{2t}) \to (H_t, I_{1t}, I_{2t} + 1)$ | $\epsilon_2 \Delta t + o\Delta(t)$ |

**Master equation**

Let $p(i, j, k)(t) = \text{Prob}\{H(t) = i, I_1(t) = j, I_2(t) = k\}$, then

$$\begin{aligned}
\frac{\mathrm{d}p_{(i,j,k)}}{\mathrm{d}t} =& \Lambda p_{(i-1,j,k)} + d(i+1)p_{(i+1,j,k)} + \beta_1(i+1)(j-1)p_{(i+1,j-1,k)} \\
&+ (d+\gamma_1)(j+1)p_{(i,j+1,k)} + \beta_2(i+1)(k-1)p_{(i+1,j,k-1)} + (d+\gamma_2)(k+1)p_{(i,j,k+1)} \\
&+ \nu_1(j+1)p_{(i-1,j+1,k)} + \nu_2(k+1)p_{(i-1,j,k+1)} + \epsilon_1 p_{(i,j-1,k)} + \epsilon_2 p_{(i,j,k-1)} \\
&- \left[\Lambda + di + \beta_1 ij + (d+\gamma_1)j + \beta_2 ik + (d+\gamma_2)k + \nu_1 j + \nu_2 k + \epsilon_1 + \epsilon_2\right] p_{(i,j,k)}
\end{aligned} \tag{A.3.2}$$

This master equation (A.3.2) is then used to work out the *Kramers-Moyal expansion* that led to the derivation of the *Fokker-Planck equation* below.

**Derivation of Fokker-Planck Equation**

Now, let

$$p(i,j,k) = \int_{ih-\frac{h}{2}}^{ih+\frac{h}{2}} \int_{jh-\frac{h}{2}}^{jh+\frac{h}{2}} \int_{kh-\frac{h}{2}}^{kh+\frac{h}{2}} u(x,y,z)dxdydz + o(h^4),$$

let also $x = ih, y = jh, z = kh$ and $h = \frac{1}{N}$. We then performed *Kramers-Moyal expansion* to derived the following Fokker-Planck equation which is given as follows.

$$\begin{aligned}
\partial_t u(x,y,t) = & -\partial_x\{h\lambda - dx - \beta_1 xy - \beta_2 xz + \nu_1 y + \nu_2 z\}u(x,y,z) \\
& -\partial_y\{\beta_1 xy - (d+\gamma_1)y - \nu_1 y + h\epsilon_1\}u(x,y,z) \\
& -\partial_z\{\beta_2 xy - (d+\gamma_2)y - \nu_2 y + h\epsilon_2\}u(x,y,z) \\
& +\frac{h}{2}\partial_{xx}\{\lambda + dx + \beta_1 xy + \beta_2 xz + \nu_1 y + \nu_2 z\}u(x,y,z) \\
& -h\partial_{xy}\{\beta_1 xy + \nu_1 y\}u(x,y,z) \\
& +\frac{h}{2}\partial_{yy}\{\beta_1 xy + (d+\gamma_1)y + \nu_1 y + \epsilon_1\}u(x,y,z) \\
& -h\partial_{xz}\{\beta_2 xz + \nu_2 z\}u(x,y,z) \\
& +\frac{h}{2}\partial_{zz}\{\beta_2 xy + (d+\gamma_1)y + \nu_2 y + \epsilon_2\}u(x,y,z)
\end{aligned} \tag{A.3.3}$$

**Linear Transformation of the Fokker-Planck equation**

**Theorem.** *The linear Fokker-Planck equation for the above non-linear Fokker-Planck can be written more compactly as follows*

$$\frac{\partial P(y,t)}{dt} = -\sum_{ij}^{3} M_{ij}\frac{\partial}{\partial y_i} y_i P(y,t) + \frac{1}{2}\sum_{ij}^{3} N_{ij}\frac{\partial^2}{\partial y_i \partial y_j} P(y,t) \tag{A.3.4}$$

*where $y = (x,y,z), N_{ij}$ is symmetric and positive definite, its solution is give as*

$$P(y,t) = (2\pi)^{\frac{1}{2}} det(\Sigma)^{\frac{1}{2}} exp(-\frac{1}{2} y\Sigma^{-1}y^T)$$

*with*

$$\Sigma^{-1} = 2\int_0^\infty e^{-Mt} N e^{-Mt} dt.$$

**Theorem.** *For every matrix $N$ which is symmetric and positive-definite, there a unique solution $\Sigma^{-1}$ to the following equation known as Lyapunov equation*

$$M\Sigma^{-1} + \Sigma^{-1}M^T = N$$

*where $\Sigma^{-1}$ is symmetric, positive-definite and equal to*

$$\Sigma^{-1} = \int_0^\infty e^{-Mt} N e^{-M^T t} dt.$$

The above theorem known as Lyapunov theorem which gives us the opportunity to compute covariance matrix more easily since matrices $M$ and $N$ are constant matrices,the only unknown is $\Sigma^{-1}$ matrix. We use MATLAB to obtain the covariance matrix $\Sigma^{-1}$ numerically. The stochastic matrices $M$ and $N$ for the system without quiescence are similar to those that of the system with quiescence.

## A.4 Stochastic Matrices of the Linear Fokker-Planck equation

$$M = \begin{pmatrix} -d-\beta_1 I_1^*-\beta_1 I_2^* & -\beta_1 H^*+\nu_1 & -\beta_1 H^*+\nu_2 & 0 & 0 \\ \beta_1 I_1^* & \beta_1 H^*-d-\gamma_1-\nu_1-\rho_1 & 0 & \zeta_1 & 0 \\ \beta_1 I_2^* & 0 & \beta_1 H^*-d-\gamma_2-\nu_2-\rho_2 & 0 & \zeta_2 \\ 0 & \rho_1 & 0 & -\zeta_1-d & 0 \\ 0 & 0 & \rho_2 & 0 & -\zeta_2-d \end{pmatrix}$$

$$N = \begin{pmatrix} n_{11} & -(\beta_1 H^* I_1^*+\nu_1 I_1^*) & -(\beta_1 H^* I_2^*+\nu_1 I_2^*) & 0 & 0 \\ -(\beta_1 H^* I_1^*+\nu_1 I_1^*) & n_{22} & 0 & -(\rho_1 I_1^*+\zeta_1 Q_1^*) & 0 \\ -(\beta_1 H^* I_2^*+\nu_1 I_2^*) & 0 & n_{33} & 0 & -(\rho_2 I_2^*+\zeta_2 Q_2^*) \\ 0 & -(\rho_1 I_1^*+\zeta_1 Q_1^*) & 0 & n_{44} & 0 \\ 0 & 0 & -(\rho_2 I_2^*+\zeta_2 Q_2^*) & 0 & n_{55} \end{pmatrix}$$

where

$$\begin{aligned} n_{11} &= \lambda + dH^* + \beta_1 H^* I_1^* + \beta_1 H^* I_2 + \nu_1 I_1^* + \nu_2 I_2^*, \\ n_{22} &= \beta_1 H^* I_1^* + (d+\gamma_1) I_1^* + \nu_1 I_1^* + \rho_1 I_2^* + \zeta_1 Q_1^* + \epsilon_1, \\ n_{33} &= \beta_1 H^* I_2^* + (d+\gamma_2) I_2^* + \nu_2 I_2^* + \rho_2 I_2^* + \zeta_2 Q_2^* + \epsilon_2, \\ n_{44} &= \rho_1 I_1^* + \zeta_1 Q_1^* + dQ_1^*, \\ n_{55} &= \rho_2 I_2^* + \zeta_2 Q_2^* + dQ_2^* \end{aligned}$$

and

$$H^*, I_1^*, I_2^*, Q_1^*, Q_2^*$$

are equilibrium solutions of (3.2.1) (rearranged in such away that healthy compartment comes first equation in the system. The order of the other compartments remains unchanged).

# List of Figures

# List of Tables

# Bibliography


[1] Hamid A Adamu, Murtala Muhammad, A Jingi, and Mahmud Usman. Mathematical modelling using improved sir model with more realistic assumptions. *Int. J. Eng. Appl. Sci*, 6(1):64–69, 2019.

[2] Martin S Alilio, Ib C Bygbjerg, and Joel G Breman. Are multilateral malaria research and control programs the most successful? lessons from the past 100 years in africa. In *The Intolerable Burden of Malaria II: What's New, What's Needed: Supplement to Volume 71 (2) of the American Journal of Tropical Medicine and Hygiene*. American Society of Tropical Medicine and Hygiene, 2004.

[3] Samuel Alizon, Jacobus C de Roode, and Yannis Michalakis. Multiple infections and the evolution of virulence. *Ecology letters*, 16(4):556–567, 2013.

[4] Linda JS Allen. *An introduction to stochastic processes with applications to biology*. CRC press, 2010.

[5] Linda JS Allen. Stochastic population and epidemic models. *Mathematical biosciences lecture series, stochastics in biological systems*, 2015.

[6] Linda JS Allen. A primer on stochastic epidemic models: Formulation, numerical simulation, and analysis. *Infect. Dis. Model.*, 2(2):128–142, 2017.

[7] LJ Allen, F Brauer, P van den Driessche, and J Wu. *Mathematical Epidemiology*. Springer, Verlag Berlin Heidelberg, 1 edition, 2008.

[8] Roy M Anderson and Robert M May. Population biology of infectious diseases: Part i. *Nature*, 280(5721):361–367, 1979.

[9] Roy M Anderson and Robert M May. *Infectious diseases of humans: dynamics and control*. Oxford university press, 1992.

[10] Roy M Anderson and Robert M May. *Infectious diseases of humans: dynamics and control*. Oxford university press, 1992.

[11] Håkan Andersson and Tom Britton. *Stochastic Epidemic Models and Their Statistical Analysis*. Springer, New York, 2000.

[12] Norman TJ Bailey et al. *The mathematical theory of infectious diseases and its applications*. Charles Griffin & Company Ltd, 5a Crendon Street, High Wycombe, Bucks HP13 6LE., 1975.

[13] Nathalie Q Balaban, Jack Merrin, Remy Chait, Lukasz Kowalik, and Stanislas Leibler. Bacterial persistence as a phenotypic switch. *Sci.*, 305(5690):1622–1625, 2004.

[14] Oliver Balmer and Marcel Tanner. Prevalence and implications of multiple-strain infections. *The Lancet Infect. Dis.*, 11(11):868–878, 2011.

[15] Lais Baroni, Marcel Pedroso, Christovam Barcellos, Rebecca Salles, Samella Salles, Balthazar Paixão, Alvaro Chrispino, Gustavo Guedes, and Eduardo Ogasawara. An integrated dataset of malaria notifications in the legal amazon. *BMC Research Notes*, 13(1), jun 2020.

[16] Katherine E Battle, Peter W Gething, Iqbal RF Elyazar, Catherine L Moyes, Marianne E Sinka, Rosalind E Howes, Carlos A Guerra, Ric N Price, J Kevin Baird, and Simon I Hay. The global public health significance of plasmodium vivax. *Advances in parasitology*, 80:1–111, 2012.

[17] Maria A Bautista, Changyi Zhang, and Rachel J Whitaker. Virus-induced dormancy in the archaeon sulfolobus islandicus. *MBio*, 6(2):e02565–14, 2015.

[18] Daniel Bernoulli. Essai d'une nouvelle analyse de la mortalité causée par la petite vérole, et des avantages de l'inoculation pour la prévenir. *Histoire de l'Acad., Roy. Sci.(Paris) avec Mem*, pages 1–45, 1760.

[19] Jochen Blath, Felix Hermann, and Martin Slowik. A branching process model for dormancy and seed banks in randomly fluctuating environments. *arXiv preprint arXiv:2007.06393*, 2020.

[20] Jochen Blath and András Tóbiás. Invasion and fixation of microbial dormancy traits under competitive pressure. *Stoch. Processes and their Appl.*, 130(12):7363–7395, 2020.

[21] Jochen Blath and András Tóbiás. Virus dynamics in the presence of contact-mediated host dormancy. *arXiv preprint arXiv:2107.11242*, 2021.

[22] T. Bousema, B. Kreuels, and R. Gosling. Adjusting for heterogeneity of malaria transmission in longitudinal studies. *Journal of Infectious Diseases*, 204(1):1–3, may 2011.

[23] Guillaume Cantin, Cristiana J Silva, and Arnaud Banos. Mathematical analysis of a hybrid model: Impacts of individual behaviors on the spreading of an epidemic. *Networks & Heterogeneous Media*, 2022.

[24] Paul E Carson, C Larkin Flanagan, CE Ickes, and Alf S Alving. Enzymatic deficiency in primaquine-sensitive erythrocytes. *Science*, 124(3220):484–485, 1956.

[25] Cindy S Chu, Aung Pyae Phyo, Khin Maung Lwin, Htun Htun Win, Thida San, Aye Aye Aung, Rattanaporn Raksapraidee, Verena I Carrara, Germana Bancone, James Watson, et al. Comparison of the cumulative efficacy and safety of chloroquine, artesunate, and chloroquine-primaquine in plasmodium vivax malaria. *Clinical Infectious Diseases*, 67(10):1543–1549, 2018.

[26] Cindy S Chu, Aung Pyae Phyo, Claudia Turner, Htun Htun Win, Naw Pet Poe, Widi Yotyingaphiram, Suradet Thinraow, Pornpimon Wilairisak, Rattanaporn Raksapraidee, Verena I Carrara, Moo Kho Paw, Jacher Wiladphaingern, Stéphane Proux, Germana Bancone, Kanlaya Sriprawat, Sue J Lee, Atthanee Jeeyapant, James Watson, Joel Tarning, Mallika Imwong, François Nosten, and Nicholas J White. Chloroquine versus dihydroartemisinin-piperaquine with standard high-dose primaquine given either for 7 days or 14 days in plasmodium vivax malaria. *Clin. Infect. Dis.*, 68(8):1311–1319, aug 2018.

[27] Anthony R. M. Coates, editor. *Dormancy and Low Growth States in Microbial Disease*, volume 3. Cambridge University Press, UK,US, jun 2003.

[28] Nadia R Cohen, Michael A Lobritz, and James J Collins. Microbial persistence and the road to drug resistance. *Cell Host & Microbe*, 13(6):632–642, 2013.

[29] Francis EG Cox. History of the discovery of the malaria parasites and their vectors. *Parasites & Vectors*, 3(1):1–9, 2010.

[30] Derek AT Cummings, Sopon Iamsirithaworn, Justin T Lessler, Aidan McDermott, Rungnapa Prasanthong, Ananda Nisalak, Richard G Jarman, Donald S Burke, and Robert V Gibbons. The impact of the demographic transition on dengue in thailand: insights from a statistical analysis and mathematical modeling. *PLoS medicine*, 6(9):e1000139, 2009.

[31] Derek AT Cummings, Sopon Iamsirithaworn, Justin T Lessler, Aidan McDermott, Rungnapa Prasanthong, Ananda Nisalak, Richard G Jarman, Donald S Burke, and Robert V Gibbons. The impact of the demographic transition on dengue in thailand: insights from a statistical analysis and mathematical modeling. *PLoS medicine*, 6(9):e1000139, 2009.

[32] DJ Daley and J Gani. Models for the spread of infection via pairing at parties. In *Applied Probability and Stochastic Processes*, pages 95–113. Springer, 1999.

[33] John N Darroch and Eugene Seneta. On quasi-stationary distributions in absorbing continuous-time finite markov chains. *Journal of Applied Probability*, 4(1):192–196, 1967.

[34] Imane El Meouche, Yik Siu, and Mary J Dunlop. Stochastic expression of a multiple antibiotic resistance activator confers transient resistance in single cells. *Sci. Rep.*, 6(1):1–9, 2016.

[35] Stephanie Evans, Emily Agnew, Emilia Vynnycky, James Stimson, Alex Bhattacharya, Christopher Rooney, Ben Warne, and Julie Robotham. The impact of testing and infection prevention and control strategies on within-hospital transmission dynamics of covid-19 in english hospitals. *Philosophical Transactions of the Royal Society B*, 376(1829):20200268, 2021.

[36] Juliano Ferrari Gianlupi, Tarunendu Mapder, TJ Sego, James P Sluka, Sara K Quinney, Morgan Craig, Robert E Stratford Jr, and James A Glazier. Multiscale model of antiviral timing, potency, and heterogeneity effects on an epithelial tissue patch infected by sars-cov-2. *Viruses*, 14(3):605, 2022.

[37] Daniel T Gillespie. A general method for numerically simulating the stochastic time evolution of coupled chemical reactions. *J. Comput. Phys.*, 22(4):403–434, 1976.

[38] Daniel T Gillespie. Exact stochastic simulation of coupled chemical reactions. *The J. Phys. Chem.*, 81(25):2340–2361, 1977.

[39] S. Jake Gonzales, Raphael A. Reyes, Ashley E. Braddom, Gayani Batugedara, Sebastiaan Bol, and Evelien M. Bunnik. Naturally acquired humoral immunity against plasmodium falciparum malaria. *Frontiers in Immunology*, 11, oct 2020.

[40] Erin E Gorsich, Rampal S Etienne, Jan Medlock, Brianna R Beechler, Johannie M Spaan, Robert S Spaan, Vanessa O Ezenwa, and Anna E Jolles. Opposite outcomes of coinfection at individual and population scales. *Proceedings of the National Academy of Sciences*, 115(29):7545–7550, 2018.

[41] Andrea L Graham, Tracey J Lamb, Andrew F Read, and Judith E Allen. Malaria-filaria coinfection in mice makes malarial disease more severe unless filarial infection achieves patency. *The Journal of infectious diseases*, 191(3):410–421, 2005.

[42] Johan Grasman and Onno A. van Herwaarden. *Asymptotic Methods for the Fokker—Planck Equation and the Exit Problem in Applications*. Springer, Berlin Heidelberg, 1999.

[43] Bryan T Grenfell, Andrew P Dobson, and HK Moffatt. *Ecology of infectious diseases in natural populations*, volume 7. Cambridge University Press, 1995.

[44] Emily C Griffiths, Amy B Pedersen, Andy Fenton, and Owen L Petchey. The nature and consequences of coinfection in humans. *Journal of Infection*, 63(3):200–206, 2011.

[45] The Medical Invincible Group. World MALARIA Day. https://medicalinvincible.blogspot.com/2015/04/world-day-25-malaria-isa-protozoal.html, 2015. [Online; last accessed on 02-February-2023].

[46] Nil Gural, Liliana Mancio-Silva, Alex B Miller, Ani Galstian, Vincent L Butty, Stuart S Levine, Rapatbhorn Patrapuvich, Salil P Desai, Sebastian A Mikolajczak, Stefan HI Kappe, et al. In vitro culture, drug sensitivity, and transcriptome of plasmodium vivax hypnozoites. *Cell Host & Microbe*, 23(3):395–406, 2018.

[47] Donovan Guttieres, Anthony J Sinskey, and Stacy L Springs. Modeling framework to evaluate vaccine strategies against the covid-19 pandemic. *Systems*, 9(1):4, 2021.

[48] Karl P. Hadeler and Thomas Hillen. Coupled dynamics and quiescent phases. In *Math Everywhere*, pages 7–23. Springer Berlin Heidelberg.

[49] Karl Peter Hadeler. *Topics in Mathematical Biology*. Springer International Publishing, 2017.

[50] K.P. Hadeler. Quiescent phases and stability. *Linear Algebra and its Applications*, 428(7):1620–1627, apr 2008.

[51] Nelson G Hairston Jr and Bart T De Stasio Jr. Rate of evolution slowed by a dormant propagule pool. *Nat.*, 336(6196):239–242, 1988.

[52] Frédéric M Hamelin, Linda JS Allen, Vrushali A Bokil, Louis J Gross, Frank M Hilker, Michael J Jeger, Carrie A Manore, Alison G Power, Megan A Rúa, and Nik J Cunniffe. Coinfections by noninteracting pathogens are not independent and require new tests of interaction. *PLoS Biol.*, 17(12):e3000551, 2019.

[53] P W Hedrick. Population genetics of malaria resistance in humans. *Heredity*, 107(4):283–304, mar 2011.

[54] João Hespanha. *Linear systems theory*. Princeton university press, 2nd edition, 2018.

[55] Herbert W Hethcote. The mathematics of infectious diseases. *SIAM review*, 42(4):599–653, 2000.

[56] Herbert W Hethcote and Pauline van den Driessche. Two sis epidemiologic models with delays. *Journal of Mathematical Biology*, 40(1):3–26, 2000.

[57] Frank M Hilker, Linda JS Allen, Vrushali A Bokil, Cheryl J Briggs, Zhilan Feng, Karen A Garrett, Louis J Gross, Frédéric M Hamelin, Michael J Jeger, Carrie A Manore, et al. Modeling virus coinfection to inform management of maize lethal necrosis in kenya. *Phytopathology*, 107(10):1095–1108, 2017.

[58] Rosalind E Howes, Katherine E Battle, Kamini N Mendis, David L Smith, Richard E Cibulskis, J Kevin Baird, and Simon I Hay. Global epidemiology of plasmodium vivax. *The American journal of tropical medicine and hygiene*, 95(6 Suppl):15, 2016.

[59] Riedel S Edward Jenner. the history of smallpox and vaccination. In *Baylor University Medical Center Proceedings*, volume 18, pages 21–5, 2005.

[60] Sona John, Mélissa Verin, Wolfgang Stephan, Aurélien Tellier, et al. Neutral genomic signatures of host-parasite coevolution. *BMC Evol. Biol.*, 19(1):1–11, 2019.

[61] Richard A. Johnson and Dean Wichern. *Multivariate Analysis*. Wiley, sep 2014.

[62] Anssi Karvonen, Jukka Jokela, and Anna-Liisa Laine. Importance of sequence and timing in parasite coinfections. *Trends in parasitology*, 35(2):109–118, 2019.

[63] Matt J. Keeling and Pejman Rohani. *Modeling Infectious Diseases in Humans and Animals*. Princeton University Press, sep 2011.

[64] Matt J Keeling, Mark EJ Woolhouse, Darren J Shaw, Louise Matthews, Margo Chase-Topping, Dan T Haydon, Stephen J Cornell, Jens Kappey, John Wilesmith, and Bryan T Grenfell. Dynamics of the 2001 uk foot and mouth epidemic: stochastic dispersal in a heterogeneous landscape. *Science*, 294(5543):813–817, 2001.

[65] William Ogilvy Kermack and Anderson G McKendrick. A contribution to the mathematical theory of epidemics. *Proceedings of the royal society of london. Series A, Containing papers of a mathematical and physical character*, 115(772):700–721, 1927.

[66] H. Kestelman and F. R. Gantmacher. The theory of matrices. *Biometrika*, 48(1/2):237, jun 1961.

[67] Oleg Kogan, Michael Khasin, Baruch Meerson, David Schneider, and Christopher R Myers. Two-strain competition in quasineutral stochastic disease dynamics. *Phys. Rev. E.*, 90(4):042149, 2014.

[68] Bendix Koopmann, Johannes Müller, Aurélien Tellier, and Daniel Živković. Fisher–wright model with deterministic seed bank and selection. *Theor. Popul. Biol.*, 114:29–39, 2017.

[69] Sunil Lakhani. Early clinical pathologists: Edward jenner (1749-1823). *Journal of clinical pathology*, 45(9):756, 1992.

[70] Jay T Lennon and Stuart E Jones. Microbial seed banks: the ecological and evolutionary implications of dormancy. *Nat. Rev. Microbiol.*, 9(2):119–130, 2011.

[71] Isac da SF Lima and Elisabeth C Duarte. Factors associated with timely treatment of malaria in the brazilian amazon: a 10-year population-based study. *Revista panamericana de salud publica*, 41:e100, 2017.

[72] A Lindberg, J Brownlie, G Gunn, H Houe, V Moening, HW Saatkamp, T Sandvik, and PS Valle. The control of bovine viral diarrhoea virus in europe: today and in the future. *Plurithematic issue of the Scientific and technical review, 2006*, pages 961–979, 2006.

[73] Manuela López-Villavicencio, Odile Jonot, Amélie Coantic, Michael E Hood, Jérôme Enjalbert, and Tatiana Giraud. Multiple infections by the anther smut pathogen are frequent and involve related strains. *PLoS Pathogens*, 3(11):e176, 2007.

[74] Francesca A Lovell-Read, Silvia Shen, and Robin N Thompson. Estimating local outbreak risks and the effects of non-pharmaceutical interventions in age-structured populations: Sars-cov-2 as a case study. *Journal of Theoretical Biology*, 535:110983, 2022.

[75] Alexander G Maier, Kai Matuschewski, Meng Zhang, and Melanie Rug. Plasmodium falciparum. *Trends in parasitology*, 35(6):481–482, 2019.

[76] Sergei Maslov and Kim Sneppen. Well-temperate phage: optimal bet-hedging against local environmental collapses. *Scientific Reports*, 5(1):10523, 2015.

[77] PW Mason and MJ Grubman. Controlling foot-and-mouth disease with vaccines?, 2001.

[78] Robert M May and Roy M Anderson. Population biology of infectious diseases: Part ii. *Nature*, 280(5722):455–461, 1979.

[79] Kimberly F McManus, Angela M Taravella, Brenna M Henn, Carlos D Bustamante, Martin Sikora, and Omar E Cornejo. Population genetic analysis of the darc locus (duffy) reveals adaptation from standing variation associated with malaria resistance in humans. *PLoS genetics*, 13(3):e1006560, 2017.

[80] Johannes Müller and Christina Kuttler. *Methods and Models in Mathematical Biology*. Springer, 2015.

[81] Coleen T Murphy and Patrick J Hu. Insulin/insulin-like growth factor signaling in c. elegans. https://www.ncbi.nlm.nih.gov/books/NBK179230, 2018.

[82] Ingemar Nåsell. On the quasi-stationary distribution of the stochastic logistic epidemic. *Mathematical biosciences*, 156(1-2):21–40, 1999.

[83] Ingemar Nåsell. Stochastic models of some endemic infections. *Mathematical biosciences*, 179(1):1–19, 2002.

[84] Ingemar Nåsell. *Extinction and quasi stationarity in the stochastic logistic SIS model*. Springer, 2011.

[85] Meksianis Z Ndii and Yudi Ari Adi. Modelling the transmission dynamics of covid-19 under limited resources. *Commun. Math. Biol. Neurosci.*, 2020:Article–ID, 2020.

[86] Government of Canada. Public Health Agency of Canada- Notifiable diseases on-line. https://diseases.canada.ca/notifiable/charts?c=ppd. [Online; last accessed on 02-February-2023].

[87] Augustine Okolie and Johannes Müller. Exact and approximate formulas for contact tracing on random trees. *Mathematical biosciences*, 321:108320, 2020.

[88] World Health Organization. Key malaria facts. Technical report.

[89] James M Ortega. *Matrix theory: A second course*. Springer Science & Business Media, 1987.

[90] Trevor N Petney and Ross H Andrews. Multiparasite communities in animals and humans: frequency, structure and pathogenic significance. *International journal for parasitology*, 28(3):377–393, 1998.

[91] Graham F Raggett. Modelling the eyam plague. *Bull. Inst. Math. and its Applic*, 18(221-226):530, 1982.

[92] Stefan Riedel. Edward jenner and the history of smallpox and vaccination. In *Baylor University Medical Center Proceedings*, volume 18, pages 21–25. Taylor & Francis, 2005.

[93] Thierry Rigaud, Marie-Jeanne Perrot-Minnot, and Mark JF Brown. Parasite and host assemblages: embracing the reality will improve our knowledge of parasite transmission and virulence. *Proceedings of the Royal Society B: Biological Sciences*, 277(1701):3693–3702, 2010.

[94] Leanne J Robinson, Rahel Wampfler, Inoni Betuela, Stephan Karl, Michael T White, Connie SN Li Wai Suen, Natalie E Hofmann, Benson Kinboro, Andreea Waltmann, Jessica Brewster, et al. Strategies for understanding and reducing the plasmodium vivax and plasmodium ovale hypnozoite reservoir in papua new guinean children: a randomised placebo-controlled trial and mathematical model. *PLoS medicine*, 12(10):e1001891, 2015.

[95] Shigeharu Sato. Plasmodium a brief introduction to the parasites causing human malaria and their basic biology. *Journal of physiological anthropology*, 40(1):1–13, 2021.

[96] Kristan Alexander Schneider and Carola Janette Salas. Evolutionary genetics of malaria. *Frontiers in Genetics*, 13, nov 2022.

[97] Shelby M Scott and Louis J Gross. Covid-19 and crime: Analysis of crime dynamics amidst social distancing protocols. *PloS one*, 16(4):e0249414, 2021.

[98] Jon Seger. What is bet-hedging? *Oxford Surv. Evol. Biol.*, 4:182–211, 1987.

[99] Thibaut Sellinger, Johannes Müller, Volker Hösel, and Aurélien Tellier. Are the better cooperators dormant or quiescent? *Math. Biosci.*, 318:108272, 2019.

[100] Michael Sieber, Lucía Pita, Nancy Weiland-Bräuer, Philipp Dirksen, Jun Wang, Benedikt Mortzfeld, Sören Franzenburg, Ruth A Schmitz, John F Baines, Sebastian Fraune, et al. Neutrality in the metaorganism. *PLoS Biol.*, 17(6):e3000298, 2019.

[101] Robert W Snow, Carlos A Guerra, Abdisalan M Noor, Hla Y Myint, and Simon I Hay. The global distribution of clinical episodes of plasmodium falciparum malaria. *Nature*, 434(7030):214–217, 2005.

[102] Ian Sorrell, Andrew White, Amy B Pedersen, Rosemary S Hails, and Mike Boots. The evolution of covert, silent infection as a parasite strategy. *Proceedings of the Royal Society B: Biological Sciences*, 276(1665):2217–2226, 2009.

[103] Hanna Susi, Benoit Barrès, Pedro F Vale, and Anna-Liisa Laine. Co-infection alters population dynamics of infectious disease. *Nature communications*, 6(1):1–8, 2015.

[104] Aimee R Taylor, James A Watson, Cindy S Chu, Kanokpich Puaprasert, Jureeporn Duanguppama, Nicholas PJ Day, Francois Nosten, Daniel E Neafsey, Caroline O Buckee, Mallika Imwong, et al. Resolving the cause of recurrent plasmodium vivax malaria probabilistically. *Nature communications*, 10(1):1–11, 2019.

[105] Aimee R Taylor, James A Watson, Cindy S Chu, Kanokpich Puaprasert, Jureeporn Duanguppama, Nicholas PJ Day, Francois Nosten, Daniel E Neafsey, Caroline O Buckee, Mallika Imwong, et al. Resolving the cause of recurrent plasmodium vivax malaria probabilistically. *Nature communications*, 10(1):1–11, 2019.

[106] Howard M. Taylor and Samuel Karlin. Introduction. In *An Introduction to Stochastic Modeling*, pages 1–43. Elsevier, 1984.

[107] Aurélien Tellier, James KM Brown, Mike Boots, and Sona John. Theory of host–parasite coevolution: From ecology to genomics. *eLS*, 2:1–10, 2021.

[108] Alan R Templeton and Donald A Levin. Evolutionary consequences of seed pools. *The Am. Nat.*, 114(2):232–249, 1979.

[109] Neil H Timm. *Applied multivariate analysis*. Springer, New York, Berlin Heidelberg, 2002.

[110] Renu Tuteja. Malaria- an overview. *The FEBS journal*, 274(18):4670–4679, 2007.

[111] Veterinary Vaccinology. Edited by pastored, pp; blancou, j; verschueren, c. *Elseiver Science BV*, 1997.

[112] Minus van Baalen and Maurice W. Sabelis. The dynamics of multiple infection and the evolution of virulence. *The Am. Nat.*, 146(6):881–910, dec 1995.

[113] Onno A Van Herwaarden and Johan Grasman. Stochastic epidemics: major outbreaks and the duration of the endemic period. *Journal of mathematical biology*, 33(6):581–601, 1995.

[114] N.G. van Kampen. *STOCHASTIC PROCESSES*. Elsevier, 2007.

[115] Elise Vaumourin, G V, Patrick Gasqui, and Muriel Vayssier Taussat. The importance of multiparasitism: examining the consequences of coinfections for human and animal health. *Parasites and vectors*, 8(1):1–13, 2015.

[116] Mélissa Verin and Aurélien Tellier. Host-parasite coevolution can promote the evolution of seed banking as a bet-hedging strategy. *Evolution*, 72(7):1362–1372, 2018.

[117] Jan Votỳpka, David Modrỳ, Miroslav Oborník, Jan Šlapeta, Julius Lukeš, et al. Apicomplexa. *Handbook of the Protists*, 2:1–56, 2016.

[118] Nicholas J White. Determinants of relapse periodicity in plasmodium vivax malaria. *Malar. J.*, 10(1):1–36, 2011.

[119] WHO. Malaria report. 2019.

[120] Alexandre WIEFELS, Bruna Wolfarth-COUTO, Naziano FILIZOLA, Laurent DURIEUX, and Morgan MANGEAS. Accuracy of the malaria epidemiological surveillance system data in the state of amazonas. *Acta Amazonica*, 46(4):383–390, dec 2016.

[121] Thomas K Wood, Stephen J Knabel, and Brian W Kwan. Bacterial persister cell formation and dormancy. *Appl. Environ. Microbiol.*, 79(23):7116–7121, 2013.

[122] Duolong Zhu, Joseph A Sorg, and Xingmin Sun. Clostridioides difficile biology: sporulation, germination, and corresponding therapies for c. difficile infection. *Front. cell. and infect. Microbiol.*, 8:29, 2018.